INVESTIGATING THE ROLE OF MLLT11 IN THE DEVELOPMENT OF CORTICAL HEM DERIVATIVES AND HIPPOCAMPAL NEUROGENESIS

by

Samantha Amelia Moore

Submitted in partial fulfilment of the requirements
for the degree of Master of Science

at

Dalhousie University
Halifax, Nova Scotia
March 2021

DEDICATION

This thesis is dedicated wholeheartedly to my beloved parents and brothers who have been my source of inspiration, who gave me strength to pursue my passions, and who continue to provide unwavering support and encouragement.

Especially to my twin brother, for always being there, for your advice, technical skills, friendship, and for making me smile.

And of course, to Lorelai.

TABLE OF CONTENTS

LIST OF TABLES

LIST OF FIGURES

ABSTRACT

The mammalian Cortical Hem plays a key role in orchestrating the formation of Cajal-Retzius cells, the Choroid Plexus, and hippocampus, a structure crucial to cognition and spatial learning. While several key regulators of Cortical Hem development have been identified, the downstream processes they regulate have remained obscure. This thesis explores the role of Mllt11, originally viewed as only an oncogenic factor, in the development of the Cortical Hem and the Dentate Gyrus region of the hippocampus. This is the first study to report the expression of *Mllt11* in postnatal and adult mouse hippocampus and provides insights into its function in the developing Cortical Hem region and its derivatives. Through use of a genetic Cre-lox strategy, the *Mllt11* gene was conditionally ablated from cells in the developing Cortical Hem and hippocampus. Part of the genetic strategy involved activating the expression of the fluorescence reporter gene tdTomato within the same cells that lacked *Mllt11,* to monitor the behaviour of mutant cells. The loss of *Mllt11* disrupted the formation of tissues derived from the Cortical Hem, including Cajal-Retzius cells and the lateral ventricular Choroid Plexus. Furthermore, *Mllt11* loss greatly impacted hippocampal neurogenesis, in part due to the aberrant position of type-1 radial glial progenitors within the developing Dentate Gyrus. As a consequence, type-1 progenitors rapidly transitioned to amplifying neural progenitors and neuroblasts, which ultimately enhanced formation of immature granule cells in the postnatal hippocampus. Taken together, the findings reported herein demonstrate the critical role of Mllt11 in maintaining the hippocampal radial glial phenotype and the balance between neural progenitor proliferation and terminal differentiation. It is also demonstrated that Mllt11 is required for the proper migration of neural progenitors to fuel the growth of the Choroid Plexus, and invasion of Cajal-Retzius cells into the pallial neocortex.

LIST OF ABBREVIATIONS USED

ALS	Amyotrophic Lateral Sclerosis
BMP	Bone Morphogenetic Proteins
BrdU	Bromodeoxyuridine
CA	Cornu Ammonis
CH	Cortical Hem
ChP	Choroid Plexus
CNS	Central Nervous System
CR	Cajal-Retzius
CreERT2	Cre Fused to Estrogen Ligand-Binding Domain 2
CSF	Cerebrospinal Fluid
Cux2	Cut-Like Homeobox Protein 2
DAPI	4′,6-Diamidino-2-Phenylindole
DG	Dentate Gyrus
DMSO	Dimethyl Sulfoxide
DNA	Deoxyribonucleic Acid
DNE	Dentate Neuroepithelium
DTM	Dorsal Telencephalic Midline
E	Embryonic Day
EdU	5-Ethynyl-2'-Deoxyuridine
Emx2	Homeobox Protein Emx2
GCL	Granule Cell Layer
GFAP	Glial Fibrillary Acidic Protein
Gli3	Zinc Finger Protein Gli3
HEK293	Human Embryonic Kidney 293 Cells
HF	Hippocampal Fissure
HNE	Hippocampal Neuroepithelium
IML	Inner Molecular Layer
IRES	Internal Ribosome Entry Site
ISH	*in situ* Hybridization

cKO	Conditional Knockout
Lhx2	LIM/Homeobox Protein
LoxP	Locus of X-Over P1
LV	Lateral Ventricle
Mllt11/Af1q	Myeloid/Lymphoid or Mixed-Lineage Leukemia; Translocated to Chromosome 11/All1 Fused Gene from Chromosome 1q
mRNA	Messenger Ribonucleic Acid
NeuN	RNA Binding Fox-1 Homolog 3
NeuroD1	Neurogenic Differentiation 1
NRSF	Neuron-Restrictive Silencer Factor
NP	Neural Progenitor
OTX1/2	Homeobox Protein OTX1/2
P	Postnatal
p53	Tumor Protein 53
p73	Tumor Protein 73
Pax6	Paired Box Protein Pax6
PBS	Phosphate Buffered Saline
PBT	Phosphate Buffered Saline with TritonX-100
PFA	Paraformaldehyde
Prox1	Prospero Homeobox Protein 1
PSA-NCAM	Polysialylated Neuronal Cell Adhesion Molecule
REST	Repressor Element 1 Silencing Transcription Factor
RGL	Radial-Glia-Like
SGZ	Subgranular Zone
SOD1	Superoxide Dismutase 1
Sox2	Sex Determining Region Y-Box 2
SVZ	Subventricular Zone
TuJ1	Neuron-Specific Class III B-Tubulin
VZ	Ventricular Zone
Wnt	Wingless/Int
XtJ	Extra-toes-J

ACKNOWLEDGEMENTS

To my supervisor, Dr. Angelo Iulianella, thank you for fostering scientific curiosity and for imparting your knowledge and expertise during the course of my time with you. Thank you for your compassion and unwavering support during personal challenges, without which this degree would not have been possible. Thank you for granting me the opportunity to grow as a scientist, for your encouragement and the fostering of passion and excitement for research. You have made me strive to reach higher goals as a student, and I am forever grateful.

Thank you to the members of my supervisory committee, Dr. Kazue Semba and Dr. Stefan Krueger for your knowledge, feedback, and guidance over the past two years enabling me to become a better researcher.

To Danielle Stanton-Turcotte, my colleague and forever friend. Thank you for your constant support, vast knowledge, and advice both in and outside of the lab. Thank you for your friendship, for the laughs, and the memories that kept me sane. You are the person, without whom I would not have made it through. I am grateful to have shared this graduate school experience with you, may you go on to do amazing things.

To Karolynn Hsu, aka lab mom, thank you for sharing your knowledge and expertise in all things research. Thank you for the advice, coffee breaks, and for the photos and videos of your adorable kiddos. Your friendship has been a source of encouragement both in and outside of the lab.

Finally, thank you to the numerous friends and colleagues in the Department of Medical Neuroscience.

CHAPTER 1. INTRODUCTION

Developmental neuroscience is devoted to understanding the mechanisms by which the complex nervous system develops and emerge with extensive cell diversity and understanding how neurons establish functional connections with immense precision and complexity. Neurogenesis was thought to occur only during embryonic stages in the mammal, until the pioneering studies by Altman and his colleagues (Altman and Das, 1965), provided the first evidence for the presence of newly generated dentate granule cells in the postnatal rat hippocampus.

Advancements in molecular and genetic techniques have aided our understanding of factors that support adult neurogenesis, maintain proliferative cell populations, and support differentiation of progenitors into their specific cell fate (Patel et al., 1997; Lee et al., 1998; Nottebohm, 2002; Alvarez-Buylla and Lim, 2004; Lledo et al., 2006; Duan et al., 2008; Lou et al., 2008). Numerous studies have shown that neurogenesis occurs at a low level in adults, with new neurons continually integrating into established neuronal circuits (Paton and Nottebohm, 1984; Reynolds and Iiss, 1992; Richards et al., 1992; Eriksson et al., 1998; Kempermann and Ehninger, 2008). These findings will allow for great inroads into the understanding of neurological disorders and disease, as our knowledge of the molecular regulation of neurogenesis and how newborn neurons integrate into developing circuits remains incomplete. The purpose of this thesis is to explore the role of Mllt11 in regulating the formation of the Cortical Hem (CH) region, its derivatives, and hippocampal neurogenesis.

1.1. The Telencephalon

The early central nervous system (CNS) begins as a simple neural plate that will ultimately form the intricate network of cells that contribute to the functional brain (Wilson and

Houart, 2004). The telencephalon is the largest, most complex part of the mammalian CNS, divided into numerous functionally specialized paired telencephalic hemispheres including the neocortex and associated structures such as the basal ganglia, hypothalamus and thalamus. Patterning of the telencephalon occurs through an elaborate and highly regulated process involving calculated proliferation of progenitors, onset of neurogenesis, migration and progressive fate restriction, and ultimately the formation of spatially and temporally distinct cell types (Wilson and Rubenstein, 2000; Rallu et al., 2002; Wilson and Houart, 2004). The precise coordination of growth and patterning of both adjacent and distant developing tissues along the anterior-posterior and dorsal-ventral axes is crucial to ensuring harmonious patterning.

Development of the telencephalic neuroepithelium is carefully orchestrated by a series of morphogens secreted from signaling centers that control the expression of specific transcription factors in a graded pattern along the coordinate axes (Assimacopoulos et al., 2003; Remedios et al., 2007; Subramanian et al., 2009). This leads to progressive subdivisions forming the neocortex, a six-cortical laminae structure (layers of neuronal cell bodies), dorsally and the archicortex, a smaller phylogenetically older cortical area developing medially (Rockland and DeFelipe, 2018). The archicortex includes the hippocampus proper, with subfields termed the Cornu Ammonis (CA) 1, CA2, CA3, the dentate gyrus (DG), and the subiculum (van Strien et al., 2009).

1.2. The Cortical Hem and its Derivatives

Regulation of patterning mechanisms in the early embryo has been of great interest for years, which has led to the identification of signaling centers. During development of the telencephalon, around embryonic day 10.5 (E10.5), the dorsal telencephalic midline (DTM) region folds inward to form complementary telencephalic vesicles and the resulting midline

tissue is reorganized to generate a structure known as the CH (Subramanian and Tole, 2009). The CH is functionally distinct from the bordering pseudostratified cortical neuroepithelium and plays a crucial role as a classical developmental organizer (Monuki et al., 2001; Caronia-Brown et al., 2014). The CH was first described as a potential signaling center at the telencephalic midline owing to its enriched expression of the Wingless/Int (Wnt) and Bone Morphogenetic Protein (BMP) families of morphogens (Furuta et al., 1997; Grove et al., 1998). By E12.5, the CH is clearly marked by the expression of three Wnt genes, Wnt2b, Wnt3a and Wnt5a, forming a distinct boundary with the hippocampal primordia dorsally and the CH ventrally (Grove et al., 1998).

There is now definitive evidence supporting the role of the CH in neural development. For example, several studies have assessed the spontaneously occurring mutation known as extra toes-J (XtJ) that causes defects in both neural and limb development. Mice homozygous for the *XtJ* mutation are deficient in both Wnt and BMP expression within the DTM and lack an identifiable CH (Caronia-Brown et al., 2014). Importantly, the loss of the CH is accompanied by a disruption in the development of the hippocampus and the telencephalic choroid plexus (ChP), with both structures no longer detectable by molecular or morphological markers (Furuta et al., 1997; Grove et al., 1998). Specifically, the CH is optimally situated to regulate the induction and appropriate structural organization of the hippocampal primordia dorsally, and the ChP ventrally (Machon et al., 2007; Mangale et al., 2008; Subramanian and Tole, 2009; Roy et al., 2014).

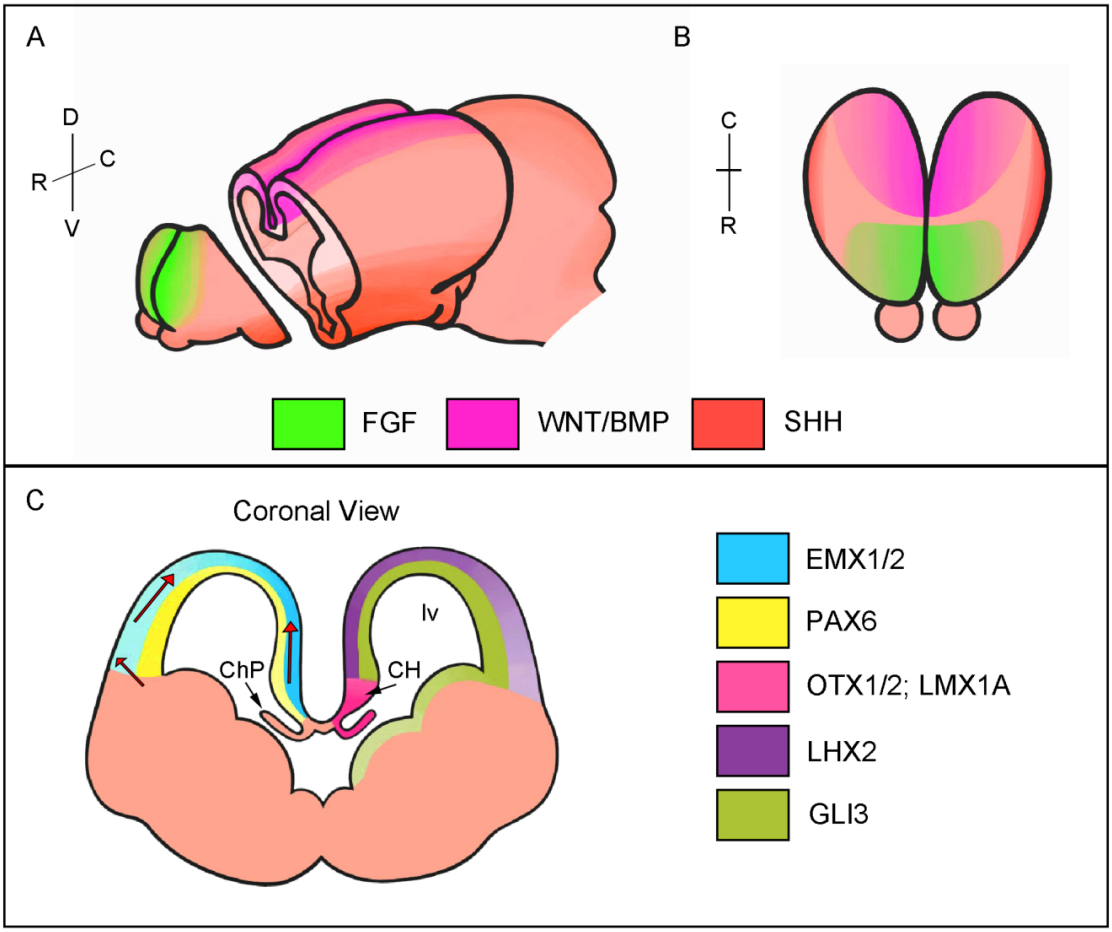

Figure 1.1. Signaling proteins and transcription factors that pattern the dorsal midline. (A, B) Schematic depiction of prominent morphogen families expressed in the telencephalon include Wingless/Int (Wnt) and Bone Morphogenetic Protein (BMP) that regulate the patterning of the cortical hem and its derivatives. In addition to Fibroblast Growth Factor (FGF) signaling in the Rostral Telencephalic Organizer (RTO) and Sonic hedgehog (Shh) from the Ventral Telencephalic Midline (VTM). (C) Key transcriptional regulators that pattern the telencephalon include Emx2 and Pax6 as well as Lhx2 and Gli3 expressed in opposing gradients important in patterning of the cortex and limiting the extent of the cortical hem. In addition to OTX1/2 and Lmx1a important in the induction and formation of the cortical hem.

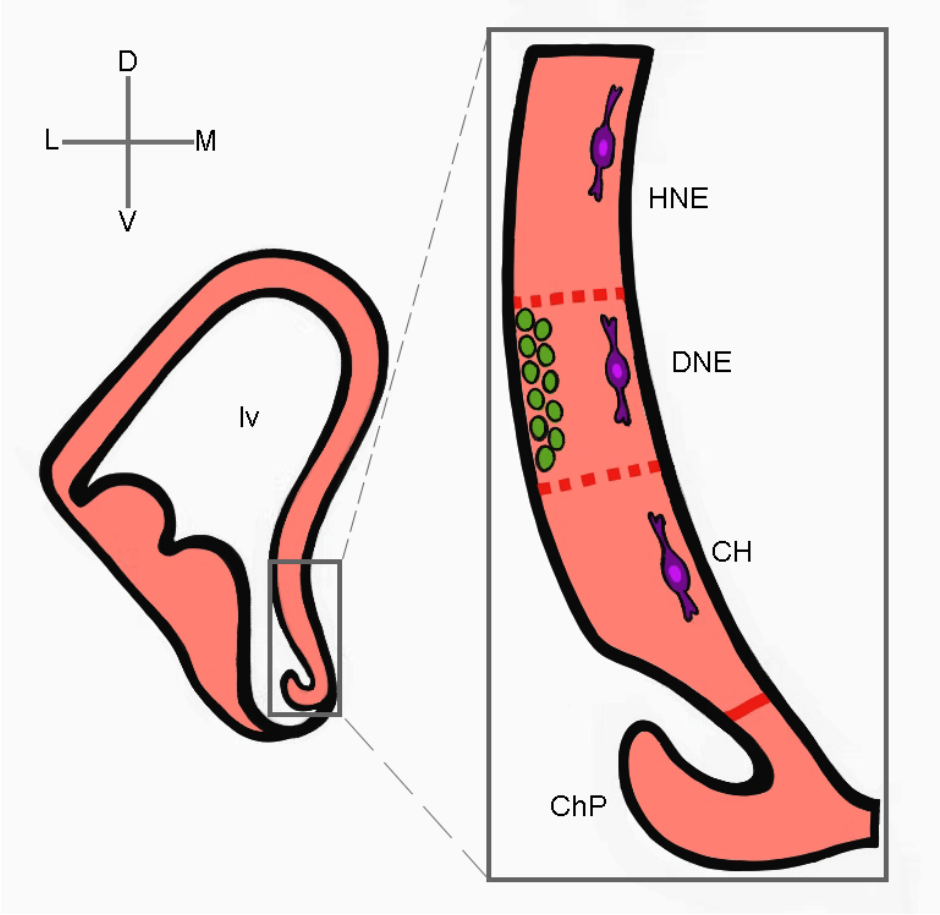

Figure 1.2. Schematic depiction of fetal cortical hem anatomy. Left side: coronal section at E14.5 displaying the telencephalic midline structures. The CH regulates induction and formation of hippocampal primordia dorsally and the choroid plexus ventrally. The presumptive DNE is located between the HNE and the CH. Right side: DG precursors (green circles) of the primary matrix are located in the VZ of the ventromedial LV. These precursors migrate to the pial side of the cortex to form the secondary matrix of the DG. CR cells (purple) of CH origin line the pial side of the cortex. Abbreviations: CH, Cortical Hem; ChP, Choroid Plexus; D, Dorsal; DG, Dentate Gyrus; DNE, Dentate Neuroepithelium; HNE, Hippocampal Neuroepithelium; LV, Lateral Ventricle; L, Lateral; M, Medial; V, Ventral.

1.2.1. Cajal-Retzius Cells

During development recognition molecules provide necessary signals for the formation of neural connections and axonal pathfinding. In some regions these cues are provided in part by specific cells that exist only transiently in development. Ramon y Cajal (1899) and Retzius (1893) described morphologically complex cells located in the marginal zone of the fetal and early postnatal human neocortex, known today as Cajal-Retzius (CR) cells (Retzius, 1893; Ramon y Cajal, 1899). Recent work has centered on the molecular signature and the developmental origin of these cells. The most well documented function of CR cells is their expression of the extracellular glycoprotein Reelin to control neural cell migration and detailed cortical lamination (Yoshida et al., 2006). However, additional functions have been proposed as in the regulation of the radial glial phenotype (Supèr et al., 2000) and in the development of hippocampal connections (Quattrocolo and Maccaferri, 2014).

During cortical development, CR cells are among the earliest neuronal subtypes to be born. These enigmatic cells arise from discrete sources within the telencephalon, including the medial CH region of the pallium. The CH forms the principal source of CR cells within the neocortex, which co-express Reelin and p73, a transcription factor of the p53-family (Abraham et al., 2004). Reelin is a multifunctional protein and plays a critical role in promoting neuronal migration and cortical lamination in the developing brain through cell-cell interactions (Yoshida et al., 2006). P73 plays an essential role in brain development, regulating the neurogenic pool *via* promotion of self-renewal and proliferation of immature neural progenitor (NP) cells and functions as a prosurvival factor of mature postmitotic neurons (Talos et al., 2010).

Upon complete inactivation of the *p73* gene in mutant mice, CR cells lack the expression of both Reelin and p73, which interestingly did not have the effect one would expect (Meyer,

2010). In fact, residual Reelin-expressing neurons in the marginal zone is sufficient to ensure normal development and prevent a *reeler* phenotype (Yang et al., 2000; Meyer, 2010). The production and maintenance of the predominant CR cell population depends on p73, but this study also demonstrates that the mouse cortex tolerates the loss of CH-derived Reelin-expressing cells (Meyer, 2010).

1.2.2. The Choroid Plexus

The ChP of the lateral ventricle is one of the main sources of Cerebrospinal Fluid (CSF), but its development remains a relatively understudied process. Only recently has research moved to the application of modern technologies to examine development and maturation of the ChPs and their potential role in neural development (Liddelow, 2015; Ghersi-Egea et al., 2018).

Structure of the Choroid Plexuses

The ChPs are modified epithelial structures that protrude into all four cerebral ventricles. They consist of a central stroma that is highly vascularized with fenestrated, leaky blood vessels and connective tissue (Johansson, 2014). The initial development of the ChPs begins around E11 and is largely complete by E14 in the mouse (Dziegielewska et al., 2001). The development of these four critical components begins with the fourth hindbrain ventricular ChP developing first. This is followed by the differentiation of the lateral ventricular ChPs and finally differentiation of the third ventricular ChP (Dziegielewska et al., 2001). The ChPs are of dual embryonic origin, as neuroepithelial cells give rise to the epithelial component and mesenchymal cells establish the stromal component (Johansson, 2014). The epithelial cells of each ventricular ChP matures through the same stereotypical stages before reaching maturity as comparative functional postnatal structures.

In Stage I, the ChP epithelial cells appear pseudostratified with centrally located nuclei. At this early point, there is little to no villous elaboration. Transition to Stage II involves a change to columnar epithelium with apically located nuclei and emerging basal connective tissue with sparse villi-like extensions. This is followed by a transition to Stage III, in which the epithelial cells flatten to become more cuboidal in shape, with centrally or apically located nuclei and more complex villi. By the final stage, Stage IV, the epithelial cells have fully transitioned to a cuboidal morphology, becoming slightly smaller in size and defined by centrally-to-basally located nuclei (Ek et al., 2003). Shortly after formation, the ChPs acquire barrier, secretory and transport capacities with additional cells continuously added to each ChP throughout early development (Ek et al., 2003; Johansson et al., 2006; Johansson, 2014). These epithelial cells are added from the proliferative zone, located at the 'root' of each plexus, as they transition through the stages outlined above (Liddelow et al., 2010).

The complex molecular relationship between the CH and the developing ChPs has been analyzed extensively. Several studies report telencephalic ChP formation requires signals from the dorsal midline, including expression of BMPs and Wnts originating from the CH (Grove et al., 1998; Wang et al., 2000; Hébert et al., 2002; Lun et al., 2015). For example, Wnt genes in the CH are upregulated as the ChPs begin to form, supporting a role for CH signaling in the induction of the ChP structures (Grove et al., 1998). Specifically, in the *XtJ* homozygous mouse mutant, which carries a deletion in *Gli3*, a transcriptional regulator of Wnt, it was found that Wnt gene expression is deficient in the CH (Grove et al., 1998). The coordination of Wnt signaling in the CH is important in upregulating the repressor form of Gli3, which in turn represses Sonic hedgehog (Shh) signaling. This represents a mechanism that regulates anterior-posterior patterning in the development of forebrain neuronal subtypes (Wang et al., 2000). Consequently,

the telencephalic ChP of the *XtJ* homozygous mouse mutant fails to develop. Grove et al. suggest that the loss of the telencephalic ChP of the homozygous *XtJ* mouse mutants is due to defects in the CH that include misregulation of Wnt expression (Grove et al., 1998). In addition, the CH provides a source of BMPs, crucial for the formation of the telencephalic ChPs (Lun et al., 2015). It is thought that high levels of BMPs are required to induce ChP formation and generation of the thin monolayer of secretory epithelium (Hébert et al., 2002). More specifically, BMPs may regulate morphogenesis of the telencephalic ChPs by establishing a balance between restricted cell proliferation and local cell death (Hébert et al., 2002). Several studies further support the critical interplay of the CH in the formation of the ChPs, as mutants lacking the CH also lack the ChPs (Grove et al., 1998; Lee et al., 2000; Yoshida et al., 2006).

Expression of numerous transcription factors are also crucial to the development of the CH and in turn the ChPs. For example, one study reports that Emx2 and Pax6 function in cooperation with OTX1 and OTX2 to ensure the proper development of the caudal forebrain which includes the CH and adjacent structures (Kimura et al., 2005). More recent work has revealed that transcription factor OTX2 is a master regulator of ChP development. Specifically, OTX2 has been reported to be essential for these structures to appear. Through the deletion of OTX2 by way of a tamoxifen inducible $OTX2^{CreERT2}$ driver line, Johansson et al. outline its critical role during development. They found that deletion of *OTX2* during the initial stages of development rapidly affects ChP formation. The most striking result established as early as E9.5 with tamoxifen mediated Cre-induction of recombination, they reported complete absence of OTX2-immunopositive cells by E11.5 and almost complete absence of all ChP tissue (Johansson et al., 2013). Together this work supports the important signal induction role of CH during ChP initiation and development.

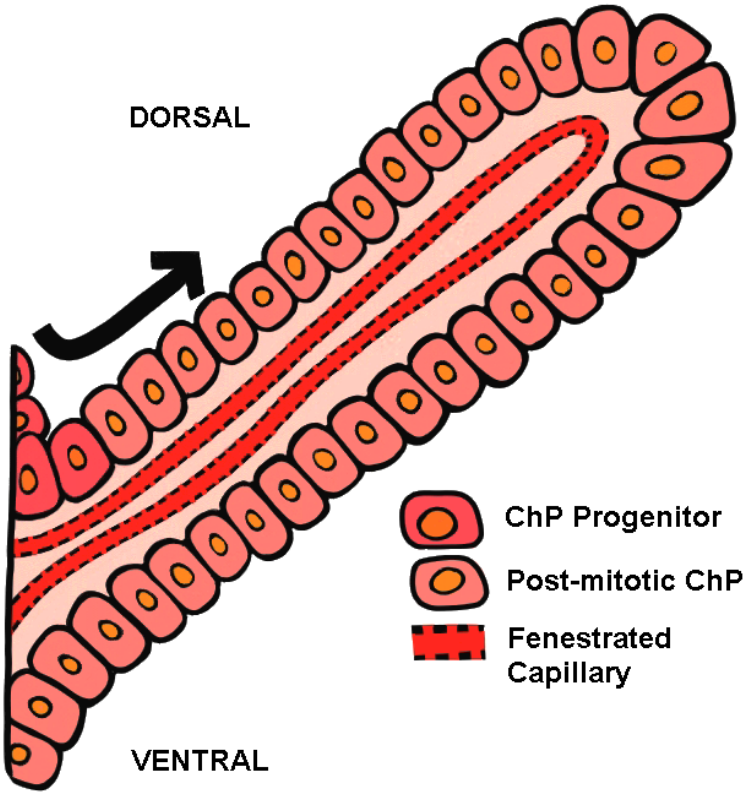

Figure 1.3. Schematic depiction of choroid plexus anatomy at E14.5. The ChPs are highly vascularized tissue located within each ventricle of the brain. Each ChP consists of a monolayer of cuboidal epithelial cells surrounding a stromal core of capillaries and loose connective tissue. ChP neuroepithelial cells originating from the ventricular zone are "pushed" out from the root of the ChP in the upper (dorsal) arm only, by newly divided cells, and migrate towards the tip of the stalk (black arrow indicating direction of cell migration). Abbreviations: ChP, Choroid Plexus. Figure adapted from (Liddelow et al., 2010).

Choroid Plexus Functions

During development, NPs are regulated by both intrinsic and extrinsic sources. One site of origin of extrinsic regulation is the CSF, a clear body fluid found in the brain and spinal cord that contains a variety of signaling factors (Lehtinen et al., 2011). Furthermore, NPs are located at the apical (ventricle facing) surface of the developing brain tissue (Mirzadeh et al., 2008). Thus, the CSF has the potential to influence cell behaviour at the ventricular surface *via* the composition of the fluid and thereby neurogenesis. The possible role of CSF in regulating neurogenesis has recently received more attention in research. However, little focus has been placed on the ChP, the principal source of CSF. This evolutionarily conserved structure consists of a monolayer of cuboidal cells surrounding connective tissue stroma containing permeable capillaries (Johansson, 2014). Adjacent ChP epithelial cells are joined by tight junctions, forming the blood-CSF barrier (Lun et al., 2015). The ChP forms early in development from the neuroepithelial cells that line the ventricles and can be first detected in mice at E11.5-E12.5 (Johansson, 2014). Each ventricular ChP is essential in regulating the internal environment of the brain via the blood-CSF barrier, and secretion and modulation of CSF as soon as they first appear during development (Liddelow et al., 2010). The fact that neural development occurs after the development of the ChPs points to the significance of these structures and the need to elucidate their role in CSF production and ultimately neurogenesis.

Recent studies have in fact shown that the ChPs produce and secrete growth factors that promote neuronal differentiation (Sawamoto et al., 2006; Huang et al., 2010). For example, deletion of Shh from the hindbrain ChP using a $Wnt1^{Cre}$ resulted in more than 50% decrease in the proliferation of NPs within the nearby cerebellum (Huang et al., 2010). This work revealed for the first time, that the ChPs act as potential modulators of Wnt-signaling in the developing

brain through the production of CSF fluid. Furthermore, CSF flow has been shown to promote neuronal migration (Sawamoto et al., 2006). This suggests that signaling molecules secreted from the ChPs into the CSF, which is in direct contact with NP populations in both the embryonic and adult brain, may regulate neurogenesis. However little research to date has placed focus on this structure, and more evidence is needed to confirm a direct link between altered ChP secretion and subsequent alterations in developmental neurogenesis.

Regulation of neurogenesis via molecules produced and/or secreted from the ChPs into the CSF could have potentially far-reaching ramifications for the understanding and treatment of both developmental disorders and pathological conditions (Falcao et al., 2012; Silva-Vargas et al., 2013; Baruch et al., 2014). The advancement of scientific techniques has enabled tremendous progress in our understanding of the role CSF plays in neurodevelopment, and more work needs to be done on the elusive ChPs and their inevitable role in neurogenesis.

1.2.3. The Hippocampus

The hippocampus is a critical structure of the limbic system and plays an important role in memory formation, especially the transformation of short-term memory to long-term memory (Anand and Dhikav, 2012). Also known as the archicortex, the phylogenetically oldest region of the brain, it is located at the caudomedial edge of the neocortex deep within the medial temporal lobe (Murray et al., 2018). The developed hippocampus forms a 'C' shape along its longitudinal axis, with the transverse axis divided into distinct fields. From proximal to distal, these fields are the DG, the CA3 and CA1 fields of Ammon's horn (referred to as the hippocampus proper) and CA2 the small transitional field. Each temporal lobe of the cerebral cortex contains the hippocampal formation, located along the medial portion of the lateral ventricle's inferior horn (Daugherty et al., 2016).

The DG is a separate structure, consisting of granule cells tightly packed in a laminated manner, wrapping around the end of the hippocampus proper (Amaral et al., 2007). The tri-synaptic circuit is the information pathway, whereby granule cells of the DG send their axons, termed mossy fibers, to CA3, followed by pyramidal cells of the CA3 sending their axons to CA1, while pyramidal cells of CA1 in turn send their axons to the subiculum and deep layers of the entorhinal cortex. The CA areas are filled with densely packed Pyramidal cells similar to those found in the neocortex (Scharfman, 2007; Van Strien et al., 2009; Mizuseki et al., 2011).

Entorhinal Cortex and the Tri-Synaptic Circuit

Information enters this one-way loop via the axons of the entorhinal cortex. These axons make the first connection with the granule cells of the DG. The second connection is established by the projection of mossy fibers to the dendrites of the pyramidal cells in the CA3 region (Caruana et al., 2012). The axons of these cells divide into two branches. One branch forms the commissural fibers that project *via* the corpus callosum to the contralateral hippocampus. The other branch forms the Schaffer collateral pathways, establishing the third connection in the loop with the cells in the CA1 region (Caruana et al., 2012). Lastly the axons of the cells in CA1 region project to neurons of the subiculum and the entorhinal cortex (O'Mara, 2005; Caruana et al., 2012). The connection of the ventral-medial neocortex to the hippocampus completes a tri-synaptic circuit which involves the DG, also known as the receiving portion of the hippocampus, and the subiculum, also known as the sending portion (Lee et al., 2010; Caruana et al., 2012; Kohara et al., 2014).

Formation of the Hippocampus

The CH, adjacent to the hippocampal primordia, expresses several members of the Wnt and BMP gene families (Furuta et al., 1997). These gene families encode secreted proteins

implicated in patterning and growth of adjacent structures (Grove et al., 1998; Subramanian et al., 2009). Mounting evidence confirms that the CH is involved in proper development and expansion of the caudomedial margin from which the hippocampus develops (Grove et al., 1998; Lee et al., 2000; Subramanian et al., 2009; Caronia-Brown et al., 2014). For example, Takada and colleagues (1994) found that mice lacking functional expression of *Wnt3a*, the earliest identified Wnt gene selectively expressed in the CH, displayed truncated morphology in the hippocampi. Furthermore, molecular markers of the developing hippocampal CA fields and DG are absent in the *Wnt3a* homozygous mutants. By contrast, the neighboring neocortex and telencephalic ChP appear to be relatively unaffected (Takada et al., 1994; Lee et al., 2000). Therefore, functional *Wnt3a* expression in the CH appears to be required for hippocampal development. In addition, observations in the *XtJ* mouse established a clear role of Wnt signaling in the expansion of hippocampal progenitors, with reduced NP pools detected in the homozygous *XtJ* mutant (Galceranet al., 2000; Lee et al., 2000; Fotaki et al., 2011; Hasenpusch-Theil et al., 2012).

Definitive evidence that the CH induces hippocampal fate came from an analysis of *Lhx2* null chimeric embryos and the effects of ectopic hems (Mangale et al., 2008). Specifically, Mangale et al. observed development of multiple hippocampal fields adjacent to each patch of ectopic hem tissue, recapitulating the normal spatial relationships of the CH and hippocampal formation. Together, these findings demonstrate that the CH acts as a hippocampal organizer and is sufficient to induce the specification of the hippocampal fields (Grove, 2008; Mangale et al., 2008).

Furthermore, graded expression of transcription factors is known to be important in telencephalic development, particularly the very early expression patterns of *Emx2* and *Pax6*.

Kimura et al. analyzed embryo mutants of *Emx2* and *Pax6*, in the background of heterozygous *OTX* mutants. They reported that these compound mutants are unable to develop the entire caudal telencephalic midline region, including the CH and the ChP (Kimura et al., 2005). A similar result is seen in embryos that are null for *Emx2* and lacking one copy of *OTX2* (Kimura et al., 2005). Together this data proves the CH is necessary and sufficient to induce hippocampal fields in the cortical primordium (Galceran et al., 2000; Lee et al., 2000; Mangale et al., 2008).

Development of the Hippocampus

Development of the DG begins around E12.5 in a complex process that involves the migration of proliferative progenitors away from the dentate neuroepithelium (DNE), the primary matrix, located between the hippocampal neuroepithelium and the CH (Guérout et al., 2014; Urbán and Guillemot, 2014). From a developmental point of view this is a unique process, as the formation of fated DNE precursors migrate inward, away from their sites of origin, to generate a subventricular zone (SVZ) of proliferating cells. At E14.5, CH-derived CR cells aid these precursors to begin migrating toward the pial side of the cortex to form the secondary matrix (Seri et al., 2004; Urbán and Guillemot, 2014). At this time, radial glial precursors begin to form hippocampal neurons in the adjacent hippocampal neuroepithelium. At E17.5 the hippocampal fissure is formed where dentate precursors accumulate to form the tertiary matrix (Seri et al., 2004; Urbán and Guillemot, 2014). CR cells in addition to the glial scaffold, which extends form the CH to the hippocampal fissure and pial surface, both play essential roles in migration and organization of dentate precursor cells and granule neurons (Hodge et al., 2013; Sugiyama et al., 2013). Hippocampal neurons are born and migrate along radial glial cells toward their location in the hippocampal CA fields. During DG development precursors from all three matrices produce granule cells that form the outer-granule cell layer (gcl) (Sugiyama et al.,

2013; Urbán and Guillemot, 2014). The continued proliferation and upward migration of immature granule cells contributes to the inner-gcl ultimately forming the DG in an outside-in manner (Mathews et al., 2010; Yamada et al., 2015). At birth, the characteristic blade shape of the DG forms, dictated by CR cells. Granule neurons in the DG appear first in the upper blade below the hippocampal fissure, while continuous migration of CR cells promotes the formation of the lower blade (Amaral et al., 2007). Precursors in the primary and secondary matrix soon disappear, restricting proliferation to the tertiary matrix or subgranular zone (SGZ) during postnatal DG development (Alvarez-Buylla and Lim, 2004; Sugiyama et al., 2013; Urbán and Guillemot, 2014).

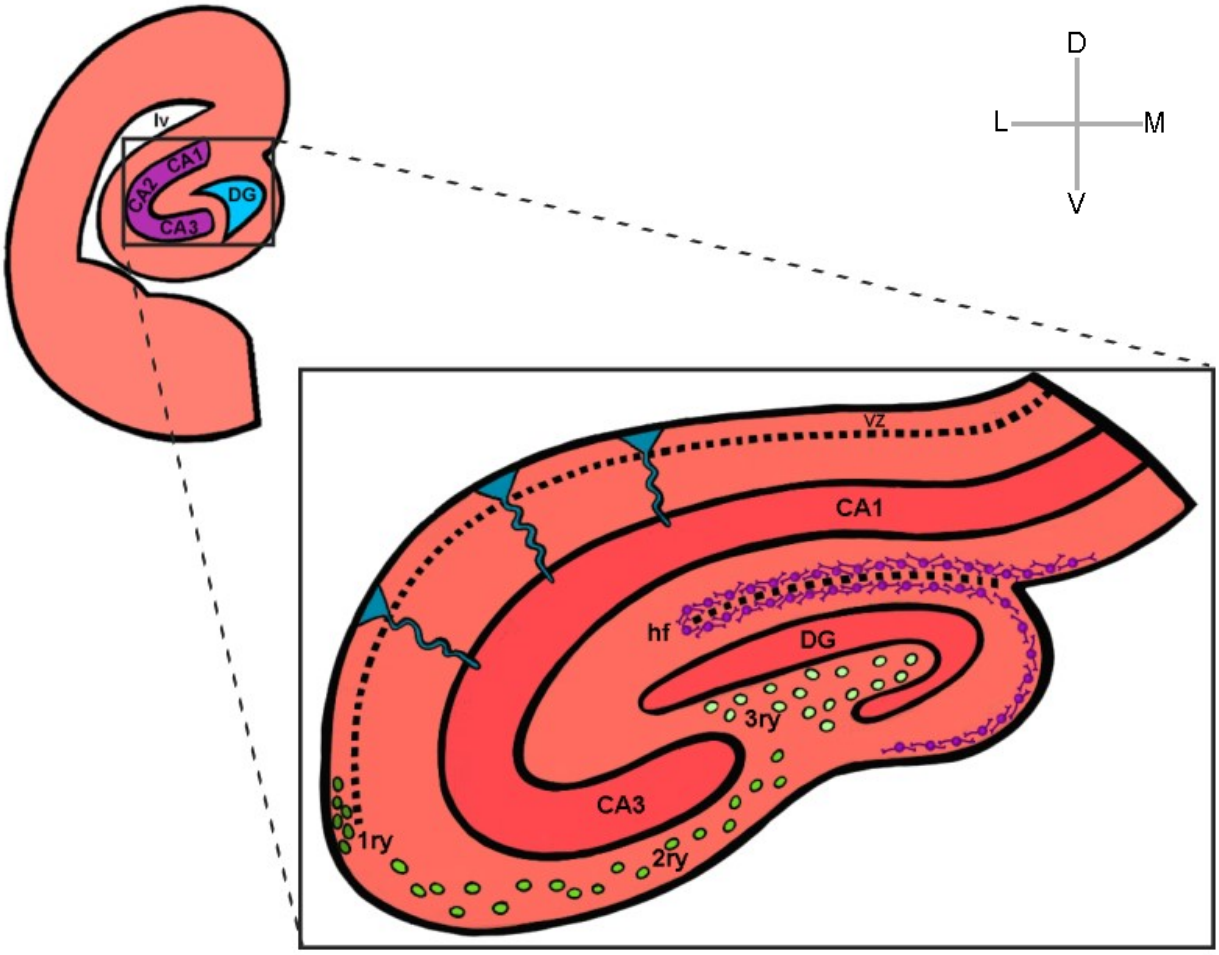

Figure 1.4. Graphic representation of the mouse hippocampus anatomy at birth. At birth, the blades of the DG begin to form. Granule cell neurons in the DG begin to first appear in the upper blade below the hippocampal fissure. The continuous migration of CR cells promotes the formation of the lower blade of the DG. Precursors cells of the primary and secondary matrix soon disappear, while cells of the tertiary matrix continue to actively divide and produce granule neurons throughout postnatal DG development. Cortical hem derived Cajal-Retzius cells (purple) are present and follow the hippocampal fissure. Abbreviations: CA1, Cornu Ammonis 1; CA3, Cornu Ammonis 3; DG, Dentate Gyrus; D, Dorsal; hf, hippocampal fissure; L, Lateral; M, Medial; V, Ventral; VZ, Ventricular Zone; 1ry, Primary Matrix; 2ry, Secondary Matrix; 3ry, tertiary matrix.

Hippocampal Neurogenesis

Traditionally it was believed that neurogenesis in the mammalian CNS occurred only during embryonic stages. However, it has more recently become generally accepted that new neurons are added in discrete regions of the adult mammalian CNS specifically the SVZ of the rostral migratory stream and the subgranular zone (SGZ) of the DG of the hippocampus (Kempermann and Ehninger, 2008; Ming and Song, 2011). Mechanisms and structures that support the proliferation and neuronal differentiation of multipotent NPs within the SVZ and SGZ is an area of intensive investigation. The finding that neurogenesis occurs within these two regions was facilitated by methodologies that allow for labeling of dividing cells. Altman and colleagues published a series of papers reporting evidence for new neurons in various regions of adult rats, including the DG of the hippocampus (Altman and Das, 1965) and olfactory bulb (Altman, 1969) through the use of radioactive [H3]-thymidine labeling. The field was revolutionized by the introduction of Bromodeoxyuridine (BrdU), a synthetic thymidine analogue (Gratzner, 1982; Taupin, 2007). In this technique, exogenous nucleotides such as BrdU are incorporated into newly synthesized DNA during the S-phase of the mitotic process and then passed on to cell progeny. This technique allows quantitative analysis of proliferation, differentiation, and survival of newborn cells through variation of injection and examination time points (Taupin, 2007). BrdU can be detected with immunohistochemistry and allows both phenotypic analysis and stereological quantification of new cells (Gratzner, 1982; Taupin, 2007).

Adult neurogenesis was observed with BrdU incorporation in all mammals examined, including samples from human patients (Eriksson et al., 1998). Combined retroviral-based lineage tracing and electrophysiological studies provided the most irrefutable evidence so far that

newborn neurons in the adult mammalian CNS are indeed functionally and synaptically integrated (Ge et al., 2008; Aimone et al., 2010; Braun and Jessberger, 2014).

Our understanding of adult neurogenesis in mammals, regarding location and fate specification of NPs, has progressed significantly over the past decade. Definitive evidence supports a neurogenic lineage within the hippocampus, as progenitors move through a series of transitionary cell types, ending in the formation of the mature functionally integrated neuron (Pleasure et al., 2000; Ambrogini et al., 2004; Zhao et al., 2006; Kempermann et al., 2015). The transition through these unique cell morphologies can be divided into individual stages, outlined below.

Stage I: Type-1 Radial-Glia Like Neural Progenitors

The putative NPs of the SGZ are known as a Radial-Glia-Like (RGL) cells as they share several astrocytic features. These cells can be identified by their distinct morphology such as the long apical process that extends into the gcl where it branches sparsely until it reaches the inner molecular layer, dispersing into many small processes. In addition to the vascular end-feet, these cells express the classical astrocytic marker Glial Fibrillary Acidic Protein (GFAP) (Seri et al., 2001; Bushong et al., 2004; Bonaguidi et al., 2012). Typical of NPs, RGL cells in the DG are mostly quiescent, and divide asymmetrically to self-renew and generate one immediate progenitor cell (Seri et al., 2001). With regard to the self-renewal capacity of hippocampal NPs, it was reported that they can only divide asymmetrically, in limited consecutive divisions before turning into inert astrocytes (Bonaguidi et al., 2012). Another study has shown that under certain circumstances RGL cells can also increase in number via symmetrical divisions (Seri et al., 2001; Bonaguidi et al., 2012). RGL cells provide the scaffolding necessary for the normal development of the DG. In addition to GFAP expression, they are also characterized by the

expression of Nestin and Sox2. RGL type-1 cells make up approximately two-thirds of the Nestin expressing cells in the SGZ in the adult mouse (Moss et al., 2016).

Stage II - III: Type-2a and Type-2b Transiently Amplifying Progenitor Cells

The next stage in the neurogenic lineage of the hippocampus involves the transition from type-1 to type-2 cells (Pleasure et al., 2000; Ambrogini et al., 2004; Zhao et al., 2006). These highly proliferative cells possess short processes that are oriented tangentially, with an irregularly shaped nucleus. They can be divided into two subtypes, 2a and 2b, based upon their expression of specific molecular markers; type-2a are characterized by expression of Nestin, and Sox2, while type-2b cells express Nestin, Sox2, and NeuroD1 (von Bohlen Und Halbach, 2007; Hodge and Hevner, 2012; Kempermann et al., 2015).

Stage IV: Type-3 Neuroblasts

The type-3 cells display a rounded or slightly triangular nucleus and exhibit the greatest changes in morphology with a progressive increase in the expression of neuronal markers. By the end of this stage the cells are vertically oriented with a clearly identifiable apical dendrite. Neuroblasts can be characterized by expression of NeuroD1, Prox1 and PSA-NCAM (von Bohlen Und Halbach, 2007; Hodge and Hevner, 2012).

Stage V: Immature Granule Cell

At this early post-mitotic stage, the cells retain their vertical orientation, with a rounded or slightly triangular nucleus and the identifiable apical dendrite (Llorens-Martín et al., 2016). It is hypothesized that this is when the new cells send out their axonal projections along mossy fiber pathways to the CA3 pyramidal cell layer. In addition, their dendrites orient in the opposite direction toward the molecular layer. Axonal contact in the target region CA3 has been found as early as 3-5 days after division (Scharfman, 2007; Amaral et al., 2007). Immature granule cells

can be further characterized by the expression of NeuN, NeuroD1, and Prox1 (Brandt et al., 2003; Gao et al., 2009; Iwano et al., 2012).

Stage VI: Mature Granule Cells

In the final stage, the dendritic arborization of the immature post-mitotic neurons increases sequentially until they become indistinguishable from the surrounding mature granule neurons (Van Praag et al., 2002; Jessberger and Kempermann, 2003; Kempermann et al., 2004). Calbindin is found in all mature granule cells, at which point these neurons establish their place in hippocampal circuitry receiving inputs from the entorhinal cortex and sending outputs to the CA3 and hilus regions (O'Mara, 2005; Lledo et al., 2006; Ge et al., 2008). Mature granule cells can be further characterized by expression of NeuN (Van Praag et al., 2002; Brandt et al., 2003; Jessberger and Kempermann, 2003).

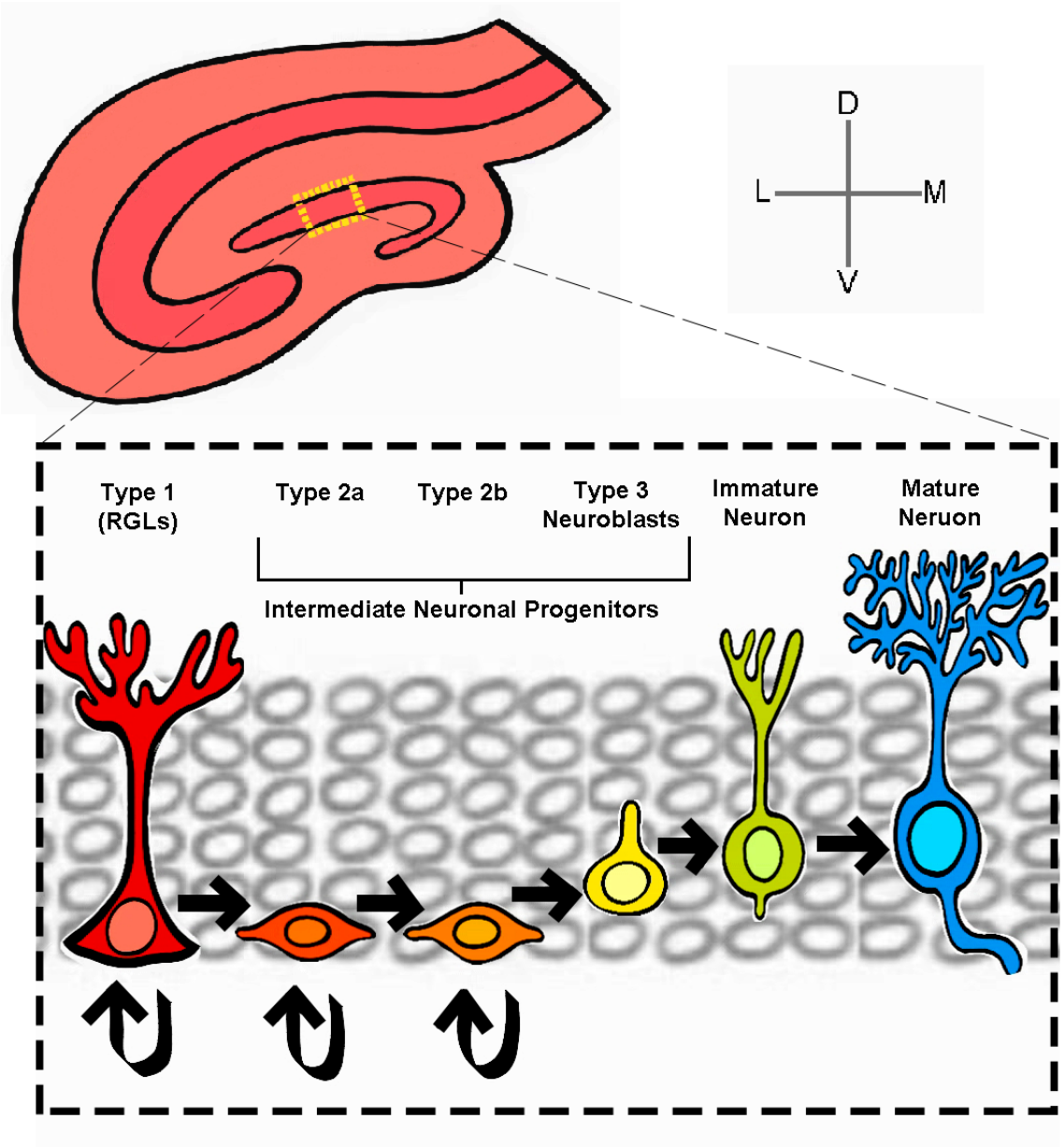

Figure 1.5. Schematic depiction of hippocampal neurogenesis. Enlarged view of the subgranular zone of the dentate gyrus depicting the developmental process of hippocampal neurogenesis. Type-1 radial glia-like neural progenitors rapidly give rise to intermediate neuronal progenitors, with type-1 and type-2 (a, b) cells maintaining the potential for self-renewal and amplification. Type-3 neuroblasts exit the cell cycle to mature into new-born neurons, ultimately integrating into existing neural networks as mature granule cells.

The demonstration of active adult neurogenesis opens possibilities in the near future of repairing the adult CNS after injury or degenerative neurological diseases through cell replacement therapy. Mounting evidence continues to illuminate the role of adult born neurons and their potential role in neurodegenerative disease and cognitive decline. Alterations in adult neurogenesis appear to be a common hallmark in different neurodegenerative diseases including Alzheimer's disease (Jin et al., 2004; Boekhoorn et al., 2006; Lazarov and Marr, 2010), Parkinson's disease (Höglinger et al., 2004; van den Berge et al., 2011; Marxreiter et al., 2013) and Huntington's disease (Curtis et al., 2003; Phillips et al., 2005; Fedele et al., 2011).

Phenotypic analysis of newborn cells requires examination of the colocalization of the cell-type specific markers. Developing neurons express distinct cell markers during their maturation process, which are outlined in Table 1.

Table 1. Transcription Factors Associated with Cortical Hem Derivatives.

Transcription Factor	Function	Reference
LIM Homeobox 2 (Lhx2)	Control the formation of the cortical hem and maintain its neuroepithelial stem cells in a proliferative mode	Bulchand et al., 2001 Roy et al., 2014
Empty Spiracles Homeobox 2 (Emx2)	Specifies the formation of the hippocampal primordia	Tole et al., 2000 Zhao et al., 2006
Tumor Protein P73	Expressed in the cortical hem, Cajal-Retzius cells, and the choroid plexus	Meyer et al., 2002 Talos et al., 2010
Reelin	Extracellular glycoprotein regulating neuronal migration	Pappas et al., 2002 Marín et al., 2010
Nerve Growth Factor Receptor (P75)	Nerve growth factor receptor stimulates neuronal cells to survive and differentiate	Spuch and Carro, 2011 Meier et al., 2019
Orthodenticle Homeobox 1 and 2 (OTX1/2)	Critical regulator of choroid plexus development	Larsen et al., 2010 Johansson et al., 2013
Paired box protein 6 (Pax6)	Type-1 and Type-2a cells	Maekawa et al., 2005 Hodge et al., 2013
Sex determining region Y-box 2 (Sox2)	Type-1 and Type-2a cells	Ferri et al., 2004 Favaro et al., 2009
Glial Fibrillary Acidic Protein (GFAP)	Type III intermediate filament protein expressed in astrocytes	Catalani et al., 2002 Choi et al., 2016
Neurogenic Differentiation 1 (NeuroD1)	Type-2b, Type-3 and immature neurons	Roybon et al., 2009 Gao et al., 2009
T-box brain protein 1 (Tbr1)	Immature neurons and mature neurons	Englund et al., 2005 Roybon et al., 2009
Prospero Homeobox protein 1 (Prox1)	Type-3 cells, immature and mature neurons	Lavado et al., 2010 Iwano et al., 2012
Calbindin	Calcium-binding protein expressed in mature granule cell neurons	Karadi et al., 2012 Li et al., 2017
Neuronal Nuclei (NeuN)	Marker of post-mitotic neurons	Wang et al., 2015 Lin et al., 2016

1.3. Mixed Lineage Leukemia Translocated to Chromosome 11

The objective of my thesis was to explore a role for Mllt11/Af1q (Myeloid/lymphoid or mixed-lineage leukemia; translocated to chromosome 11/All1 Fused Gene from Chromosome 1q) in regulating development of CH derivatives and hippocampal neurogenesis. Mllt11 was initially defined as an oncogenic factor identified in acute myeloid leukemia patients carrying the t(1;11)(q21;q23) translocation, creating a protein fused to M11 (Tse et al., 1995). Mllt11 is a novel vertebrate-specific protein that possesses a nuclear export signal, but otherwise has poorly defined functional domains. Numerous studies to date have described that aberrantly elevated *Mllt11* expression is a poor prognostic marker, commonly found in aggressive hematologic malignancies and solid tumors (Chang et al., 2008; Park et al., 2015).

Despite evidence for a role in oncogenesis, work from our laboratory and that of others, has identified Mllt11 as a potential novel regulator of neurogenesis, being highly and exclusively expressed in post-mitotic neurons during development and enriched in the developing cortical plate and hippocampal forming regions of the forebrain (Yamada et al., 2014). Lin and colleagues (2004) reported that *Mllt11* expression is up-regulated in differentiated cortical neurons, and its ectopic expression in embryonic kidney cells triggers the expression of neuronal markers. Specifically, Lin et al. reports that the ectopic expression of *Mllt11* is able to trigger the expression of the neuronal marker *TuJ1* in non-neuronal HEK cells, indicating that intact wild-type *Mllt11* may play a role in neuronal differentiation during CNS development (Lin et al., 2004).

Furthermore, a more recent report has identified a correlation between the Repressor Element 1 Silencing Transcription Factor (REST), also known as Neuron-Restrictive Silencer Factor (NRSF) and Mllt11 (Hu et al., 2015). REST is regulated differentially throughout

development, with high expression in pluripotent embryonic stem cells and minimal levels in multipotent NPs. Precise timing of NP differentiation is contingent upon differential REST levels, acting as a negative regulator of gene expression in both embryonic and adult neurogenesis (Hu et al., 2015). This critical role is supported by mounting evidence reporting that REST overexpression in differentiating neurons blocks migration and greatly delays neural differentiation by interfering with neural gene expression, ultimately resulting in axon guidance errors (Mandel et al., 2011; Mozzi et al., 2017). In contrast to the disappearance of expression in differentiating neurons, REST expression is reported to increase progressively in the nuclei of cortical and hippocampal neurons in healthy aging adults (Baldelli and Meldolesi, 2015). Specifically, REST promotes up-regulation of protective genes and the down-regulation of genes related to neural degeneration (Lu et al., 2014; Mozzi et al., 2017).

Hu and colleagues (2015) demonstrate that REST is a key transcriptional factor participating in the down-regulation of *Mllt11* gene expression through direct binding to a neuron-restrictive silencer element at -383 to -363 bp of human *Mllt11* promoter. Importantly, the expression of REST and *Mllt11* are negatively correlated during neurodevelopment, implying that the activation of *Mllt11* expression may be essential for neurogenesis (Hu et al., 2015). However, there has yet to be a published study examining the role of Mllt11 *in vivo.*

In addition to a potential function of Mllt11 during neurogenesis, its potential role in neuronal maintenance and neurodegeneration is unknown. One study detected down-regulated genes in sporadic, non-SOD1 linked ALS through gene-based analysis of microarray data (Lederer et al., 2007). Of the depleted promoters, there was a group of genes, including *Mllt11*, involved in neurodifferentiation and axonal/dendritic maintenance with clear implications for a role in neuronal survival (Lederer et al., 2007).

1.4. Rationale for the Establishment of a Conditional *Mllt11* Mutant Mouse

An exciting development in the field of adult neurogenesis is the generation of animal models that allow visualization and specific manipulation of newborn neurons in the adult CNS. These approaches may allow manipulation of a specific population of adult-generated neurons in a temporally and spatially precise manner for mechanistic and functional analysis of adult neurogenesis *in vivo.*

One of the most widely used genetic strategies in the field of neurodevelopment is the classical Cre/LoxP recombination system (Kim et al., 2018). This system enables cell- or tissue-specific control of Cre expression by unique gene promoters. Cre-expressing mice are in turn mated with mice containing a floxed gene of interest bearing the LoxP recognition sequences, forming a transgenic conditional mouse line in which recombination is under the control of a promoter.

In this study, I utilize a $Cux2^{IRESCre/+}$ driver line to generate a conditional *Mllt11* knockout from a floxed allele. Cut-like transcription factor 2 (Cux2) is a novel discriminatory marker for neurogenic progenitors. Previous work from our lab shows that Cux2 is required for neurogenesis in the developing spinal cord and olfactory epithelium (Iulianella et al., 2014). Additional studies have implicated Cux2 in the regulation of cortical pyramidal neuron formation form SVZ progenitors (Zimmer et al., 2004; Cubelos et al., 2008; Franco et al., 2012). While more recently, our lab reported that Cux2 is expressed in the developing CH at E14.5 and its activity defines non-self-renewing neural progenitors in the SGZ from E14.5 onwards, which contributes to the formation of gcl neurons in an outside-in manner (Yamada et al., 2015). Interestingly, Lmx1a, a critical regulator of cell-fate decisions within the telencephalic CH region, was recently identified as a positive regulator of the Cux2 CH enhancer and is both

necessary and sufficient for Cux2 activation in the Dorsal Telencephalic Midline (DTM) (Fregoso et al., 2019). The Cux2 locus is therefore well-suited to explore gene function during both development of the CH derivatives and hippocampal neurogenesis. For this reason, I employed the *Cux2*$^{IRESCre/+}$ driver line to inactivate *Mllt11* in the CH and developing hippocampus using a *Mllt11*$^{flox/flox}$ mouse line.

I created a *Cux2*$^{IRESCre/+}$*; Mllt11*$^{flox/flox}$ conditional mouse knockout (cKO) line by intercrossing the *Cux2*$^{IRESCre/+}$ driver with the *Mllt11* floxed allele. Furthermore, I combined these alleles with the *Rosa26*$^{tdTomato/tdTomato}$ reporter mouse line to monitor the activity of the *Cux2*$^{IRESCre/+}$driver. The Cre/LoxP strategy has contributed significantly to the understanding of neurodevelopment and gene function (Madisen et al., 2010). Using this conditional inactivation strategy, this thesis work has illuminated the role of *Mllt11* in Cux2-expressing cells within the developing CH derivatives and hippocampal neurogenesis.

1.5. Hypothesis and Objectives

Fundamental questions that remain at the forefront of neurodevelopment concern the acquisition and maintenance of cell diversity and how establishment of connections between neural networks is achieved. In addition, a more contemporary paradigm shift has occurred in regard to the view of plasticity and stability of neurons in the adult brain, with adult neurogenesis gaining more acceptance. This study aims to improve our understanding of the development of CH derivatives and hippocampal neurogenesis, and to delineate any function *Mllt11* may play. The three main derivatives assessed in this study include CR cells, the ChP, and the hippocampus. In addition, further analysis of perinatal and postnatal hippocampal neurogenesis is evaluated.

The molecular and cellular mechanisms involved in the development of the CH and its derivatives remain largely unknown. Similarly, while our understanding of the regulation of neurogenesis has progressed markedly within the last two decades, the mechanism underlying the transition from fetal to postnatal hippocampal neurogenesis remains unclear. Further research is required to reveal how the formation and migration of CH derivatives, including the hippocampus, is regulated. This study aims to look at the roles of *Mllt11* as a critical regulator of the development of these DTM structures using a conditional knockout approach.

Hypothesis: The hypothesis I addressed here is whether *Mllt11* gene function is required for the development and migration of CH derivatives, and hippocampal neurogenesis. To achieve this, immunofluorescence microscopy was carried out on embryonic and postnatal brains derived from mice lacking *Mllt11* and compared to wild-type littermate controls.

To address this hypothesis, I pursued the following objectives:

1. Create a conditional *Mllt11 cKO* allele using the $Cux2^{IRESCre/+}$ driver combined with the $Rosa26^{tdTomato}$ reporter. This will remove Mllt11 in the CH region and developing hippocampus.
2. Examine the role of Mllt11 in the development of the CH and its derivatives: the ChP and CR cells.
3. Elucidate the role of Mllt11 in perinatal hippocampal neurogenesis.

This thesis study will further our understanding of the roles for Mllt11 during the development of DTM structures and hippocampal neurogenesis. The findings reported here has implications for our understanding of the cellular and molecular mechanisms that lead to neurodevelopmental disorders and offers insights in the development of therapeutic approaches for neuronal injury and neurodegeneration.

CHAPTER 2. MATERIAL AND METHODS

2.1. Generation of Mice

Construct inserted into the 3' untranslated region (3'UTR) of exon 3 of *Mllt11* in a C57 background. Crossed with flpO mouse to excise the extraneous LoxP site to flox exon 3. Crossed with $Rosa26^{tdTomato}$ reporter line maintained in an FVB background to generate $Mllt11^{flox/flox}$;$Rosa26^{tdTomato}$. I utilized a $Cux2^{IRESCre/+}$driver line previously described by Yamada et al., 2014. This line contains an internal ribosome entry site (IRES) and nuclear localized Cre recombinase targeted to the 3'UTR region of the Cux2 locus. $Cux2^{IRESCre/+}$ maintained in a C57 background was then crossed into tdTomato reporter line, maintained in FVB background to generate $Cux2^{IRESCre/+}$; $Rosa26^{tdTomato/tdTomato}$. This line was then crossed with $Mllt11^{flox/flox}$; $Rosa26^{tdTomato/tdTomato}$ to generate $Cux2^{IRESCre/+}$; $Rosa26^{tdTomato/tdTomato}$; $Mllt11^{flox/+}$ to be backcrossed with $Mllt11^{flox/flox}$; $Rosa26^{tdTomato/tdTomato}$ or $Mllt11^{flox/+}$; $Rosa26^{tdTomato/tdTomato}$. All experiments were performed with $Cux2^{IRESCre/+}$; $Rosa26^{tdTomato/tdTomato}$; $Mllt11^{+/+}$ as the wild-type control or **WT**, and $Cux2^{IRESCre/+}$; $Rosa26^{tdTomato/tdTomato}$; $Mllt11^{flox/flox}$ as the conditional knockout or **cKO**. See figure below (Figure 2.1) for workflow used to establish the experimental mouse line.

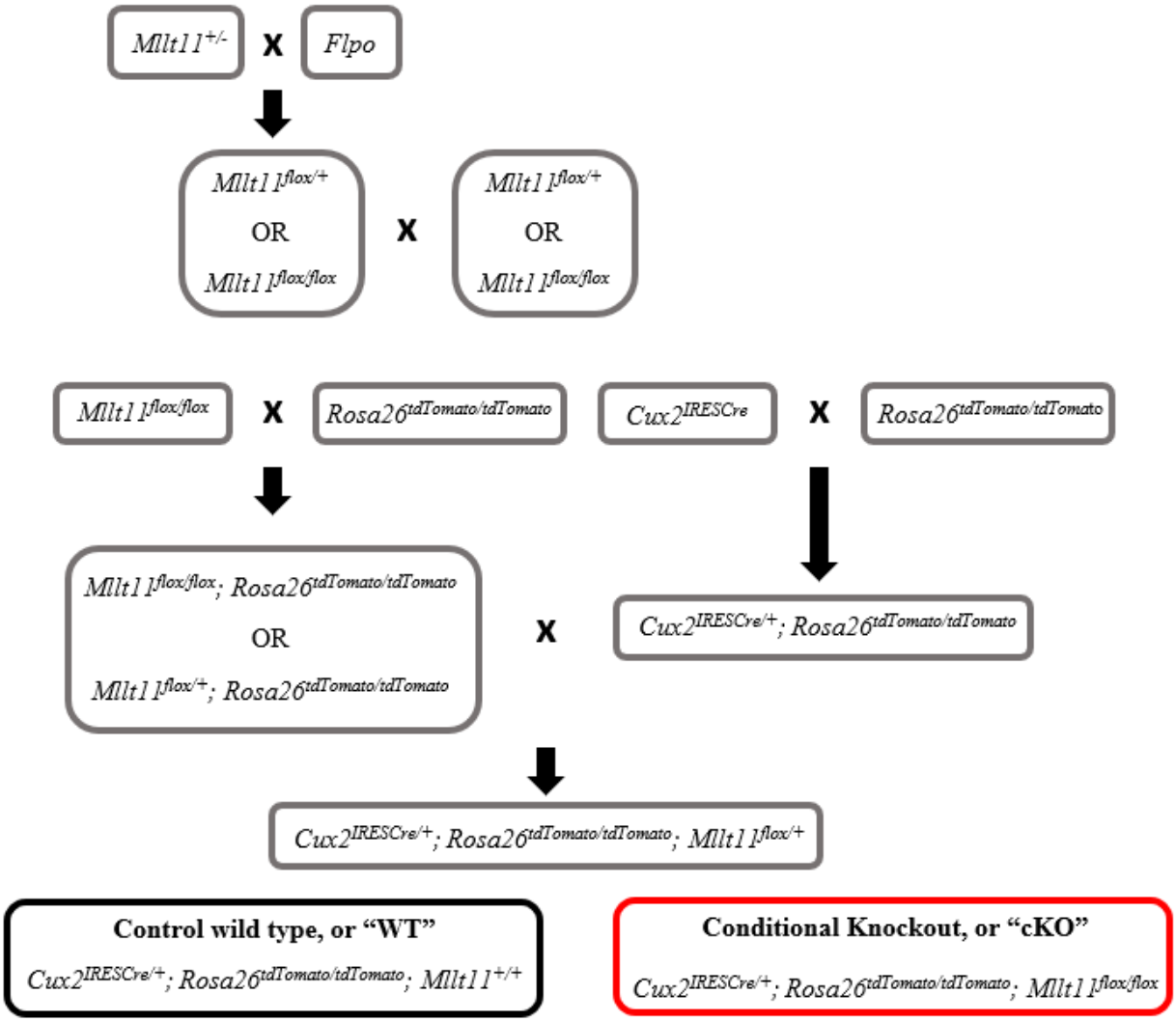

Figure 2.1. Workflow used to generate *Mllt11* conditional knockout mouse strain.

2.2. Preparation of Tissues

Timed matings of C57BL/6 (The Jackson Laboratory, Bar Harbor, ME) mice were conducted to obtain whole brains at embryonic day (E)12.5, E14.5, E16.5, E18.5, postnatal day (P)7, P14, and 6 weeks after birth, for a comprehensive analysis, with noon of the day of vaginal plug taken to represent 0.5 post conception (E0.5). For embryonic stage analysis pregnant dams were sacrificed by cervical dislocation and litters were harvested at the stages described above, while for postnatal stages litters were anesthetized by intraperitoneal injection of 100µl of 4:1 Ketamine:Xylazine. In the absence of foot-retraction reflex, an abdominal incision was made to expose the diaphragm. The thoracic cavity was accessed to reveal the heart using two lateral incisions, allowing the ribcage to be retracted. A cannula made from a 23-gauge hypodermic needle attached to a perfusion pump was inserted in the aorta via the left ventricle. The right atrium was cut allowing clearing of the blood from circulation. Perfusion with PBS was followed by perfusion with PBS and 4% paraformaldehyde (PFA). Whole brains were fixed in 4% PFA (0.1m phosphate buffer) at 4C for 2 hours to overnight depending on the embryonic or postnatal stage. This was followed by 3 x 10 minutes washes in PBS and cryoprotection in 15% and then 30% sucrose. Once equilibrated, whole brains were embedded and snap frozen in Optimum Cutting Temperature compound (O.C.T.; Tissue-Tek, Torrance, CA) and stored at -80C°. This study was approved by the Dalhousie animal ethics committee and the animals were handled in accordance with the institutional regulations and guidelines of the Canadian Council on Animal Care.

2.3. Immunohistochemistry

Coronal sections were cut at 12μm using a Leica CM1850 cryostat with sections placed onto superfrost slides (VWR, Radnor, PA). Ten slides were mounted at a time to allow for multiple axial levels to be captured on each slide. At least three animals were sectioned and analyzed for each embryonic stage. Sections were permeabilized with a wash in PBS+ 0.5% TritonX100 (PBT) for 10 minutes and subsequently blocked in 5% Donkey Serum in PBS for 1 hour at room temperature. This was followed with overnight incubation with primary antibodies in blocking buffer, extensive washing with PBS and 1-hour incubation with secondary antibodies in blocking buffer at room temperature. Secondary antibodies were rinsed with PBS and the nuclei were counterstained with DAPI (4'6-diamidino-2-phenylindole; Sigma, St. Louis, MS) for 5 minutes at room temperature followed by a final PBS wash and coverslips mounted with Dako Fluorescent Mounting Medium. Multiple axial levels were analyzed per animal and images were captured using a Zeiss AxioObserver fluorescence microscope equipped with an Apotome 2 illumination device.

The following primary antibodies were used: rabbit anti-Calbindin (1:1000, Abcam), mouse anti-NeuN (1:500, Millipore, Temecula, CA), rabbit anti-OTX1/2 (1:500, Abcam), mouse anti-ZO1 (1:100, Invitrogen), rabbit anti-p73 (1:500, Abcam), conjugated mouse anti-Reelin488 (1:500, Sigma), rabbit anti-Pax6 (1:500, Hybridoma), mouse anti-Ki67 (1:25, R+D Biosystems), goat anti-Sox2 (1:200, Santa Cruz), mouse anti-NeuN (1:200, Millipore), goat anti-NeuroD1 (1:300, Santa Cruz), rabbit anti-Tbr1 (1:200, Millipore), goat anti-Nestin (1:200, Santa Cruz), rabbit anti-p75 (1:200, Abcam), rabbit anti-Prox1 (1:1000, Sigma), mouse anti-Calretinin (1:500), rabbit anti-MLLt11 (1:50), rabbit anti-Cleaved Caspase (1:500), rabbit anti-GFAP (1:500, Abcam). Secondary antibodies were used at 1:1500 included donkey anti-rabbit Alexa-

Fluor 647, donkey anti-rabbit Alexa-Fluor 488, donkey anti-goat Alexa-Fluor 647, donkey anti-mouse 647 (Invitrogen). Images were captured from multiple axial levels from each animal to ensure analyses were being completed throughout the DTM region of the brain.

2.4. EdU (5-ethynyl-2´-deoxyuridine) *in vivo* Labeling

10 mM EdU solution was prepared in DMSO and administered via intraperitoneal injection into dams. EdU was dosed at 30mg/kg body in a solution of 10mg/ml PBS (pH 7.35). A series of time points for injection and harvesting were used for full assessment of CH derivatives. Including: dose at E14.5 harvest at E18.5, dose at E16.5 harvest at E18.5 and finally dose at E18.5 harvest at P14. Detection of proliferative cells is based on a copper catalyzed covalent reaction between an azide and an alkyne. In this application the alkyne is found in the ethynyl moiety of EdU while the azide used is coupled to Alexa-Fluor 647 or Alexa-Fluor 488 dyes.

EdU staining was conducted using Click-iT EdU imaging kit according to the manufacturer's protocol (Invitrogen). The immunohistochemistry protocol was adapted such that EdU staining was performed before the addition of the primary antibody. EdU Click-iT reaction cocktail containing Click-iT reaction buffer, CuSO4, Alexa Fluor 647 or 488 Azide, and reaction buffer additive for 30 minutes. The slides were rinsed with 3 x 10 minutes PBS before adding the primary antibody.

2.5. Sampling Methodology

To ensure consistency among samples, cell counts obtained at E18.5, P7, P14 and 6 weeks after birth, were restricted to a total of 10 counting frames (50µm x 50µm) randomly placed on the entire DG starting from the midline to the lateral end of the DG according to systematic-random sampling method (Mouton, 2002). The base of each counting frame was adjusted to align along the lower edge of the SGZ to ensure cells within the hilus region were not included in counts. A total of 40 coronal sections were obtained from 3-4 separate individuals at 12 µm thickness obtained from WT or cKO mice at E18.5, P7, P14 and 6 weeks. Analysis of the SVZ and the ChP stalk at E12.5 and E14.5 was conducted similarly with counting frames of 50µm x 50µm. Cells positively labeled with each IHC marker were counted within the $50\mu m^2$ frame using ImageJ (FIJI) (Schindelin et al., 2012). To analyze DG thickness, equivalent coronal sections were selected and examined from each littermate control and conditional *Mllt11* cKO mutant animal and repeated for a total of 10 mice. Measured values were averaged to create one representative value for each animal. A portion of the DG with uniform thickness was selected as a rectangular area of interest. The area was then divided by the length of the rectangular area with the thickness calculated from the proximal areas to the crest where the two blades connect (Watanabe et al., 2016). Analysis of the density of ZO-1 staining of the ChP at E14.5 was assessed using features found in FIJI. From these measurements, population averages of WT and cKO mice were compared. Images were captured using a Zeiss AxioObserver inverted fluorescent microscope with x20 and x40 oil objectives and Apotome2 Structural Illumination. Montages were assembled using Photoshop CS6.

2.6. Statistical Analysis

All statistical analyses were performed using PRISM. Statistical significance was obtained by performing unpaired t-tests to compare the means and standard deviations between the control data set and the experimental data set. In all quantification studies, statistical differences were challenged using the Student's t-test (two-tailed), with significance level set at $P \leq 0.05$ (*$P \leq 0.05$, **$P \leq 0.01$, ***$P \leq 0.001$, ****$P \leq 0.0001$). For all experiments, a minimum of 3 WT and 3 cKO individuals were analyzed and cells counts were reported as an average analysis (n identifies the number of individuals per WT and cKO data set). Cell counts were performed blinded to genotype to avoid potential counting bias. Data was presented as Scatter plots, with each point representing an individual with results presented as mean ± SEM.

CHAPTER 3. RESULTS

3.1. *Mllt11* Expression in the Embryonic and Adult Brain

Mllt11 is a pan-neuronal marker, expressed in post-mitotic neurons in the developing marginal zone of the cortex and spinal cord (Yamada et al., 2014). In addition, transcription of *Mllt11* is reported to be up-regulated during neurogenesis (Lin et al., 2004) and down-regulated by RE1 silencing transcription factor, a key factor involved in regulating neural differentiation (Hu et al., 2015). Preliminary work from our lab reports a role for Mllt11 in regulating cortical specification and localization within the maturing cortical plate, possibly by regulating dynamic cytoskeletal processes.

The initial step in this study was to provide an expression profile of *Mllt11* in the adult hippocampus by *in situ* hybridization (ISH) experiments on control C57BL/6 mice over a series of postnatal time points. I report high levels of *Mllt11* mRNA expression at P7 throughout the DG and hippocampus proper, with tapered levels by P28 (Figure 3.1. A-D). NP cells exist throughout life, restricted to the SGZ of the DG. Between P0 and P14 the majority of neurons are born, and the resulting mature granule neurons of the DG consolidate to form axonal connections targeting neurons in the CA region of the hippocampus (Yasuda et al., 2011). The early postnatal period is critical for the generation of the adult NP pool, with neurogenesis declining exponentially over time (Ben Abdallah et al., 2010; Encinas et al., 2011). These critical time periods coincide with the enriched levels and duration of *Mllt11* expression seen in the results of the ISH.

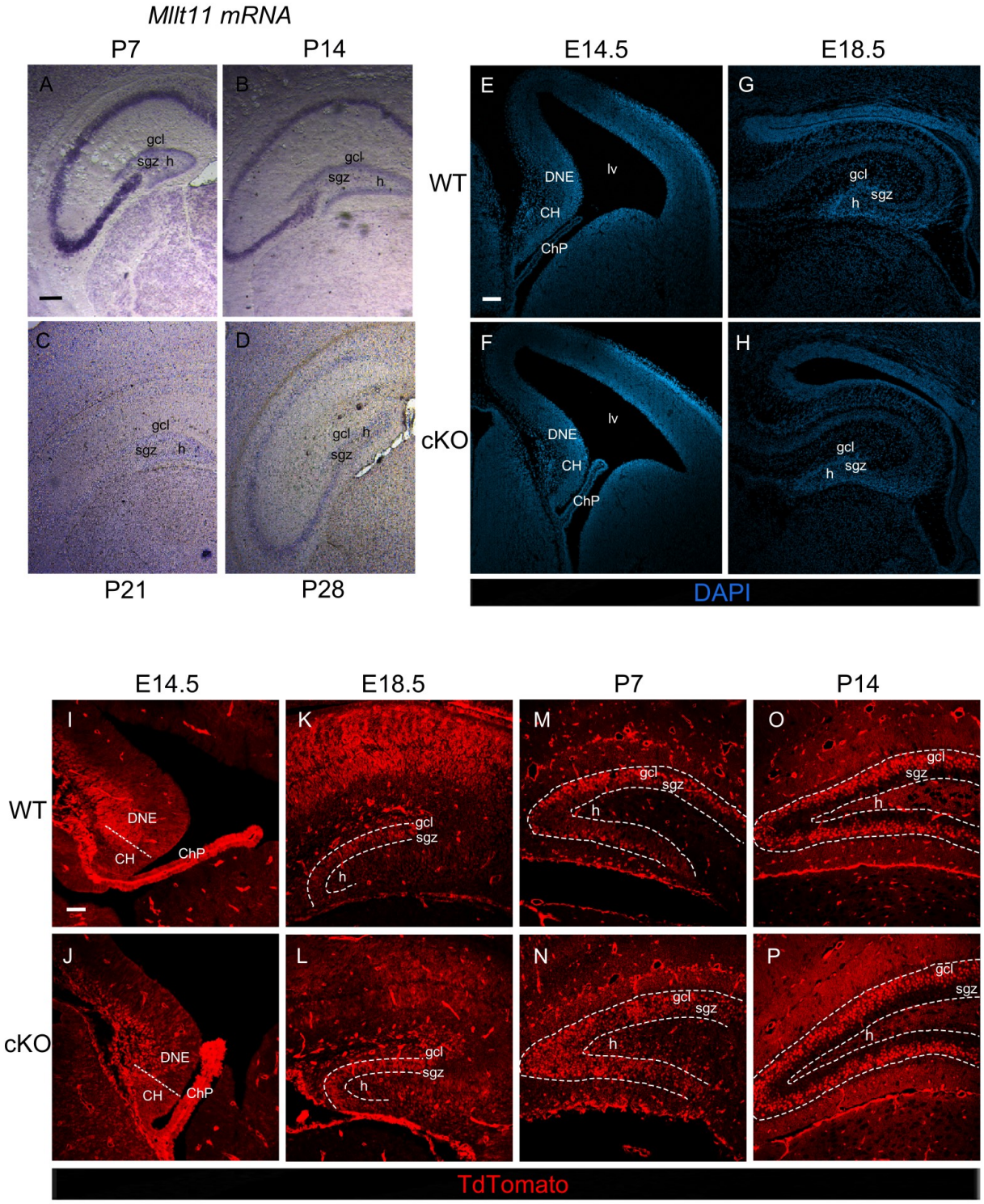
Mllt11 mRNA
P7
P14
E14.5
E18.5
A
B
E
G
gcl
sgz
h
WT
DNE
lv
CH
ChP
C
D
F
H
cKO
P21
P28
DAPI
E14.5
E18.5
P7
P14
I
K
M
O
J
L
N
P
TdTomato

Figure 3.1.

Figure 3.1. *Mllt11* expression profile in the embryonic and adult brain.

(A- D) Images show *in situ* hybridization staining in coronal tissue sections of C57BL/6 mice at P0, P14, P21 and P28. *Mllt11* mRNA expression detected at high levels in the DG and CA regions of the hippocampus with highest levels during peak neurogenesis P0, dissipating by P28. Scale bar = 50µm. (E-F) DAPI staining in the DTM at E14.5 in WT and *Mllt11* cKO mouse. Note the truncated structure of the ChP in the cKO. Scale bar = 100µm. (G-H) DAPI staining of a dorsal DG from an E18.5 cKO mouse. Scale bar = 100µm. (I-P) Coronal sections of forebrains from WT vs cKO embryos showing tdTomato (red) fluorescence as a readout for recombination. Top panel: coronal section from WT control mouse; bottom panel: coronal section from a comparative cKO mouse. (I, J) E14.5: Highest levels of tdTomato labeling occurred within the developing ChP. (K, L) E18.5: Recombination throughout the developing hippocampus, and most prominently in the developing DG. (M, N) P7: DG displayed highest tdTomato labeling in the gcl. (O, P) P14: tdTomato labeling in the gcl of the DG. Highest levels of labeling occurred in the ol, with occasional low levels in the SGZ. Scale bar = 50µm. Abbreviations: DG, dentate gyrus; DTM, dorsal telencephalic midline; DNE, dentate neuroepithelium; CH, cortical hem; ChP, choroid plexus; gcl, granule cell layer; ol, outer layer; SGZ, subgranular zone; h, hilus.

The expression of *Mllt11* mRNA throughout the embryonic and adult hippocampus suggested a role in the formation and/or maintenance of this structure. I therefore decided to generate an *Mllt11* cKO to assess its role during hippocampal neurogenesis. Given that the hippocampus is ultimately derived from the CH region, I also explored its role in the development of the DTM. I utilized a Cre/LoxP strategy to generate a $Cux2^{IRESCre/+}$ driven *Mllt11* cKO. Cux2 is dynamically expressed in complex spatiotemporal patterns within the developing mouse forebrain and developing CH and hippocampus (Zimmer et al., 2004; Yamada et al., 2015). This makes the $Cux2^{IRESCre/+}$ driver a suitable choice to inactivate *Mllt11* during forebrain development and hippocampal neurogenesis. Lineage tracing of tdTomato+ cells in $Cux2^{IRESCre/+};Rosa26^{tdTomato/tdTomato}$ brains from E14.5, E18.5, P7 and P14 revealed Cre activity within the DTM and hippocampus. Specifically, strong tdTomato activity was detected as early as E14.5 in the ventricular region of the medial telencephalon. This stage corresponds with the formation of the DG matrices and migration of hippocampal NPs from the germinal wall of the SVZ. Our lab previously characterized the activity of the Cux2 locus in SGZ progenitors and nascent granule cell neurons in the postnatal brain, revealing selective labeling of the forming DG in an outside-in manner (Yamada et al., 2015). For this thesis project, *Mllt11* WT vs cKO mice were analyzed at E14.5 when the DTM is reorganized into two distinct structures, the CH and the ChP epithelium, and followed through until postnatal day 14, when the bulk of hippocampal neurogenesis is underway.

An initial neuroanatomical assessment of *Mllt11* WT vs cKO was conducted utilizing a DAPI counterstain to reveal nuclear staining (Figure 3.1. E-H). The gross morphology of the CH at E14.5 (Figure 3.1. E-F) appeared largely normal, however a notable difference was observed in the length of the ChP stalk in the cKOs relative to the WT controls. No outward

morphological changes could be detected in the developing DG at E18.5 (Figure 3.1. G-H). At postnatal stages, cKO mice appeared normal in comparison to their WT littermates with the conditional mouse strain able to breed and maintain the transgenic line.

The *Cux2*$^{IREScre/+}$ driver removed the *Mllt11* gene in *Cux2*-expressing cells within the CH region and the developing hippocampus. The conditional strategy removed *Mllt11* while activating tdTomato expression, allowing for well-defined, fate labeled cells (Figure 3.1. I-P). Tomato fate labeling occurred early in the mouse fetus at stages corresponding to the formation of the dentate germinal matrices and migration of granule cell precursors from the germinal wall of the forebrain SVZ. At E14.5 the CH region was highly labeled by red fluorescent protein with significant labeling along the entire ChP stalk (Figure 3.1. I-J). By E18.5 the developing DG was well defined by tdTomato expression, localized principally in the SGZ region of the dentate knot (Figure 3.1. K-L). At postnatal stages, I found that the anterior hippocampus was highly labeled by red fluorescent protein. Specifically, at P7 and P14 (Figure 3.1. M-P), when postnatal neurogenesis is ongoing, tdTomato expression was limited to the gcl of the DG. By P14, tomato labeling progressed to encompass more granule cells of the DG, with a distinct band defining the outer-gcl.

3.2. Loss of *Mllt11* Results in Increased Dentate Gyrus Thickness

I next assessed whether there were any distinct morphological changes in the dentate blades of the developed hippocampus. I evaluated the dentate blades at P7, P14 and 6 weeks after birth, when dentate formation is complete and ongoing hippocampal neurogenesis is occurring. The yellow rectangle in Figure 3.2. A. provides a representation of how this calculation was conducted for each section. Interestingly, I report a significant increase in the dentate blade thickness within the cKO at all stages examined (Figure 3.2 A-I) (P7: p=<0.0001, n=10; P14:

p=<0.0001, n=10; 6Wks: p= 0.0357, n=3). However, no significant changes in total DAPI + cell numbers per 50μm^2 were observed (E18.5: p=0.4998, n=10; P7: p=0.6420, n=10; P14: p=0.1290, n=10) (Figure 3.2. J). There was also no increase in apoptosis made evident by unaltered levels of cleaved caspase-3 (E18.5: p=0.5277, n=4; P7: p=0.2764, n=4; P14: p=0.1127, n=4) (Figure 3.2. K). These findings suggest that *Mllt11* loss altered the cytoskeletal structure of the DG, resulting in thicker blades with no change in cell number. The next step in this study was to provide a more in-depth analysis of the developing CH region and its derivatives in the *Mllt11* cKO.

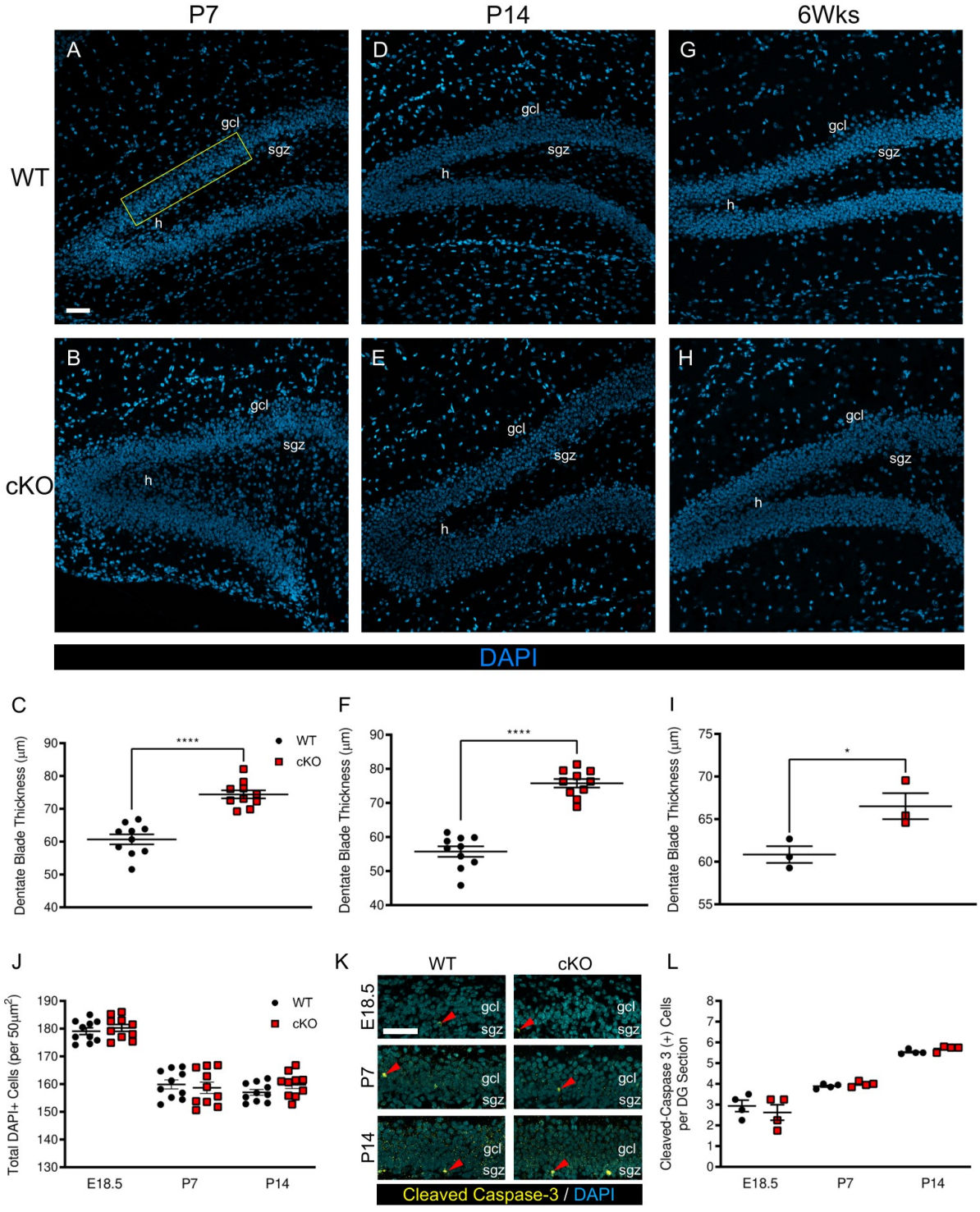
P7
P14
6Wks
WT
cKO
A
B
D
E
G
H
gcl
sgz
h
DAPI
C
F
I
Dentate Blade Thickness (μm)
WT
cKO
****
*
J
K
L
Total DAPI+ Cells (per 50μm²)
E18.5
P7
P14
Cleaved Caspase-3 / DAPI
Cleaved-Caspase 3 (+) Cells per DG Section

Figure 3.2.

Figure 3.2. *Mllt11* loss results in an increase in dentate gyrus thickness.

(A, B) DAPI stained coronal sections of dorsal DG at P7 in the WT and conditional cKO *Mllt11* mouse. Yellow box in (A) identifying representative region used for thickness calculation. (C) Scatter plot identifying a significant increase in DG thickness (μm) in cKO sections compared to WT controls ($P < 0.0001$; n=10). (D, E) DAPI stained coronal sections of dorsal DG at P14 in the WT and cKO. (F) Scatter plot identifying a significant increase in DG thickness (μm) in cKO sections ($P < 0.0001$; n=10). (G, H) DAPI stained coronal sections of dorsal DG at 6 weeks. (I) Scatter plot identifying a significant increase in DG thickness (μm) in cKOs relative to WTs ($P= 0.0357$; n=3). (J) Scatter plot showing no significant changes in total number of DAPI+ cells per $50\mu m^2$ at E18.5 ($P = 0.4998$; n=10), P7 ($P = 0.6420$; n=10) and P14 ($P = 0.1290$; n=10). (K) WT and cKO sections of DG at E18.5, P7, and P14 stained for cleaved caspase-3 (yellow) and counterstained with DAPI (blue) to assess cell death. Red arrowheads indicate co-stained cells. (L) Scatter plot showing number of cleaved caspase-3 positive cells per DG section analyzed. No significant changes were identified at E18.5 ($P = 0.5277$; n=4), P7 ($P = 0.2764$; n=4) and P14 ($P = 0.1127$; n=4). Quantification of data presented as mean ± SEM. Scale bars = 50μm**.**

Abbreviations: DG, dentate gyrus; gcl, granule cell layer; h, hilus; sgz, subgranular zone.

3.3. THE ROLE OF *Mllt11* IN THE FORMATION OF THE CORTICAL HEM AND CHOROID PLEXUS

3.3.1. *Mllt11* Loss Alters the Developing Dorsal Telencephalic Midline

The patterning of the cerebral cortex into distinct subregions begins early in development. As described in the Introduction, the CH region forms a specialized nexus at the tip of the pallial cortex that is enriched in signaling proteins and transcription factors that act to pattern telencephalon along into medial-lateral, and ventral–dorsal axes. This region is also the source of CR cells and supplies progenitors that fuel the development of the hippocampus.

I first assessed the role Mllt11 in the development of the CH region by examining the expression of transcription factors that play a role in patterning the telencephalic midline. One key transcription factor is Lhx2, which acts as a selector gene for cerebral cortical fate and plays a critical role in patterning the forebrain midline and CH (Monuki et al., 2001). Targeted disruption of *Lhx2* at E12.5 resulted in missing or extreme underdevelopment of the entire medial telencephalic neuroepithelium (Bulchand et al., 2001). Lhx2 is involved in the critical first step in patterning of the DTM, dividing it into the presumptive cortical neuroepithelium, and the CH. Loss of *Lhx2* disrupts this division and results in expansion of the CH at the expense of the cortical neuroepithelium (Roy et al., 2014). This makes Lhx2 an excellent candidate to assess the initial stages of CH development in the *Mllt11* cKO.

IHC was performed against Lhx2 to identify any initial differences in the division of the developing DTM (Figure 3.3. A-B). I reported an elevated number of Lhx2+ cells at E14.5 within the SVZ in the *Mllt11* cKO when compared to the WT controls ($p=0.0004$; $n=6$) (Figure 3.3. C). Since Lhx2 is critical in establishing accurate division of the DTM, I then assessed

whether there were any notable changes specifically in the CH region. By analyzing the transcription factor OTX1/2, a known regulator in CH development. I noted that the CH area, outlined by the hatched yellow line, was significantly smaller in the *Mllt11* cKO in comparison to the control (p=0.0033; n=6) (Figure 3.3 D-F). As the CH is a critical signaling center in the formation of various forebrain derivatives, I suspect that the increase in Lhx2+ cells and the minor changes in CH area may lead to changes in CH derived CR cells and development of the ChP.

3.3.2. *Mllt11* Loss Disrupts the Formation of Cortical Hem Derived Cajal-Retzius Cells

CR cells co-express p73, a regulator of cell survival and apoptosis, and the glycoprotein Reelin, a chemoattractant crucial for radial migration of newborn cortical pyramidal neurons (Meyer et al., 2002). I assessed coronal sections of the DTM at E14.5 when the CR cells line the pial surface of the SVZ and promote the migration of the dentate precursor cells and E18.5 when they have migrated out along the fimbrial radial glial scaffold and settled in the hippocampal marginal zone to aid in the formation of the dentate blades. Interestingly, I report a significant and transient decrease in the number of p73+/Reelin+ cells at E14.5 (p=0.0001, n=5) with a with no significant difference by E18.5 (p=0.1280, n=4) (Figure 3.3. G-L).

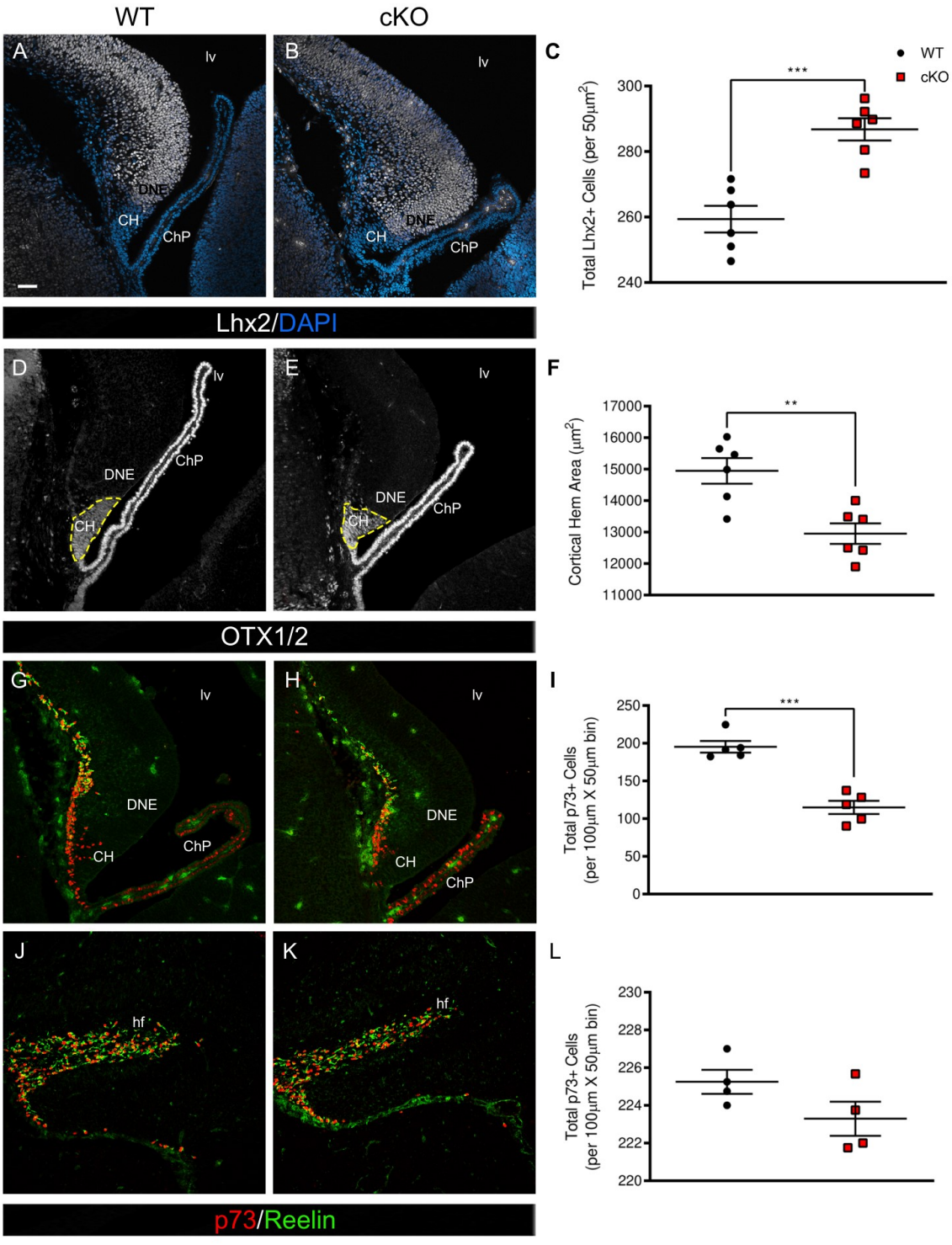
WT
cKO
A
B
lv
DNE
CH
ChP
Lhx2/DAPI
C
WT
cKO
***
Total Lhx2+ Cells (per 50μm²)
300
280
260
240
D
E
F
**
Cortical Hem Area (μm²)
17000
16000
15000
14000
13000
12000
11000
OTX1/2
G
H
I
***
Total p73+ Cells (per 100μm X 50μm bin)
250
200
150
100
50
0
J
K
L
hf
230
228
226
224
222
220
p73/Reelin

Figure 3.3.

Figure 3.3. *Mllt11* loss alters development of dorsal telencephalic midline structures.
(A, B) Coronal sections of DTM region at E14.5 WT vs *Cux2*$^{IRESCre/+}$driven *Mllt11* cKO stained for Lhx2 (white) counterstained with DAPI (blue). (C) Scatter plot identifying the total number of Lhx2+ cells per 50μm^2. A significant increase was reported in the cKO relative to WT controls (P = 0.0004; n=6). (D, E) Coronal sections of DTM region at E14.5 WT vs. cKO stained for OTX1/2 (white) to identify the CH region. (F) Scatter plot identifying the total CH area in μm^2. A significant decrease is observed in the CH area in the cKO in comparison to WT controls (P = 0.0033; n=6). (G, H) Coronal sections of DTM region at E14.5 WT vs cKO stained for p73 (red) and Reelin (green). (I) Scatter plot identifying the total number of p73+/Reelin+ cells per 50μm X 100μm. A significant decrease was identified in the cKOs in comparison to WT controls (P= 0.0001; n=5). (J, K) Coronal sections of hf region at E18.5 WT vs. cKO stained for p73 (red) and Reelin (green). (L) Scatter plot identifying the total number of p73+/Reelin+ cells per 50μm X 100μm. No significant difference was observed in cKOs (P= 0.1280; n=4). Scale bars= 50μm. Quantification of data presented as mean ± SEM**.** Abbreviations: CH, cortical hem; ChP, choroid plexus; DNE; dentate neuroepithelium; DTM, dorsal telencephalic midline; hf, hippocampal fissure.

3.3.3. *Mllt11* Loss Decreased Choroid Plexus Stalk Length

With the reported decrease in CH area and the corresponding decrease in CH derived CR cells I expected to identify changes in the ChP, an additional derivative of the CH. I evaluated the ChP at E14.5 when development is at its peak, specifically evaluating the critical ChP regulator OTX1/2 (Johansson et al., 2013). The ChP stalk length was significantly shorter in the *Mllt11* cKO in comparison to the WT controls ($p=<0.0001$, $n=9$) (Figure 3.4. C). No significant difference in ChP stalk thickness was observed between control and cKOs ($p=0.0501$, $n=9$) (Figure 3.4. D). I found a clear difference in the distribution of cells *Mllt11* cKOs relative to WTs. Specifically, there was a progressive pattern of more OTX1/2+ cells being clustered at the base of the cKO ChP relative to the tip 350µm away from the base (Figure 3.4. E).

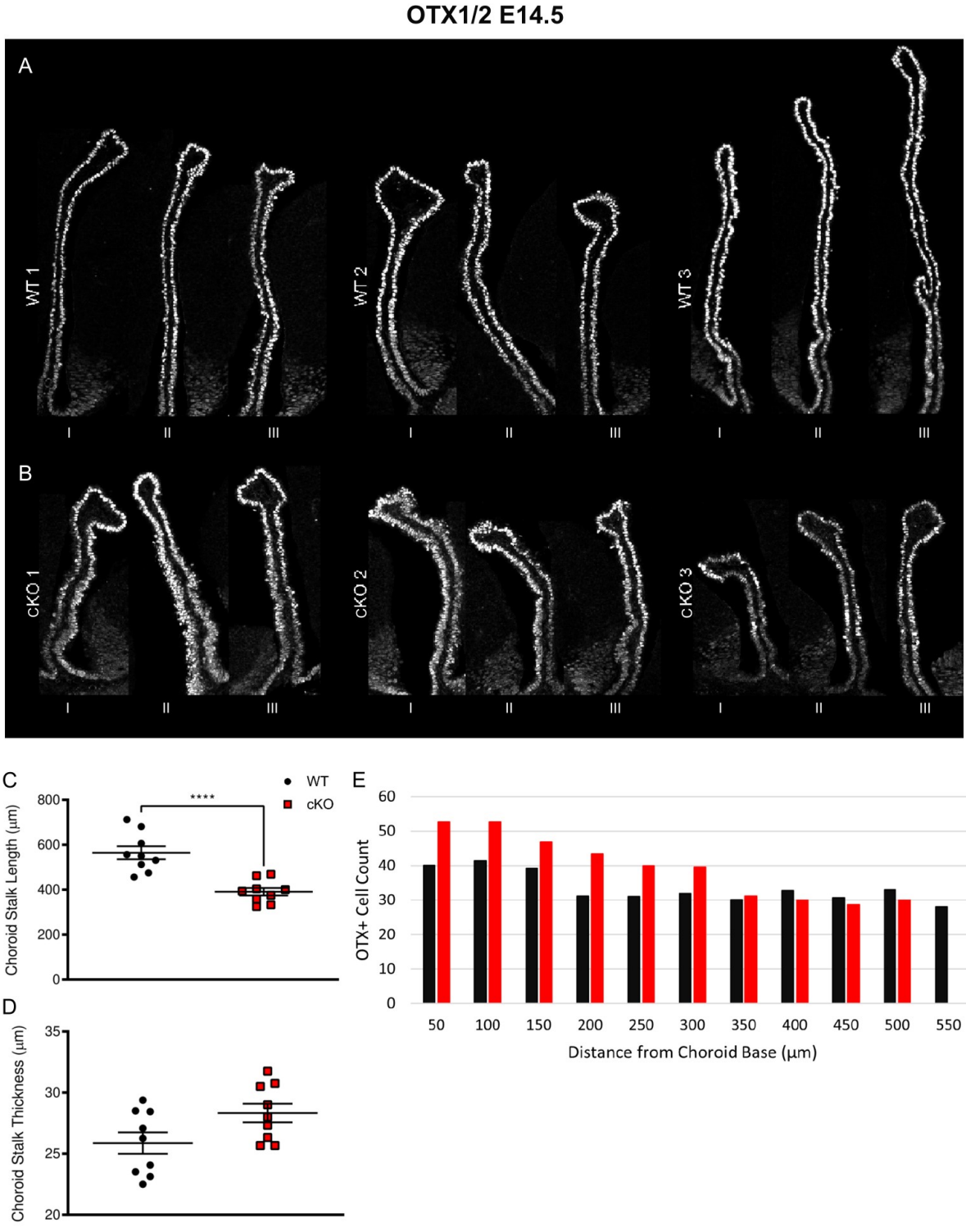
OTX1/2 E14.5
A
WT 1
WT 2
WT 3
I
II
III
B
cKO 1
cKO 2
cKO 3
C
WT
cKO
****
Choroid Stalk Length (µm)
800
600
400
200
0
D
Choroid Stalk Thickness (µm)
35
30
25
20
E
OTX+ Cell Count
60
50
40
30
20
10
0
50
100
150
200
250
300
350
400
450
500
550
Distance from Choroid Base (µm)

Figure 3.4.

Figure 3.4. *Mllt11* loss results in truncated telencephalic choroid plexus.

(A, B) Cross sections of telencephalic ChPs from WT and *Mllt11* cKO fetuses at E14.5 stained for OTX1/2 with three serial sections obtained from three different specimens. (C) Scatter plot identifying ChP stalk length in μm. Telencephalic ChP stalk length was significantly shorter in the cKOs relative to WT controls (P= <0.0001, n=9). (D) Scatter plot quantifying ChP stalk thickness in μm. cKO fetuses displayed no significant difference in ChP thickness relative to WT controls (P= 0.0501, n=9). (E) Bar chart quantifying total OTX1/2+ cells per 50μm^2, beginning at the base of the ChP stalk and counted in 50μm increments. Quantification of data presented as mean ± SEM. Abbreviations: ChP, Choroid Plexus.

3.3.4. *Mllt11* Loss Affected the Choroid Plexus Basement Membrane

Due to the apparent clustering of OTX1/2+ cells at the base of the ChP I next assessed the basement membrane structure of the ChP epithelium utilizing *Zona Occludens*-1 (ZO-1). ZO-1 is normally expressed in epithelial and endothelial cells and acts as a scaffold protein cross-linking and anchoring tight junctions (McNeil et al., 2006). I observed a significant increase in ZO-1 density (mean area covered) in the *Mllt11* cKO ChP relative to WT controls ($p=0.0164$, $n=3$). I noted a marked change in the typical stratified epithelial organization of the ChP in the cKOs, with mutant cells being positioned aberrantly along the width of the ChP (green arrowheads; Figure 3.5. B, D). It appears as though there is more bridging between the individual cells, indicated by the increased density of ZO-1 staining along the width of the ChP stalk (Figure 3.5. A-D).

3.3.5. *Mllt11* Loss Results in a Proliferative Defect in the Choroid Plexus

To assess whether the truncated ChP in the *Mllt11* mutants reflected a failure of OTX1/2 progenitors to migrate properly into ChP stalk, I exposed cKO and WT controls to a short pulse of EdU to label newly divided neuroepithelial cells contributing the ChP. I noted a significant decrease in the number of OTX1/2+/EdU+ cells in the cKOs relative to WT controls at E14.5 ($p=0.0148$, $n=3$) (Figure 3.5. E-J). Moreover, EdU-labeled newly formed cells rarely made it to the tip of the ChP stalk of the *Mllt11* mutants (green open arrow, Figure 3.5, H, J), suggesting that a migration defect underlies the shortened ChP phenotype in the mutants.

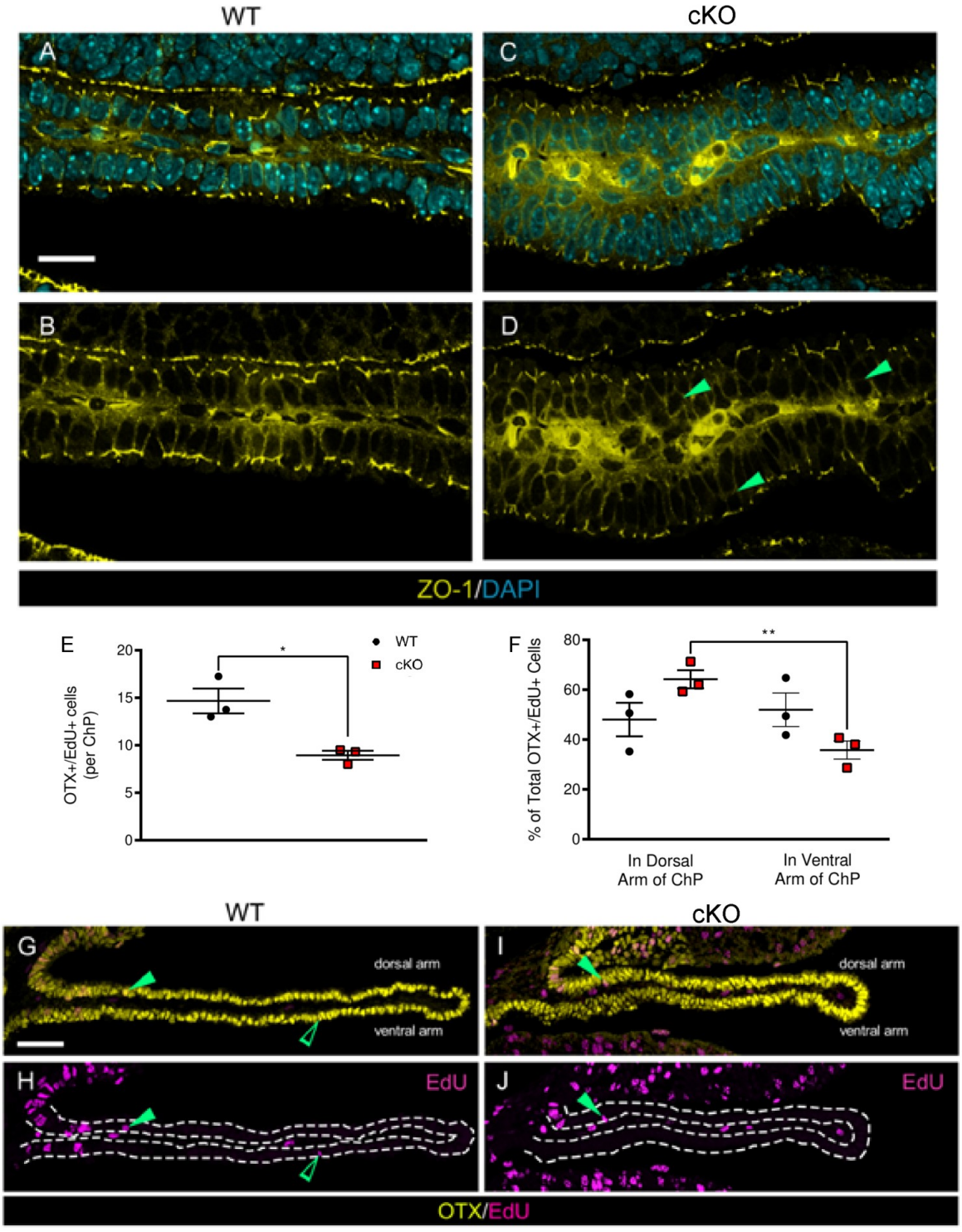
WT
cKO
A
C
B
D
ZO-1/DAPI
E
WT
cKO
OTX+/EdU+ cells (per ChP)
20
15
10
5
0
*
F
% of Total OTX+/EdU+ Cells
80
60
40
20
0
**
In Dorsal Arm of ChP
In Ventral Arm of ChP
WT
cKO
G
I
dorsal arm
ventral arm
H
J
EdU
OTX/EdU

Figure 3.5.

Figure 3.5. *Mllt11* loss alters the epithelial anatomy of the choroid plexus.
(A-D) Cross-sectional view of WT and *Mllt11* cKO telencephalic ChP stained for ZO-1 (yellow) and DAPI (blue). Green arrowheads (D) identify the disorganized placement of cKO ChP epithelial cells relative to the single cell layer organization of WT ChP. (E) Scatter plot identifying OTX1/2+/EdU+ cells per ChP stalk, reporting a significant decrease in cKOs (P= 0.0148, n=3). (F) Scatter plot identifying the percent total of OTX1/2+/EdU+ cells in the dorsal arm of the stalk and the ventral arm of the stalk, reporting a significant decrease in percent of OTX1/2+/EdU+ in the ventral arm of the cKOs relative to the dorsal arm (P= 0.0052, n=3). (G-H) Cross section of WT and cKO ChP strained for OTX1/2 (yellow) and EdU (violet). Solid and open green arrowheads identify OTX1/2+/EdU+ cells in the dorsal arm and the ventral arm of the stalk, respectively. Scale bar= 50μm. Quantification of data presented as mean ± SEM. Abbreviations: ChP, Choroid Plexus.

3.4. THE ROLE OF *Mllt11* IN HIPPOCAMPAL NEUROGENESIS

3.4.1. *Mllt11* Loss Enhanced Progression of Type-1 to Type-2a Progenitors

I assessed whether the development of hippocampal progenitor cells was dependent on *Mllt11* expression. I analyzed the maturation of progenitor cells of the DG in the embryonic and developing hippocampus (P7 and P14) when the population of differentiating progenitor cells is at its peak (Nicola et al., 2015; Yamada et al., 2015). IHC analysis of hippocampal neurogenesis repeated for a total of at least 3 mice within each the WT and cKO groups. My aim was to focus on both embryonic and postnatal aspects of the development of the DG and formation of the neurogenic niche in the SGZ in the cKO mouse model. To this end I performed all analyses at E18.5, P7 and P14 time points.

During the first stage of hippocampal neurogenesis, newly generated cells express the markers GFAP and Sox2 (Catalani et al., 2002). These putative NPs in the SGZ are thought to represent a subset of astrocytes that give rise to new granule cells (Seri et al., 2001). Interestingly I report a transient increase at E18.5 in the number of GFAP+/Sox2+ type-1 radial glial NPs ($p=0.0047$, $n=3$) (Figure 3.6. A-C). While in contrast at P7 and P14, I report a significant reduction in the number of GFAP+/Sox2+ type-1 radial glial NPs (P7: $p=0.0004$, $n=5$; P14: $p=0.0008$, $n=4$) (Figure 3.6. D-I). I also assessed the expression of Pax6, a radial glial NP maker which has been reported as necessary for the maintenance of the GFAP+ early progenitor cells in the SGZ. I report a significant increase in the number of Pax6+ cells at E18.5 ($p=0.0088$, $n=4$), a significant decrease at P7 ($p=0.0001$, $n=5$) and no significant change at P14 ($p=0.4157$, $n=5$) (Figure 3.8. A-I). Along with GFAP+/Sox2+ analysis, this suggest that *Mllt11* loss led to a transient burst in production of type-1 cells in the late fetal hippocampus, which is followed by a loss of type-1 cells within the first week of life.

I examined the role of Mllt11 in regulating the formation of type-2a NPs in the hippocampus, which are characterized by the expression of Sox2 and absence of GFAP (GFAP-/Sox2+). These type-2a cells represent a developmental state in which the transient amplifying cells differentiate into immature neurons in the SGZ. They are highly proliferative progenitors thought to commit to a neuronal lineage (Kempermann et al., 2015). *Mllt11* cKOs displayed a significant and transient increase in the number of GFAP-/Sox2+ type-2a cells at E18.5 ($p=0.0036$, $n=3$) and P7 ($p=0.0001$, $n=5$) with no significant difference at P14 ($p=0.1377$, $n=4$) (Figure 3.6. A-I). Importantly, these cells appeared to be unmoored with their radial glial processes failing to traverse the thickness from the hilus to maturing granule cells in the DG (Figure 3.6. J, L). The P7 *Mllt11* cKO hippocampus also showed expanded $Cux2^{IRESCre/+}$ fate mapped tdTomato+ cells, suggesting increased generation DG cells (Figure 3.6. M).

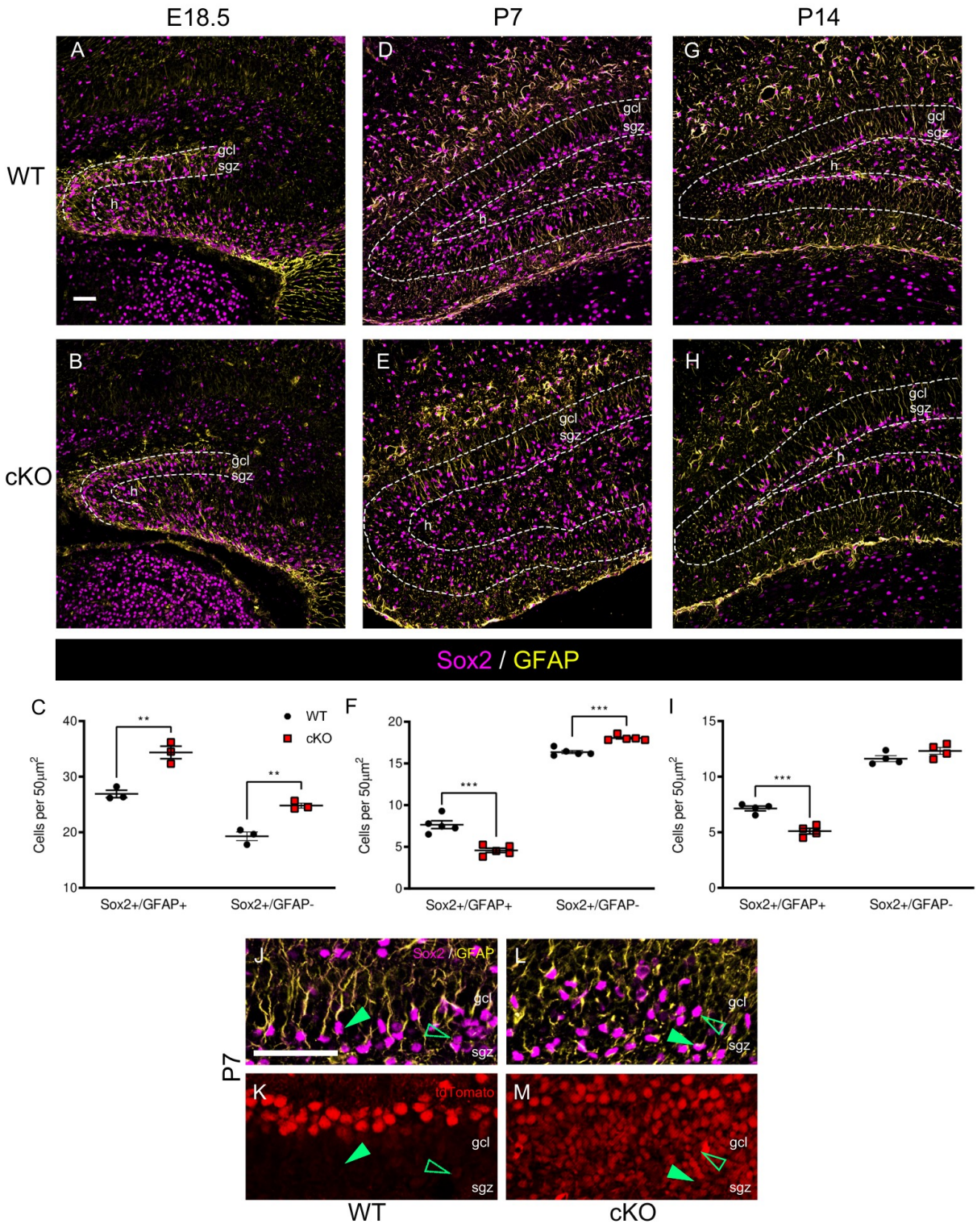
E18.5
P7
P14
WT
cKO
A
B
D
E
G
H
gcl
sgz
h
Sox2 / GFAP
C
F
I
WT
cKO
Cells per 50μm²
Sox2+/GFAP+
Sox2+/GFAP-
J
K
L
M
P7
tdTomato
WT
cKO

Figure 3.6.

Figure 3.6. *Mllt11* loss alters the formation of type-1 and type-2a cells.

(A, B) Coronal sections of the developing dk at E18.5 in the WT and *Mllt11* cKO mouse brain stained for Sox2 (violet) and GFAP (yellow). Sox2+/GFAP+ co-stain identifies type-1 cells and Sox2+/GFAP- cells identifies type-2a cells. (C) Scatter plot identifying a significant increase in both type-1 (P= 0.0047, n=3) and type-2a (P= 0.0036, n=3) cells in the embryonic dk region in cKOs compared to WT controls (D, E) Coronal sections of the dorsal hippocampus at P7 in the WT and cKO mouse stained for Sox2 and GFAP. (F) Scatter plot identifying significant decrease in type-1 cells (P= 0.0004, n=5) with a corresponding increase in type-2a cells (P= 0.0001, n=5). (G, H) Coronal sections of the dorsal hippocampus at P14 in the WT and cKO mouse stained for Sox2 and GFAP. (I) Scatter plot identifying significant decrease in type-1 cells (P= 0.0008, n=4) with no significant difference in type-2a cell numbers (P= 0.1377, n=4) in cKO sections compared to WT controls. (J-M) Magnified cross-sectional view of the DG identifying the SGZ and gcl of WT and cKO. Top panel stained for Sox2 (violet) and GFAP (yellow), lower panel identifying recombined tdTomato+ cells in the identical DG region. Solid arrowheads in (J-M) identify GFAP+/Sox2+ type-1 NP cells. Empty arrowheads in (J-M) identify type-2a NP cells. (K-M) tdTomato-fate mapped cells of the P7 DG did not localize with GFAP+ astroglia. (L. M) P7 *Mllt11* cKO displayed expanded GFAP-/Sox2+ NPs, and tdTomato-fate mapped cells. Scale bars = 50µm**.** Data presented as mean ± SEM. Abbreviations: dk, dentate knot; gcl, granule cell layer; h, hilus; SGZ, subgranular zone.

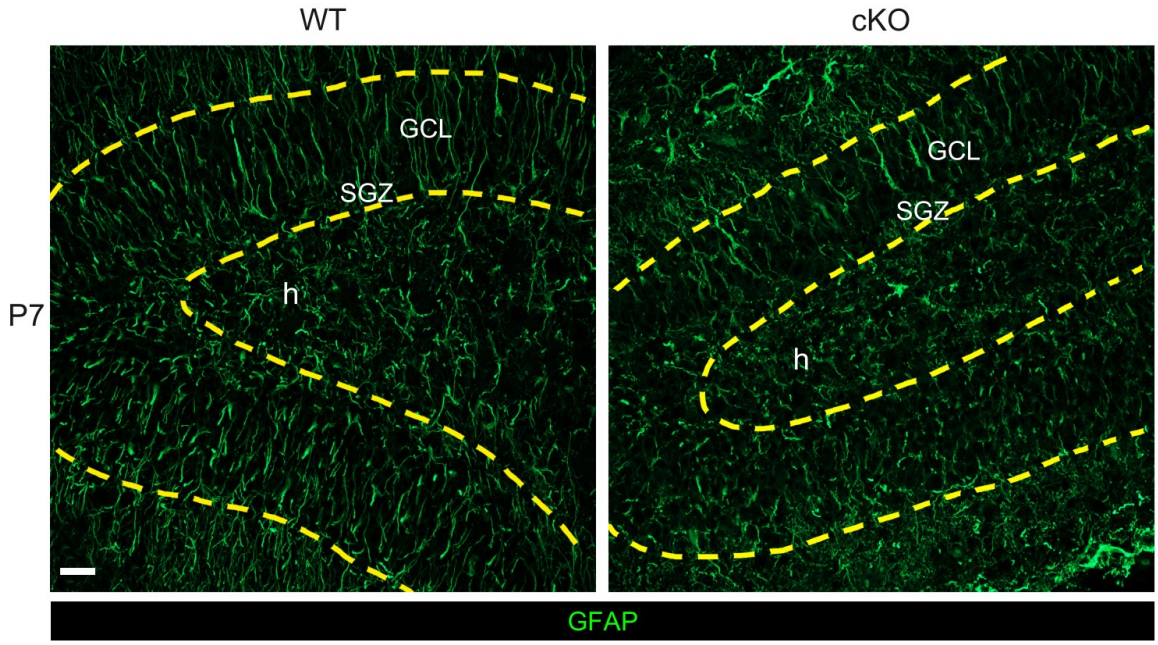

Figure 3.7. *Mllt11* loss alters radial glial fiber length and orientation.

Coronal sections of WT control and *Mllt11* cKO DG imaged at 40xOil magnification. GFAP staining identifying decreased expression and disorganized orientation of radial glial fibers in the cKO. Scale bar= 50μm. Abbreviations: DG, dentate gyrus; GCL, granule cell layer; h, hilus; SGZ, subgranular zone.

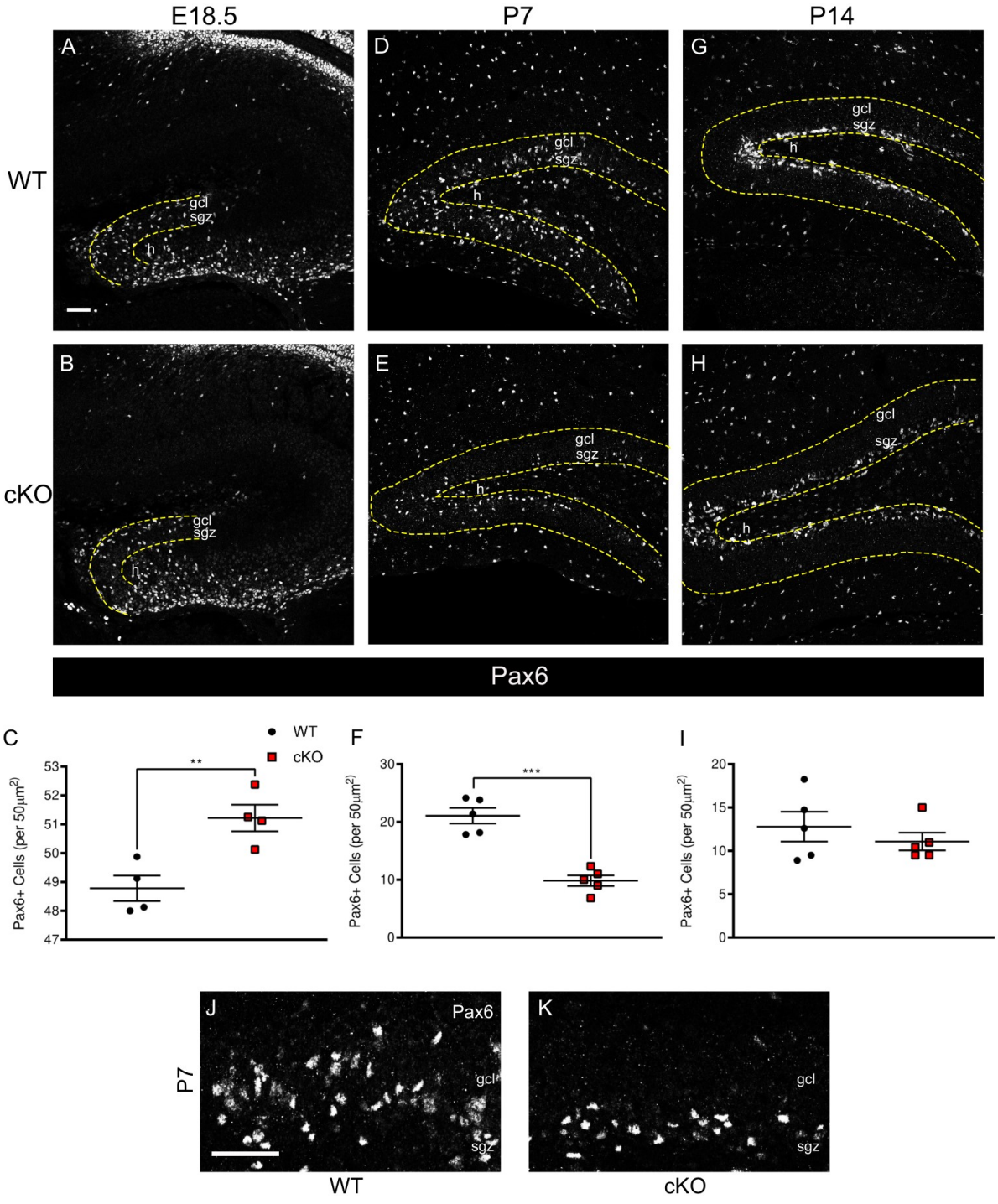
E18.5
P7
P14
A
D
G
WT
gcl
sgz
h
B
E
H
cKO
Pax6
C
F
I
WT
cKO
**
***
Pax6+ Cells (per 50μm²)
J
K
P7
Pax6
WT
cKO

Figure 3.8.

Figure 3.8. *Mllt11* loss differentially impacts early postnatal hippocampal progenitors. (A, B) Coronal sections of the developing dk at E18.5 in the WT and cKO mouse stained for Pax6 (white) identifying type-1 cells. (C) Scatter plot identifying a significant difference in type-1 cells in the cKO in comparison to WT controls (P= 0.0088, n=4). (D, E) Coronal sections of the dorsal hippocampus at P7 in the WT and cKO mouse stained for Pax6. (F) Scatter plot identifying a significant decrease in type-1 cells in the cKO relative to WT controls (P= 0.0001, n=5). (G, H) Coronal sections of the dorsal hippocampus at P14 in the WT and cKO mouse stained for Pax6. (I) Scatter plot quantifying a no significant change in type-1 cells in cKOs (P= 0.4157, n=5). (J, K) Magnified cross-sectional view of the DG identifying the SGZ and gcl of WT and cKO stained for Pax6. Scale bars = 50µm**.** Data presented as mean ± SEM. Abbreviations: dk, dentate knot; gcl, granule cell layer; h, hilus; SGZ, subgranular zone.

Cux2 fate-mapped cells are primarily gcl neurons (Yamada et al., 2015). This finding is supported by the fact that GFAP+/Sox2+ NPs were distributed in a complementary non-overlapping pattern to that of tdTomato-fate mapped cells (Figure 3.6. J-M). This confirms the previous finding from our lab that Cux2+ hippocampal progenitors gave rise to neuroblasts that transitioned to mature calbindin granule cells populating the DG in an outside-in manner (Yamada et al., 2015).

In comparison to the WT controls, *Mllt11* cKO embryos exhibited a transient increase in both Sox2+/GFAP+ and Pax6+ NPs (Figures. 3.6 and 3.8), demonstrating a requirement for Mllt11 in controlling the differentiation of hippocampal progenitors. The *Mllt11* mutants displayed a loss of radial glial morphology in the DG, as evidenced by GFAP staining (Figure 3.7). The loss of function analysis in this study supports a role for Mllt11 in regulating the organization and cytoskeletal structure of type-1 hippocampal NPs, which in turn affects the balance of progenitor self-renewal and differentiation.

3.4.2. *Mllt11* Loss Increased Formation of Hippocampal Neuroblasts

To determine the effect of *Mllt11* loss on the generation of more differentiated cells types in the neonatal DG, I next evaluated markers for granule cell neurogenesis. This allowed me to segment the phenotypic analysis by carefully choosing markers that more conclusively identify *transit amplifiers*, *migrating neuroblasts*, and *newly formed neurons*.

Neuroblasts are progenitors that have left their niche and begun to terminally differentiate into granule cell neurons. They are characterized by expression of NeuroD1, a pro-neural transcription factor (Kempermann et al., 2015). Interestingly, the number of NeuroD1+ cells was increased in the *Mllt11* cKO relative to WT controls at all time points observed (E18.5: p=0.0014, n=4; P7: p=0.0001, n=3; P14: p=0.0019, n=4) (Figure 3.9. A-I), consistent with a transient increase in type-2a cells (Figure 3.6. A-I). NeuroD1-staining confirmed a clear disruption in the organization of the DG region (Figure 3.9. D, E), which was also observed using markers for radial glia (Figure 3.6 and 3.7). There was a pronounced increase in NeuroD1+ cells in the hilus region (not included in counts) of the *Mllt11* cKO hippocampus, which was most notable at P7 (Figure 3.9. D, E). This coincided with expanded Pax6+ cells in mutants at P7 (Figure 3.8) thus, the ontogenetic analysis demonstrated that *Mllt11* loss impacted the maintenance of hippocampal progenitors most acutely within the first week of life, leading to a greatly expanded population of transit amplifiers.

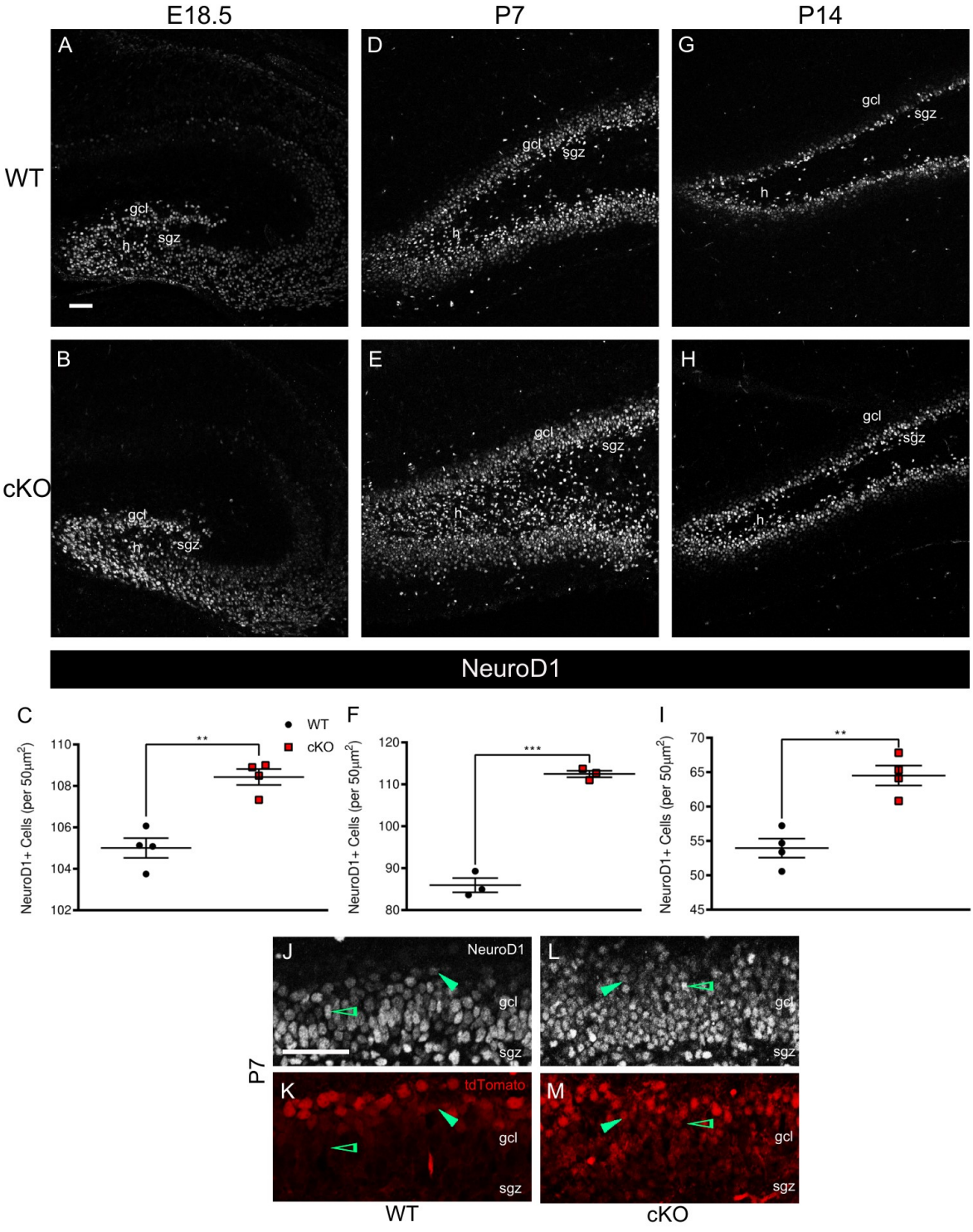
E18.5
P7
P14
WT
cKO
A
B
D
E
G
H
gcl
sgz
h
NeuroD1
C
F
I
WT
cKO
NeuroD1+ Cells (per 50μm²)
**
***
J
K
L
M
P7
tdTomato
WT
cKO

Figure 3.9.

Figure 3.9. *Mllt11* loss increased formation of NeuroD1-positive neuroblasts.
(A, B) Coronal sections of the developing dk at E18.5 in the WT and *Mllt11* cKO mouse stained for NeuroD1 identifying neuroblasts. (C) Scatter plot identifying a significant increase in NeuroD1+ neuroblasts in the cKOs relative to WT controls (P= 0.0014, n=4). (D, E) Coronal sections of the dorsal hippocampus at P7 in the WT and cKO mouse stained for NeuroD1. (F) Scatter plot quantifying a significant increase in neuroblasts in the cKOs (P= 0.0001, n=3). (G, H) Coronal sections of the dorsal hippocampus at P14 in the WT and cKO mouse DG stained for NeuroD1. (I) Scatter plot identifying a significant increase in neuroblasts in the cKOs (P= 0.0019, n=4). (J-M) Magnified view of the DG at P7 identifying the SGZ and gcl of WT (J, K) and cKO (L, M). Top panel: NeuroD1; lower panel: recombined tomato+ cells. Solid green arrowhead in (J-M) identifying neuroblast with high NeuroD1 and low tdTomato levels. Open green arrowhead in (J-M) identifying neuroblast with low NeuroD1 intensity and high tdTomato expression. Scale bars = 50µm**.** Data presented as mean ± SEM. Abbreviations: dk, dentate knot; gcl, granule cell layer; h, hilus; SGZ, subgranular zone.

3.4.3. *Mllt11* Loss Expanded the Formation of Mature Granule Cells

Next, I explored the impact of *Mllt11* loss on stage 4 of hippocampal neurogenesis. The stage is characterized by the maturation of DG granule cells, whose dendrites branch towards the molecular layer of the DG, and axons project towards the hippocampal CA3 pyramidal cell layer (Lavado et al.,2010). During this stage, the newly generated neurons become postmitotic and are identified by markers Prox1 and Tbr1 in the developing DG (Lavado et al., 2010). The loss of *Mllt11* resulted in significantly fewer Prox1+ cells at E18.5 ($p=0.0023$, $n=4$) when compared to the controls with no significant difference at P7 ($p=0.1356$, $n=4$) followed by a significant increase at P14 ($p=0.0299$, $n=4$) (Figure 3.10). No differences were noted in the numbers of Tbr1+ cells at E18.5 ($p=0.4511$, $n=3$), but significant increases were found in cKO DG at perinatal stages; namely P7 ($p=0.0014$, $n=3$) and P14 ($p=0.0015$, $n=4$) (Figure 3.11). Taken together, these findings are consistent with the observation that *Mllt11* loss initially impacted the maintenance of type-1 NPs at perinatal stages, which led to their rapid transition to amplifying progenitors within the first week of life, ultimately contributing to the enhanced formation of immature postmitotic gcl neurons.

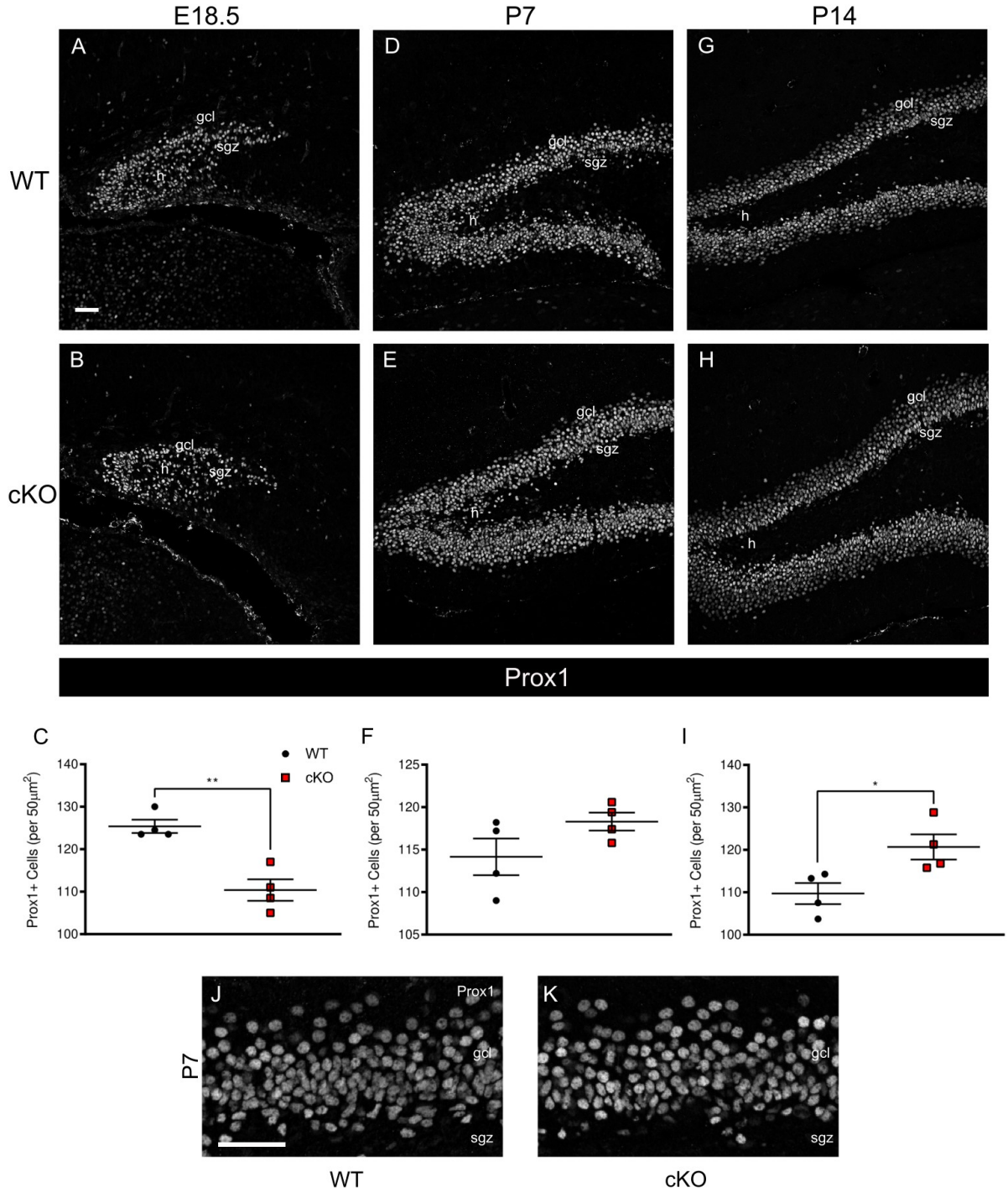
E18.5
P7
P14
A
D
G
WT
gcl
sgz
h
B
E
H
cKO
Prox1
C
F
I
WT
cKO
Prox1+ Cells (per 50μm²)
**
*
J
K
P7
Prox1
WT
cKO

Figure 3.10.

Figure 3.10. *Mllt11* loss altered the maturation of Prox1-positive granule cells.
(A, B) Coronal section of the developing dk at E18.5 in the WT and *Mllt11* cKO mouse stained for Prox1, identifying maturing GCs. (C) Scatter plot quantifying a significant decrease in maturing GCs in the cKOs (P= 0.0023, n=4). (D, E) Coronal sections of the dorsal hippocampus at P7 in the WT and cKO mouse stained for Prox1. (F) Scatter plot identifying no significant difference in maturing GCs in the cKO in comparison to WT controls (P= 0.1356, n=4). (G, H) Coronal sections of the dorsal hippocampus at P14 in the WT and cKO mouse stained for Prox1. (I) Scatter plot identifying a significant increase in maturing GCs in the cKO compared to WT controls (P= 0.0299, n=4). (J, K) Magnified cross-sectional view of the DG at P7 identifying the SGZ and gcl of WT and cKO stained for Prox1. Scale bars = 50µm**.** Data presented as mean ± SEM. Abbreviations: dk, dentate knot; gcl, granule cell layer; h, hilus; SGZ, subgranular zone.

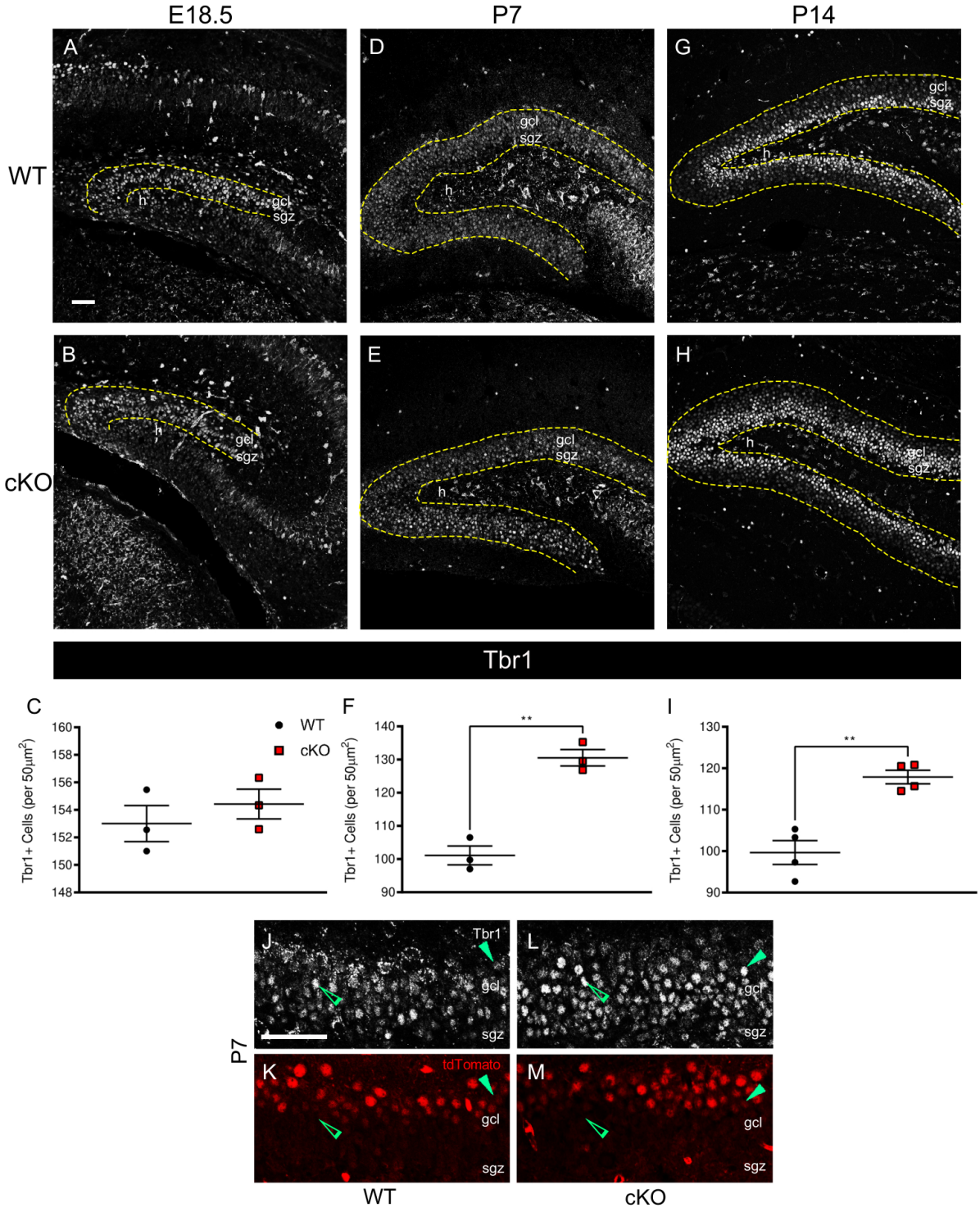
E18.5
P7
P14
WT
cKO
A
B
D
E
G
H
h
gcl
sgz
Tbr1
C
F
I
WT
cKO
Tbr1+ Cells (per 50μm²)
**
J
K
L
M
P7
tdTomato
WT
cKO

Figure 3.11.

Figure 3.11. *Mllt11* loss increased Tbr1-positive developing granule cells.

(A, B) Coronal sections of the developing dk at E18.5 in the WT and *Mllt11* cKO mouse stained for Tbr1 (white) identifying maturing GCs. (C) Scatter plot identifying no significant difference in maturing GCs in the cKO in comparison to WT controls (P= 0.4511, n=3). (D, E) Coronal sections of the dorsal hippocampus at P7 in the WT and cKO mouse stained for Tbr1. (F) Scatter plot quantifying a significant increase in maturing GCs in the cKOs (P= 0.0014, n=3). (G, H) Coronal sections of the dorsal hippocampus at P14 in the WT and cKO mouse stained for Tbr1. (I) Scatter plot quantifying a significant increase in maturing GCs in the cKOs (P= 0.0015, n=4). (J-M) Magnified cross-sectional view of the DG at P7 identifying the SGZ and gcl of WT and cKO; top panel: Tbr1 stain; lower panel: recombined tdTomato+ cells. (J-M) Solid green arrowheads identify maturing GC with high Tbr1 intensity and low tdTomato levels. Open green arrowhead identifying maturing GC with low Tbr1 intensity and high tdTomato levels. Scale bars = 50µm**.** Data presented as mean ± SEM. Abbreviations: dk, dentate knot; gcl, granule cell layer; h, hilus; SGZ, subgranular zone.

3.4.4. *Mllt11* Loss Increased Differentiation of Mature Granule Cells at Postnatal Stages

The final stage of hippocampal neurogenesis is characterized by newly formed granule neurons establishing synaptic contacts for receiving inputs from the entorhinal cortex and sending outputs to the CA3 and hilus regions (O'Mara, 2005). The calcium-binding protein Calbindin serves as a marker of nascent neurons and the nuclear phosphoprotein NeuN identifies all mature and functionally integrated GCs (Brandt et al., 2003). Conditional deletion of *Mllt11* resulted in a decrease in the number of Calbindin+ cells at E18.5 ($p=0.0438$, $n=3$) and at P7 ($p=0.0020$, $n=3$) but no significant difference was reported at P14 ($p=0.8025$, $n=3$) (Figure 3.12). In addition, *Mllt11* loss resulted in a decrease in NeuN+ cells observed at E18.5 ($p=0.0326$, $n=3$), with a contrasting significant increase in NeuN+ cells at both P7 ($p=0.0049$, $n=3$) and P14 ($p=0.0293$, $n=3$) (Figure 3.13). Thus, *Mllt11* loss led to aberrant maturation of hippocampal granule cells within the first two weeks of life, resulting in increases in makers for immature (Prox1, Tbr1) and mature (Calbindin, NeuN) GCs (Figures 3.10-3.13). However, when examining the findings from Calbindin and NeuN staining more closely, it is clear that there is a complex role of *Mllt11* in promoting the maturation of gcl neurons. A previous study in the lab highlighted Cux2 locus activity in both hippocampal progenitors and maturing DG granule cells (Yamada et al., 2015). Thus, the effect of *Mllt11* loss in the maturation of cells in the DG may reflect the progressive deletion of the *Mllt11* floxed allele in progenitors and gcl neurons when using the $Cux2^{IRESCre/+}$ mouse driver.

Taken together these findings reveal a critical role for *Mllt11* in hippocampal neurogenesis. The loss of *Mllt11* initially delays the maturation DG granule cells, which is compensated for by enhanced maturation by the second week of postnatal life. Fate mapping analysis using the $Rosa26^{tdTomato}$ reporter confirmed a transient increase in gcl neurons upon

Cux2$^{IRESCre/+}$ driven *Mllt11* deletion (Figures 3.6. K, M; 3.9. K, M; 3.12. K, M and 3.13. K, M). Altogether, these findings demonstrate that *Mllt11* loss enhanced the formation of immature GCs in the early postnatal hippocampus, while having more modest effects on the numbers of mature GCs.

To more clearly define the effect of *Mllt11* loss on hippocampal neurogenesis, I next evaluated the formation of nascent gcl neurons using a series of EdU birth dating studies. Three EdU pulse-chase time points were chosen to best reflect the outside-in formation of the DG, as previously reported by the lab (Yamada et al., 2015). This experiment revealed the formation of the earliest granule neurons arising from the primary germinative matrix in the developing DG. Specifically, EdU pulsing from E14.5-E18.5 progressively labels hippocampal progenitors initially residing in the CH SVZ region, followed by gcl precursors developing from the dentate knot region of the developing hippocampus. The conditional deletion of *Mllt11* in the hippocampal primordium led to a significant increase in of EdU+/Calbindin+ cells resulting from EdU pulsing at E14.5 followed by harvesting at E18.5 ($p= 0.0004$; WT: n=3, KO: n=4) (Figure 3.14. A-C, J-M). These reflect the formation of the earliest born gcl neurons populating the outer edge of the DG blade. While short term EdU pulsing at E16.5 revealed a significant decrease in Calbindin+/EdU+ cells in cKO neonates at E18.5 ($p=0.0147$, n=4) (Figure 3.14. D-F) and a significant increase in granule cell neurogenesis was observed when pups were dosed at E18.5 and analyzed at P14 ($p= 0.0045$, n=3) (Figure 3.14. G-I, N-Q). This reflected the contribution of granule cell neurons from the dentate knot progenitors that migrate to fill the DG blades and was consistent with the observed burst of transient amplifier formation in the DG of *Mllt11* mutants at one week of age. Subsequently, analysis at two weeks postnatally, confirmed that *Mllt11* loss enhanced neurogenesis of the earliest-born gcl neurons. When taken together with the DG

marker analysis, the EdU pulse-labeling experiment confirmed a role for Mllt11 in regulating the pace and extent of hippocampal neurogenesis.

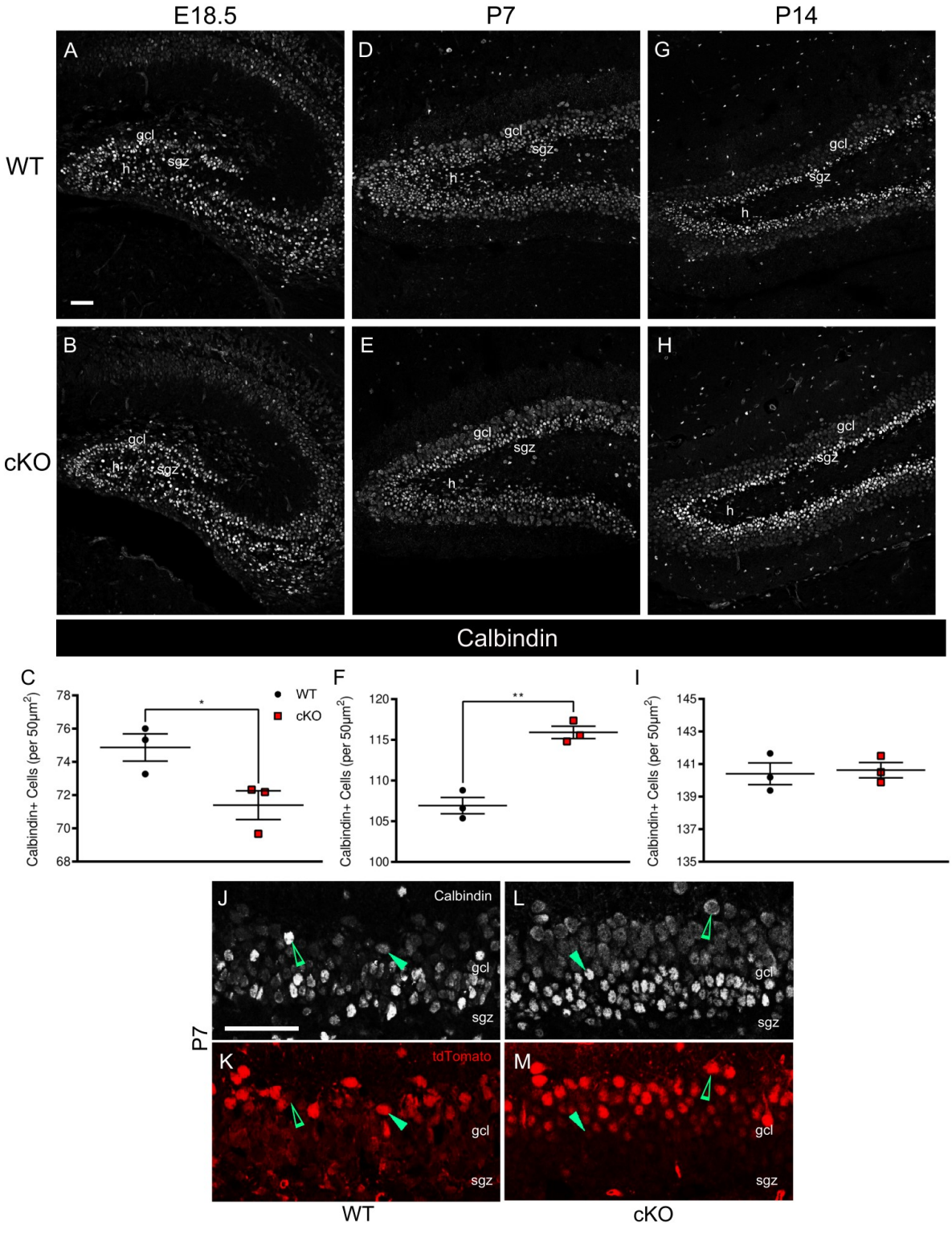
E18.5
P7
P14
WT
cKO
A
B
D
E
G
H
gcl
sgz
h
Calbindin
C
F
I
Calbindin+ Cells (per 50μm²)
WT
cKO
*
**
J
K
L
M
Calbindin
tdTomato
P7
WT
cKO

Figure 3.12.

Figure 3.12. *Mllt11* loss affected the initial formation of mature Calbindin-positive granule cells.

(A, B) Coronal sections of the developing dk at E18.5 in the WT and *Mllt11* cKO mouse stained for Calbindin (white) identifying nascent GCs. (C) Scatter plot quantifying a significant decrease in nascent GCs in the cKOs relative to WTs (P= 0.0438, n=3). (D, E) Coronal sections of the dorsal hippocampus at P7 in the WT and cKO mouse stained for Calbindin. (F) Scatter plot identifying a significant increase in the formation of nascent GCs in the cKOs (P= 0.0020, n=3). (G, H) Coronal sections of the dorsal hippocampus at P14 in the WT and cKO mouse stained for Calbindin. (I) Scatter plot quantifying no significant difference in nascent GCs in the cKO compared to WT controls (P= 0.8025, n=3). (J-M) Magnified cross-sectional view of the DG at P7 identifying the SGZ and gcl of WT and cKO. Top panel: Calbindin stain; lower panel: tdTomato+ recombined DG cells. (J-M) Solid green arrowhead identifies nascent GC with high Calbindin intensity and low tdTomato levels. Open green arrowhead identifies nascent GC with low Calbindin intensity and high tdTomato levels. Scale bars = 50µm**.** Data presented as mean ± SEM. Abbreviations: dk, dentate knot; gcl, granule cell layer; h, hilus; SGZ, subgranular zone.

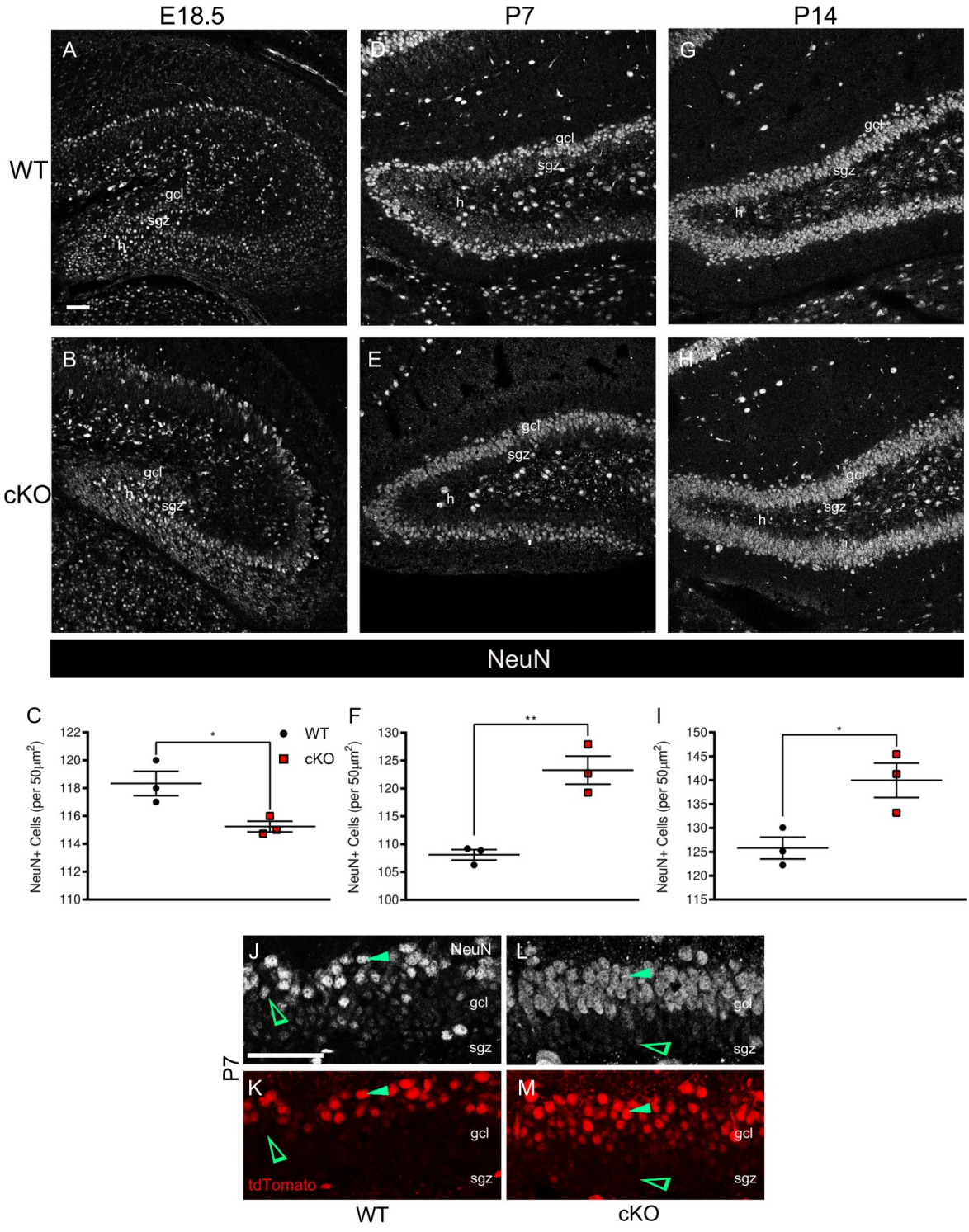
E18.5
P7
P14
WT
cKO
A
B
D
E
G
H
gcl
sgz
h
NeuN
C
F
I
WT
cKO
NeuN+ Cells (per 50μm²)
J
K
L
M
NeuN
tdTomato
P7
WT
cKO

Figure 3.13.

Figure 3.13. *Mllt11* loss alters mature granule cell numbers identified by NeuN.
(A, B) Coronal sections of the developing dk at E18.5 in the WT and conditional *Mllt11* cKO mouse stained for NeuN (white) identifying mature GCs. (C) Scatter plot identifying a significant decrease in mature GCs in the cKO relative to WT controls (P= 0.0326, n=3). (D, E) Coronal sections of the dorsal hippocampus at P7 in the WT and cKO mouse stained for NeuN. (F) Scatter plot identifying a significant increase in mature GCs in the cKOs (P= 0.0049, n=3). (G, H) Coronal sections of the dorsal hippocampus at P14 in the WT and cKO mouse stained for NeuN. (I) Scatter plot identifying a significant increase in mature GCs in the cKOs (P= 0.0293, n=3). (J-M) Magnified cross-sectional view of the DG at P7 identifying the SGZ and gcl of WT and cKO. Top panel: NeuN staining; lower panel: recombined tdTomato cells. (J-M) Solid green arrowhead identifying NeuN+/tdTomato+ mature GC. Open green arrowhead identifying NeuN+ mature GC with no tdTomato expression. Scale bars = 50μm**.** Data presented as mean ± SEM. Abbreviations: dk, dentate knot; gcl, granule cell layer; h, hilus; SGZ, subgranular zone.

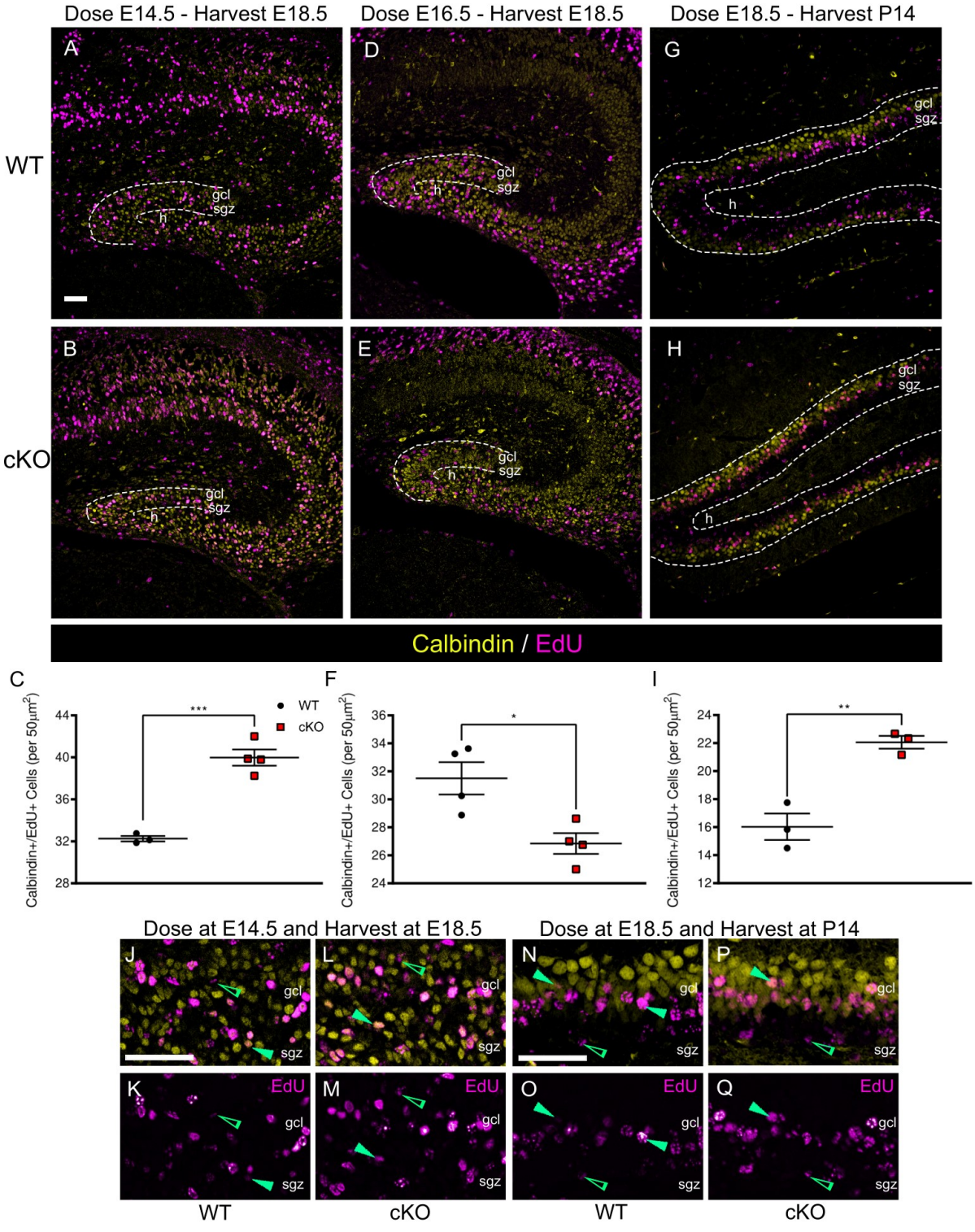
Dose E14.5 - Harvest E18.5
Dose E16.5 - Harvest E18.5
Dose E18.5 - Harvest P14
WT
cKO
A
B
D
E
G
H
gcl
sgz
h
Calbindin / EdU
C
F
I
WT
cKO
Calbindin+/EdU+ Cells (per 50μm²)
***
*
**
Dose at E14.5 and Harvest at E18.5
Dose at E18.5 and Harvest at P14
J
K
L
M
N
O
P
Q
EdU
WT
cKO
WT
cKO

Figure 3.14.

Figure 3.14. *Mllt11* loss enhanced formation of EdU-positive mature granule cells postnatally.

(A, B) Coronal sections of the developing dk in the WT and cKO mouse, dosed with EdU at E14.5 and harvested at E18.5, stained for Calbindin (yellow) and EdU (violet). (C) Scatter plot quantifying a significant increase in Calbindin+/EdU+ cells in the cKO in comparison to WT controls (P= 0.0004; WT: n=3, KO: n=4). (D, E) Coronal sections of the dorsal hippocampus at P7 in the WT and cKO mouse stained for Calbindin and EdU. (F) Scatter plot identifying a significant decrease in Calbindin+/EdU+ cells in cKOs (P= 0.0147. n=4). (G, H) Coronal sections of the dorsal hippocampus at P14 in the WT and cKO mouse stained for Calbindin and EdU. (I) Scatter plot quantifying a significant increase in Calbindin+/EdU+ cells in the cKOs (P= 0.0045, n=3). (J-M) Magnified cross-sectional view of the DG of WT and cKO mice dosed with EdU at E14.5 and harvested at E18.5, identifying labeled cells in the SGZ and gcl. Top panel: Calbindin+/EdU+ cells; lower panel: EdU+ labeling. (J-Q) Solid green arrowhead identifying a Calbindin+/EdU+ cells; open green arrowhead identifying a Calbindin-/EdU+ cells. (N-Q) Magnified cross-sectional view of the DG of WT and cKO mice dosed with EdU at E18.5 and harvested at P14, identifying the SGZ and gcl. (J-Q) Top panel: stained for both Calbindin and EdU; bottom panel: EdU+ cells. Solid arrowhead identifying Calbindin+/EdU+ cells; empty arrowhead identifying Calbindin-/EdU+ cells. Scale bars = 50µm**.** Quantification of data presented as mean ± SEM. Abbreviations: dk, dentate knot; gcl, granule cell layer; h, hilus; SGZ, subgranular zone.

CHAPTER 4. DISCUSSION

4.1. Summary of Key Findings

The embryonic DTM is patterned into critical structures including the telencephalic ChPs and HNE and DNE by way of essential signals from the CH region (Roy et al., 2014). Neural specification requires the activation of cell specific gene regulatory programs. The purpose of this thesis was to elucidate the role of Mllt11 in development of the CH, its derivatives and ultimately hippocampal neurogenesis. To this end, I utilized the genetic Cre-lox strategy to develop an *Mllt11* cKO mouse line, utilizing a Cre recombinase mouse line driven from the Cux2 locus ($Cux2^{IRESCre/+}$). When combined with $Rosa26^{tdTomato}$ reporter mouse line, I was able to powerfully interrogate, and fate map the effects of *Mllt11* loss in CH derivatives and hippocampal neurogenesis. I identified Mllt11 as a key factor that regulates cell migration to fuel the growth and organization of the ChP and promote the maintenance of type-1 NPs essential for the controlled neurogenesis in the hippocampus. Specifically, the loss of *Mllt11* led to aberrant changes to the telencephalic ChP epithelial architecture and more importantly significant alterations to the NP pool. This in turn, lead to changes in the trajectory of progenitors during neurogenesis to proliferate and differentiate into postmitotic granule cell neurons in the embryonic and postnatal hippocampus. The following general discussion provides a summary of the results presented within this thesis and suggests future work that may stem from these findings.

4.2. *Mllt11* Expression in the Postnatal and Adult Hippocampus

The first objective of this thesis characterized the expression pattern of *Mllt11* in the developed hippocampus. Our lab previously explored the spatio-temporal expression pattern of *Mllt11* during development, with abundant transcripts detected post-mitotic neurons throughout the developing central and peripheral nervous system (Yamada et al., 2014). However, its expression pattern has yet to be characterized in the hippocampus. I now show that *Mllt11* is expressed throughout the DG and CA regions of the hippocampus over the series of postnatal and adult time points. Early postnatal stages are critical for generating the adult NP pool in the SGZ of the hippocampus. The enriched levels and duration of *Mllt11* expression coincided with this critical postnatal period of the SGZ with tapering levels of expression by P28. This suggests that Mllt11 is functionally important during these early stages of hippocampal development, coinciding with a burst of perinatal neurogenesis and circuit integration. The fact that the hippocampal neural niche undergoes major development by P14 and remains nearly unchanged through adulthood (Duan et al., 2008; Urbán and Guillemot, 2014), further strengthens the speculation about the importance of Mllt11 for early developmental processes. These results have not been previously reported and will open a new avenue of investigation into the role of Mllt11 in neural development, with important implications in the analysis of key factors in postnatal neurogenesis.

4.3. *Mllt11* Loss Disrupts Formation of the Cortical Hem and its Derivatives

The second objective of this thesis characterized the role of Mllt11 in regulating the development of the CH and its derivatives by using the *Mllt11* conditional mouse mutant model described herein. Previous studies have observed that the defective formation of DTM regional specificity can give rise to downstream malformations during neurodevelopment (Monuki et al.,

2001; Hébert et al., 2002). As such, I first assessed Lhx2, a critical regulator in early forebrain development and patterning of this region. I report a significant increase in Lhx2+ cell numbers and decrease in CH area formed in *Mllt111* cKO brains. I also noted a significant decrease in the number of CH derived CR cells, which are essential for regulating the migration of newborn forebrain cells in cortex and archicortex (Marín et al., 2010). Interestingly, the decrease in number of CH derived CR cells in the *Mllt11* cKO at E14.5 was transient, since levels were comparable to the WT by E18.5. The loss of function of *Lhx2* mouse mutants showed an expanded CH region and dramatic overproduction of CR cells (Roy et al., 2014), offering an interesting contrast to the findings reported here for *Mllt11* mutants. The relationship between Mllt11 and Lhx2 is unknown, but given the complimentary phenotypes, Mllt11 may act to regulate the formation and/or migration of CH derivatives. Importantly, the CH is a major source of CR cells in the DTM, since the near complete deletion of CH-derived CR cells using the *Wnt3a*^{IRESCre} could not be compensated for by other sources of CR cells; namely those from the pallial/subpallial boundary (Yoshida et al., 2006). Interestingly, neocortical development and lamination remained largely unaffected in those mice, suggesting that CH-derived CR cells may play a more critical role in regulating migration of Hem-derived structures. In light of this, while I observed a transient reduction in CR cells in the *Mllt11* cKO brain, I subsequently observed significant perturbation in the migration of neuroepithelial cells supplying the growing ChP. Whether this is related to the transient reduction in CR cells is unknown at this time.

4.4. *Mllt11* Loss Disrupts Morphogenesis of the Telencephalic Choroid Plexus

The ChP epithelium develops from the Wnt and BMP expressing CH region in the DTM, generating a highly organized tissue that acts as an interface between the peripheral circulation and the CNS (Grove et al., 1998; Ek et al., 2003; Liddelow et al., 2010). Regulatory mechanisms

in ChP development are only just being investigated and studies remain in their infancy. Thus far, definitive evidence concludes a distal-proximal maturation process whereby proliferative cells are added to the root of the plexus, forming in a "conveyor belt" like manner (Liddelow et al., 2010). A small population of proliferative cells within the root continue to divide throughout development, with the majority of ChP epithelial cells along the length of the stalk existing in a postmitotic state (Huang et al., 2009; Liddelow et al., 2010). During typical ChP development, the epithelium progresses from the proliferative pseudostratified progenitor population and transitions into low columnar epithelium and finally into a highly polarized cuboidal epithelium necessary for important barrier functions (Ek et al., 2003; Liddelow et al., 2010).

With respect to the telencephalic ChP, I report an interesting and unexpected finding. *Mllt11* loss resulted in a significantly truncated ChP with notable defects in the underlying morphology. Typically, in the E14.5 mouse, the ChP epithelium consists of a pseudostratified structure that varies from simple low columnar to cuboidal organization (Huang et al., 2009; Liddelow et al., 2010). However, in the *Mllt11* cKO I observed loss of the tight organization of epithelial cells along the entire length of the ChP stalk. *Mllt11* mutant cells were juxtaposed with one another, and the basement membrane, outlined by ZO-1 staining, was highly disorganized. To assess whether the ChP precursor population was affected in the *Mllt11* cKO I utilized EdU-birth dating analysis by injecting at E14.5 and harvesting 2 hours post-injection. Interestingly, there was a significant reduction in the number of EdU+ cells reaching the ventral arm of the ChP stalk in the cKOs, suggesting a defect in the migration of newly born OTX1/2+ neuroepithelial precursors contributing to the formation of the stalk. Thus, the work presented here suggest that *Mllt11* function is essential for the migration and integration of neuroepithelial progenitors from the CH supplying the growth of the ChP stalk.

4.5. *Mllt11* loss Disrupts the Balance Between Proliferation and Terminal Differentiation

The third objective characterized the outcome of *Mllt11* loss on hippocampal neurogenesis both in the fetus and postnatal mouse. Embryonic and postnatal neurogenesis relies on the unique spatio-temporal sequence of cell type differentiation to maintain a necessary balance between the generation of hippocampal progenitors and terminal differentiation and maturation of postmitotic neurons (Hsieh, 2012). The role of Mlt11 in embryonic and postnatal hippocampal neurogenesis has not been explored prior to my thesis study. Here, I show that Mllt11 plays a critical role in regulating hippocampal neurogenesis. It acts by initially maintaining the radial glial architecture of type-1 cells and their tether to the SGZ niche. In the absence of *Mllt11*, type-1 cells are untethered because their glial processes are shorted and fail to maintain a connection from the hilus/SGZ boundary to the top of the DG blade. This is supported by the observed decrease in astroglia phenotype at postnatal stages identified by changes in GFAP expression in the DG (Figure 3.7.). The staining reveals a clear disruption in the orientation and length of radial glial fibers, and future work should quantify and confirm this finding. Maintenance of proper radial glial morphology is essential for the long-term self-renewal of hippocampal progenitors (Falk and Götz, 2017). As a consequence of this loss of glial tethering, *Mllt11* mutant hippocampi displayed transient increases in the numbers of amplifying NP types, such as type-2a and type-3 cells, concomitant with a burst in the formation of immature granule cells in the DG. By two weeks of age, an increase in mature GCs was seen in the conditional *Mllt11* mutants. My findings demonstrate a primary role of Mllt11 in the maintenance of a hippocampal radial glial phenotype, and that in its absence, cells rapidly transition through a series of cell states ultimately leading to enhanced GC neurogenesis, and reduction of self-renewing progenitor populations.

The balance between the generation of hippocampal progenitors and terminally differentiated postmitotic neurons shifts during development, with postnatal and adult NPs molecularly and anatomically distinguishable from their embryonic counterparts (Hardwick and Philpott, 2014). Specifically, embryonic NPs are characterized by their high proliferative rate and their situation within a dynamic niche environment (Hardwick and Philpott, 2014; Urbán and Guillemot, 2014). While adult NPs are characterized by their acquisition of quiescence and their situation in a complex but stable cellular niche at the hilus-dentae border region (Urbán and Guillemot, 2014). This shift during development must be tightly controlled and is essential to the formation of the appropriate neuronal cell numbers. Numerous studies have reported that alterations such as an increase or decrease to the original cell proliferation rate, is associated with major neurological pathologies including Alzheimer's disease (Jin et al., 2004; Lazarov and Marr, 2010), Huntington's disease (Curtis et al., 2003; Phillips et al., 2005) and Parkinson's disease (Höglinger et al., 2004; Marxreiter et al., 2013).

This thesis has revealed that the balance between hippocampal progenitors and formation of postmitotic neurons is controlled by Mllt11 during development. In the absence of *Mllt11*, a transient increase in unmoored type-1 NPs was observed and was accompanied by significant increases in the numbers of subsequent intermediate progenitors and a transient attenuation of terminal differentiation of the earliest born DG neurons. This data implies that at embryonic stages, Mllt11 controls a shift in the balance of progenitor cell activity toward self-renewal vs. differentiation. In contrast, during early postnatal neurogenesis I found that the hippocampal type-1 radial glial neural stem cell pool was significantly reduced, with a corresponding increase in the numbers of intermediate progenitors and both immature and mature postmitotic GC neurons. This data implies a shift in the maintenance of progenitor proliferation and commitment

to the neuronal cell fate due to exhaustion the type-1 radial glial NP pool. My conclusions are supported by the fate-mapping of gcl neurons using the tdTomato reporter, which showed a dramatic increase in the infilling of the DG blades in the perinatal *Mllt11* mutant hippocampus. This effect was most notable at P7, with *Mllt11* cKO mutants showing abnormal increases in the number of tdTomato+ cells fated to the GC identity suggesting aberrant activation of a granule cell fate. This was likely consequence of the transient burst of intermediate progenitors observed in the mutant hippocampus. The increased proliferation of intermediate progenitors and terminal differentiation toward a neuronal fate in the cKOs was further supported by the EdU-birth dating analysis. Specifically, *Mllt11* loss led to a significant increase in the number of Calbindin+/EdU+ cells in the cKO in comparison to the WT controls.

These results therefore identify Mllt11 as a key player required in the control of proliferation and terminal differentiation of newborn neurons during both embryonic development and postnatal hippocampal neurogenesis. The effect of Mllt11 is mostly likely a consequence of abnormal radial glia morphology of the type-1 cells in the mutant. However, Mllt11 may also play a role in regulating the expression of differentiation/survival factors required for cell cycle exit and terminal differentiation of gcl neurons. Future work should explore the downstream molecular changes using a whole transcriptome profiling approach. For example, studies of kidney disease (Zhang et al., 2017) and breast cancer (Chang et al., 2008) reveal Mllt11 promotes pathogenesis via the Wnt signaling pathway.

4.6. Canonical Wnt Signaling: A Possible Mechanism of Action to be Investigated

Wnt signaling has been found to play a crucial role in neurodevelopmental processes with complex spatio-temporal expression patterns of Wnt receptors (Ciani and Salinas, 2005). Canonical Wnt signaling is transduced by β-catenin which in turn mediates the transcription of

lymphoid enhancer factor 1/T cell-specific transcription factors (LEF1/TCFs). Consequently, various downstream genes that control early cell fate decisions are activated (Ciani and Salinas, 2005). It has been further demonstrated that β-catenin signaling impinges on the decision of NPs to proliferate or differentiate (Zechner et al., 2003). This suggests a molecular link between the functions of Mllt11 and Wnt/β-catenin signaling during neural development. In the following discussion I will make a case as to why the link between Wnt signaling and Mllt11 function deserves more attention in future studies.

4.6.1. Wnt Signaling in the Developing Choroid Plexus

The developing ChP expresses components of the Wnt signaling pathway in both the embryonic mouse and human brain, suggesting this pathway is likely crucial to its development and/or function. For example, *Wnt5a* is known to be expressed both in the CH and the telencephalic ChP (Grove et al., 1998) and a recent report identified Wnt5a as an important regulator in the development of this unique structure (Langford et al., 2020). Specifically, at E14.5 they observed disrupted ChP morphogenesis following the loss of *Wnt5a*, with the mutant telencephalic ChP displaying reduced length, varying thickness and increased distance between the proximal ends of the stalk (Langford et al., 2020). Furthermore, they found that ZO-1, which plays a critical role as a scaffold protein cross-linking and anchoring tight junction proteins to the actin cytoskeleton, was not seen on cells that had detached form the ventricular surface thus failing to produce an intact and functional basement membrane network (Langford et al., 2020). Interestingly, the findings of the *Wnt5a* KO displays similarities to the phenotypes observed in the $Cux2^{IRESCre/+}$ driven *Mllt11* cKO. The clinical importance of this finding is that normal development of the ChP is essential for the formation and maintenance of the brain and secretion

of CSF. Alteration in its structure may result in altered CSF production which has been linked to neuropathologies including Alzheimer's disease (Silverberg et al., 2001).

4.6.2. Wnt Signaling in the Hippocampus

The development and proper functioning of the hippocampus is under strict regulation from multiple signaling pathways (Lie et al., 2005; Urbán and Guillemot, 2014) which can activate or inhibit neurogenesis. In addition to promoting neuronal differentiation and maturation, several *in vitro* studies have shown that canonical Wnt signaling also affects the proliferation of hippocampal progenitors regulating both self-renewal and neurogenesis (Yu et al., 2006; Prajerova et al., 2010; Okamoto et al., 2011; Qu et al., 2013). For example, it was reported that Wnt3a and Wnt5a could both increase proliferation and stimulate neural differentiation of progenitor cells isolated from the postnatal mouse brain (Yu et al., 2006).

4.6.3. Mllt11 and the Wnt Signaling Pathway

Several *in vitro* studies using transformed cells have found Mllt11 activates canonical Wnt signaling by interacting with the T-cell specific transcription factor 7 (TCF7) activating downstream target genes of the Wnt pathway. *Mllt11* was reported to bind and subsequently stabilize *TCF7*, facilitating its translocation into the nucleus where it acts as a co-activator of LEF1/TCFs (Behrens et al., 1996; Willert et al., 2002). Immunoprecipitation studies have confirmed the interaction between *Mllt11* and *TCF7,* with a protein-protein interaction model suggesting *Mllt11* interacts with the *TCF7*/β-catenin transcriptional complex, proposing *TCF7* forms a unique shape into which *Mllt11* is fully enveloped (Park et al., 2015). These results are further corroborated by the finding that levels of β-catenin were notably enhanced in *Mllt11* overexpressed cells and accompanied by increased *TCF7* mRNA expression (Park et al., 2015).

Furthermore, they reported that knocking down *TCF7* in cells results in the elimination of *Mllt11*-mediated increase of β-catenin (Zhang et al., 2017).

Thus far there have been no studies evaluating the action of Mllt11 on the Wnt signaling pathway in regard to its influence on neurodevelopmental processes. However, given the link between Mllt11 and Wnt signaling in non-neural tissues, as well as the importance of Wnt signaling during the formation of CH derivatives, future genetic and molecular studies should focus on how Mllt11 and Wnt signaling coordinately regulate the formation of the CH and hippocampal neurogenesis.

4.7. Future Directions

Neurogenesis is a highly proliferative process that has implications for the limited regenerative abilities of the brain. Much attention has been focused on the elucidation of the mechanisms governing the birth of neurons in the SGZ of the adult brain (Alvarez-Buylla and Lim, 2004; Bonaguidi et al., 2012; Kempermann et al., 2015). Although progress has been made, our knowledge of the neurogenic factors and the origin of the progenitor cell types in the postnatal mammalian brain remain rudimentary. Here I did not include any behavioural or cognitive testing since my primary goal was to highlight the cellular role for Mllt11 in CH and hippocampus development, using a conditional loss-of-function approach in the mouse.

In the future it would be interesting to conduct behavioural phenotyping experiments to further investigate the role of Mllt11 using the $Cux2^{IRESCre/+}$ driven conditional cKOs. Behavioural studies, such as the Morris water maze (Vorhees and Williams, 2006), and the elevated plus maze (Walf and Frye, 2007) would test memory dysfunction that may arise as a result of the aberrant hippocampal neurogenesis phenotype observed in the *Mllt11* cKOs. This would provide valuable insight into the functional consequences of the inactivation of *Mllt11*

throughout adult neurogenesis. In addition to behavioural studies, it would also be important to further characterize any compromised ChP function in the *Mllt11* cKO, by evaluating junctional, enzymatic, and transporter proteins in the embryonic and adult ChP. For example, it would be interesting to utilize injectable tracers in both the embryonic and adult mouse (Tietz and Engelhardt, 2015; Langford et al., 2020) to investigate whether epithelial junctional integrity was maintained in the absence of *Mllt11* and to evaluate whether there are any lasting morphological changes to the ChP which would in turn have significant consequences on CSF secretion. With the knowledge of the role Wnt signaling plays during normal CNS development, and maintenance of the homeostatic balance of proliferation and differentiation of NPs, it would be interesting to conduct future studies to investigate the relationship between Mllt11 and Wnt signaling during the development of the CH and associated brain structures.

4.8. Conclusion

Interactions between neurogenic niches and NPs play a critical role in maintaining the balance between progenitor maintenance and differentiation in the hippocampus, and in preventing premature depletion of progenitor cells in order to maintain robust neurogenesis throughout life (Morrison and Spradling, 2008, Miller and Gauthier-Fisher, 2009). I have performed a comprehensive analysis of *Mllt11* expression in the developing and adult mouse brain CH and hippocampus formation *via* the use of conditional mutagenesis. My thesis work has demonstrated a significant role for Mllt11 in ChP development and the morphogenesis and maturation DG cells in the perinatal hippocampus. As such, this work is the first to reveal the role of Mllt11 in the maintenance and differentiation of perianal progenitors in the hippocampus, and the migration and organization of epithelial cells fueling the growth of the ChP. Further investigations into the roles of Mllt11 during neural development may provide significant insight

into the cellular behaviours crucial to the development of the nervous system and the maintenance on long-lived NPs within neurogenic niches. Furthermore, these investigations into the *in vivo* roles of Mllt11 during brain formation will shed light on pathological processes that lead to neurodevelopmental disorders.

REFERENCES

Abraham, H., Pérez-García, C., & Meyer, G. (2004). p73 and Reelin in Cajal-Retzius cells of the developing human hippocampal formation. *Cereb Cortex*, 14(5):484-95.

Aimone, J., Deng, W., & Gage, F. (2010). Adult neurogenesis: integrating theories and separating functions. *Trends Cogn Sci*, 14(7): 325–337.

Altman, J. (1969). Autoradiographic and histological studies of postnatal neurogenesis. IV. Cell proliferation and migration in the anterior forebrain, with special reference to persisting neurogenesis in the olfactory bulb. *J Comp Neurol*, 137(4):433-57.

Altman, J., & Das, G. (1965). Autoradiographic and histological evidence of postnatal hippocampal neurogenesis in rats. *J Comp Neurol*, 124(3):319-35.

Alvarez-Buylla, A., & Lim, D. (2004). For the long run: maintaining germinal niches in the adult brain. *Neuron*, 41(5), 683-6.

Amaral, D., Scharfman, H., & Lavenex, P. (2007). The dentate gyrus: fundamental neuroanatomical organization (dentate gyrus for dummies). *Prog Brain Res*, 163: 3–22.

Ambrogini, P., Lattanzi, D., Ciuffoli, S., Agostini, D., Bertini, L., Stocchi, V., . . . Cuppini, R. (2004). Morpho-functional characterization of neuronal cells at different stages of maturation in granule cell layer of adult rat dentate gyrus. *Brain Res*, 1017: 21–31.

Anand, K., & Dhikav, V. (2012). Hippocampus in health and disease: An overview. *Ann Indian Acad Neurol*, 15(4):239-246.

Assimacopoulos, S., Grove, E., & Ragsdale, C. (2003). Identification of a Pax6-Dependent Epidermal Growth Factor Family Signaling Source at the Lateral Edge of the Embryonic Cerebral Cortex. *Journal of Neuroscience*, 23(16):6399-6403.

Baldelli, P., & Meldolesi, J. (2015). The Transcription Repressor REST in Adult Neurons: Physiology, Pathology, and Diseases. *eNeuro*, 2(4):ENEURO.0010-15.2015.

Baruch, K., Deczkowska, A., David, E., Castellano, J., Miller, O., Kertser, A., . . . Schwartz, M. (2014). Aging-induced type I interferon response at the choroid plexus negatively affects brain function. *Science*, 346(6205):89-93.

Behrens, J., von Kries, J., Kühl, M., Bruhn, L., Idlich, D., Grosschedl, R., & Birchmeier, W. (1996). Functional interaction of beta-catenin with the transcription factor LEF-1. *Nature*, 382(6592):638-42.

Ben Abdallah, N., Slomianka, L., Vyssotski, A., & Lipp, H. (2010). Early age-related changes in adult hippocampal neurogenesis in C57 mice. *Neurobiol Aging*, 31(1):151-61.

Boekhoorn, K., Joels, M., & Lucassen, P. (2006). Increased proliferation reflects glial and vascular-associated changes, but not neurogenesis in the presenile Alzheimer hippocampus. *Neurobiol Dis*, 24(1):1-14.

Bonaguidi, M., Song, J., Ming, G., & Song, H. (2012). A unifying hypothesis on mammalian neural stem cell properties in the adult hippocampus. *Curr Opin Neurobiol*, 22: 754–761.

Brandt, M., Jessberger, S., Steiner, B., Kronenberg, G., Reuter, K., Bick-Sander, A., . . . Kempermann, G. (2003). Transient calretinin expression defines early postmitotic step of neuronal differentiation in adult hippocampal neurogenesis of mice. *Mol Cell Neurosci*, 24(3):603-13.

Braun, S., & Jessberger, S. (2014). Adult neurogenesis: mechanisms and functional significance. *Development*, 141: 1983-1986.

Bulchand, S., Grove, E., Porter, F., & Tole, S. (2001). LIM-homeodomain gene Lhx2 regulates the formation of the cortical hem. *Mech Dev*, 100(2):165-75.

Bushong, E., Martone, M., & Ellisman, M. (2004). Maturation of astrocyte morphology and the establishment of astrocyte domains during postnatal hippocampal development. *International Journal of Developmental Neuroscience*, 22(2), 73–86.

Caronia-Brown, G., Yoshida, M., Gulden, F., Assimacopoulos, S., & Grove, E. (2014). The cortical hem regulates the size and patterning of neocortex. *Development*, 141: 2855-2865.

Caruana, D., Alexander, G., & Dudek, S. (2012). New insights into the regulation of synaptic plasticity from an unexpected place: Hippocampal area CA2. *Learn Mem*, 19(9): 391–400.

Catalani, A., Sabbatini, M., Consoli, C., Cinque, C., Tomassoni, D., Azmitia, E., . . . Amenta, F. (2002). Glial fibrillary acidic protein immunoreactive astrocytes in developing rat hippocampus. *Mechanisms of Ageing and Development*, 123(5):481-90.

Chang, X., Li, D., Hou, Y., Wu, J., Lu, J., Di, G., . . . Shao, Z. (2008). Identification of the functional role of AF1Q in the progression of breast cancer. *Breast Cancer Res Treat*, 111(1):65-78.

Choi, M., Ahn, S., Yang, E., Kim, H., Chong, Y., & Kim, H. (2016). Hippocampus-based contextual memory alters the morphological characteristics of astrocytes in the dentate gyrus. *Mol Brain*, 9, 72.

Ciani, L., & Salinas, P. (2005). WNTs in the vertebrate nervous system: from patterning to neuronal connectivity. *Nat Rev Neurosci*, 6(5):351-62.

Cubelos, B., Sebastián-Serrano, A., Kim, S., Moreno-Ortiz, C., Miguel Redondo, J., Walsh, C., & Nieto, M. (2008). Cux-2 Controls the Proliferation of Neuronal Intermediate Precursors of the Cortical Subventricular Zone. *Cerebral Cortex*, 18(8):1758–1770.

Curtis, M., Penney, E., Pearson, A., van Roon-Mom, W., Butterworth, N., Dragunow, M., . . . Faull, R. (2003). Increased cell proliferation and neurogenesis in the adult human Huntington's disease brain. *Proc Natl Acad Sci U S A*, 100(15):9023-7.

Daugherty, A., Bender, A., Raz, N., & Ofen, N. (2016). Age differences in hippocampal subfield volumes from childhood to late adulthood. *Hippocampus*, 26(2):220-8.

Duan, X., Kang, E., Liu, C., Ming, G., & Song, H. (2008). Development of neural stem cell in the adult brain. *Curr Opin Neurobiol*, 18(1):108-15.

Dziegielewska, K., Ek, C., Habgood, M., & Saunders, N. (2001). Development of the choroid plexus. *Microsc Res Tech*, 52(1):5-20.

Ek, C., Habgood, M., Dziegielewska, K., & Saunders, N. (2003). Structural characteristics and barrier properties of the choroid plexuses in developing brain of the opossum (Monodelphis Domestica). *J Comp Neurol*, 460(4):451-64.

Encinas, J., Michurina, T., Peunova, N., Park, J., Tordo, J., Peterson, D., . . . Enikolopov, G. (2011). Division-coupled astrocytic differentiation and age-related depletion of neural stem cells in the adult hippocampus. *Cell Stem Cell*, 8(5):566-79.

Englund, C., Fink, A., Lau, C., Pham, D., Daza, R., Bulfone, A., . . . Hevner, R. (2005). Pax6, Tbr2, and Tbr1 are expressed sequentially by radial glia, intermediate progenitor cells, and postmitotic neurons in developing neocortex. *J Neurosci*, 25(1):247-51.

Eriksson, P., Perfilieva, E., Björk-Eriksson, T., Alborn, A., Nordborg, C., Peterson, D., & Gage, F. (1998). Neurogenesis in the adult human hippocampus. *Nat Med*, 4(11):1313-7.

Falcao, A., Marques, F., Novais, A., Sousa, N., Palha, J., & Sousa, J. (2012). The path from the choroid plexus to the subventricular zone: go with the flow! *Front. Cell. Neurosci*, 6:34.

Falk, S., & Götz, M. (2017). Glial control of neurogenesis. *Curr Opin Neurobiol*, 47:188-195.

Favaro, R., Valotta, M., Ferri, A., Latorre, E., Mariani, J., Giachino, C., . . . Nicolis, S. (2009). Hippocampal development and neural stem cell maintenance require Sox2-dependent regulation of Shh. *Nat Neurosci*, 12(10):1248-56.

Fedele, V., Roybon, L., Nordström, U., Li, J., & Brundin, P. (2011). Neurogenesis in the R6/2 mouse model of Huntington's disease is impaired at the level of NeuroD1. *Neuroscience*, 173:76-81.

Ferri, A., Cavallaro, M., Braida, D., Di Cristofano, A., Canta, A., Vezzani, A., . . . Nicolis, S. (2004). Sox2 deficiency causes neurodegeneration and impaired neurogenesis in the adult mouse brain. *Development*, 131(15):3805-19.

Forrest, M., Parnell, E., & Penzes, P. (2018). Dendritic structural plasticity and neuropsychiatric disease. *Nat Rev Neurosci*, 19(4): 215–234.

Fotaki, V., Price, D., & Mason, J. (2011). Wnt/β-catenin signaling is disrupted in the extra-toes (Gli3(Xt/Xt)) mutant from early stages of forebrain development, concomitant with anterior neural plate patterning defects. *J Comp Neurol*, 519(9):1640-57.

Franco, S., Gil-Sanz, C., Martinez-Garay, I., Espinosa, A., Harkins-Perry, S., Ramos, C., & Müller, U. (2012). Fate-Restricted Neural Progenitors in the Mammalian Cerebral Cortex. *Science*, 337(6095): 746–749.

Fregoso, S., Dwyer, B., & Franco, S. (2019). Lmx1a drives Cux2 expression in the cortical hem through activation of a conserved intronic enhancer. *Development*, 146(5).

Furuta, Y., Piston, D., & Hogan, B. (1997). Bone morphogenetic proteins (BMPs) as regulators of dorsal forebrain development. *Development*, 124, 2203-2212.

Galceran, G., Miyashita-Lin, E., Devaney, E., Rubenstein, J., & Grosschedl, R. (2000). Hippocampus development and generation of dentate gyrus granule cells is regulated by LEF1. *Development*, 127, 469-482.

Gao, Z., Ure, K., Ables, J., Lagace, D., Nave, K., Goebbels, S., . . . Hsieh, J. (2009). Neurod1 is essential for the survival and maturation of adult-born neurons. *Nat Neurosci*, 12(9): 1090–1092.

Ge, S., Sailor, K., Ming, G., & Song, H. (2008). Synaptic integration and plasticity of new neurons in the adult hippocampus. *J Physiol*, 586(16): 3759–3765.

Ghersi-Egea, J., Strazielle, N., Catala, M., Silva-Vargas, V., Doetsch, F., & Engelhardt, B. (2018). Molecular anatomy and functions of the choroidal blood-cerebrospinal fluid barrier in health and disease. *Acta Neuropathol*, 135, 337–361.

Gratzner, H. (1982). Monoclonal antibody to 5-bromo- and 5-iododeoxyuridine: A new reagent for detection of DNA replication. *Science*, 218(4571):474-5.

Grove, E. (2008). Neuroscience organizing the source of memory. *Science*, 319(5861):288-289.

Grove, E., Tole, S., Limon, J., Yip, L., & Ragsdale, C. (1998). The hem of the embryonic cerebral cortex is defined by the expression of multiple Wnt genes and is compromised in Gli3-deficient mice. *Development*, 125, 2315-2325.

Guérout, N., Li, X., & Barnabé-Heider, F. (2014). Cell fate control in the developing central nervous system. *Exp Cell Res*, 321(1):77-83.

Hardwick, L., & Philpott, A. (2014). Nervous decision-making: to divide or differentiate. *Trends Genet*, 30(6): 254–261.

Hasenpusch-Theil, K., Magnani, D., Amaniti, E., Han, L., Armstrong, D., & Theil, T. (2012). Transcriptional analysis of Gli3 mutants identifies Wnt target genes in the developing hippocampus. *Cereb Cortex*, 22(12):2878-93.

Hébert, J., Mishina, Y., & McConnell, S. (2002). BMP signaling is required locally to pattern the dorsal telencephalic midline. *Neuron*, 35(6):1029-41.

Hodge, R., & Hevner, R. (2012). Expression and actions of transcription factors in adult hippocampal neurogenesis. *Dev Neurobiol*, 71(8): 680–689.

Hodge, R., Garcia, A., Elsen, G., Nelson, B., Mussar, K., & Reiner, S. (2013). Tbr2 expression in Cajal-Retzius cells and intermediate neuronal progenitors is required for morphogenesis of the dentate gyrus. *J. Neurosci*, 33, 4165–4180.

Höglinger, G., Rizk, P., Muriel, M., Duyckaerts, C., Oertel, W., Caille, I., & Hirsch, E. (2004). Dopamine depletion impairs precursor cell proliferation in Parkinson disease. *Nat Neurosci*, 7(7):726-35.

Hsieh, J. (2012). Orchestrating transcriptional control of adult neurogenesis. *Genes Dev*, 26(10):1010–1021.

Hu, Y., Sun, Q., Zhang, C., Sha, Q., & Sun, X. (2015). RE1 silencing transcription factor (REST) negatively regulates ALL1-fused from chromosome 1q (AF1q) gene transcription. *BMC Molecular Biology*, 16, 15.

Huang, X., Ketova, T., Fleming, J., Wang, H., Dey, S., Litingtung, Y., & Chiang, C. (2009). Sonic hedgehog signaling regulates a novel epithelial progenitor domain of the hindbrain choroid plexus. *Development*, 136(15):2535-43.

Huang, X., Liu, J., Ketova, T., Fleming, J., Grover, V., Cooper, M., . . . Chiang, C. (2010). Transventricular delivery of Sonic hedgehog is essential to cerebellar ventricular zone development. *Proc. Natl. Acad. Sci. U.S.A*, 107, 8422–8427.

Iulianella, A., Sharma, M., Vanden Heuvel, G., & Trainor, P. (2009). Cux2 functions downstream of Notch signaling to regulate dorsal interneuron formation in the spinal cord. *Development*, 136(14): 2329–2334.

Iwano, T., Masuda, A., Kiyonari, H., Enomoto, H., & Matsuzaki, F. (2012). Prox1 postmitotically defines dentate gyrus cells by specifying granule cell identity over CA3 pyramidal cell fate in the hippocampus. *Development*, 139: 3051-3062.

Jessberger, S., & Kempermann, G. (2003). Adult-born hippocampal neurons mature into activity-dependent responsiveness. *European Journal of Neuroscience*, 18(10):2707-2712.

Jin, K., Galvan, V., Xie, L., Mao, X., Gorostiza, O., Bredesen, D., & Greenberg, D. (2004). Enhanced neurogenesis in Alzheimer's disease transgenic (PDGF-APPSw,Ind) mice. *Proc Natl Acad Sci U S A*, 101(36):13363-7.

Johansson, P. (2014). The choroid plexuses and their impact on developmental neurogenesis. *Front Neurosci*, 8:340.

Johansson, P., Dziegielewska, K., Ek, C., Habgood, M., Liddelow, S., Potter, A., . . . Saunders, N. (2006). Blood-CSF barrier function in the rat embryo. *Eur J Neurosci*, 24(1):65-76.

Johansson, P., Irmler, M., Acampora, D., Beckers, J., Simeone, A., & Götz, M. (2013). The transcription factor Otx2 regulates choroid plexus development and function. *Development*, 140(5):1055-66.

Karadi, K., Janszky, J., Gyimesi, C., Horváth, Z., Lucza, T., Doczi, T., & Kállai, J. (2012). Correlation between calbindin expression in granule cells of the resected hippocampal dentate gyrus and verbal memory in temporal lobe epilepsy. *Epilepsy & Behavior*, 25(1):110-9.

Kempermann, G., & Ehninger, D. (2008). Neurogenesis in the adult hippocampus. *Cell Tissue Res*, 331(1):243-50.

Kempermann, G., Jessberger, S., Steiner, B., & Kronenberg, G. (2004). Milestones of neuronal development in the adult hippocampus. *Trends in Neuroscience*, 27(8):447-452.

Kempermann, G., Song, H., & Gage, F. (2015). Neurogenesis in the adult hippocampus. *Cold Spring Harb Perspect Biol*, 7(9):a018812.

Kim, H., Kim, M., Im, S., & Fang, S. (2018). Mouse Cre-LoxP system: general principles to determine tissue-specific roles of target genes. *Lab Anim Res*, 34(4): 147–159.

Kimura, J., Suda, Y., Kurokawa, D., Hossain, Z., Nakamura, M., Takahashi, M., . . . Aizawa, S. (2005). Emx2 and Pax6 function in cooperation with Otx2 and Otx1 to develop caudal forebrain primordium that includes future archipallium. *J. Neurosci*, 25, 5097-5108.

Kohara, K., Pigatelli, M., Rivest, A., Jung, H., Kitamura, T., & Suh, J. (2014). Cell type-specific genetic and optogenetic tools reveal hippocampal CA2 circuits. *Nat. Neurosci*, 17, 269–279.

Langford, M., O'Leary, C., Veeraval, L., White, A., Lanoue, V., & Cooper, H. (2020). WNT5a Regulates Epithelial Morphogenesis in the Developing Choroid Plexus. *Cereb Cortex*, 30(6):3617-3631.

Larsen, K., Lutterodt, M., Møllgård, K., & Møller, M. (2010). Expression of the Homeobox Genes OTX2 and OTX1 in the Early Developing Human Brain. *J Histochem Cytochem*, 58(7): 669–678.

Lavado, A., Lagutin, O., Chow, L., Baker, S., & Oliver, G. (2010). Prox1 Is Required for Granule Cell Maturation and Intermediate Progenitor Maintenance During Brain Neurogenesis. *PLoS Biology*, 8(8).

Lazarov, O., & Marr, R. (2010). Neurogenesis and Alzheimer's disease: at the crossroads. *Exp Neurol*, 223(2):267-81.

Lederer, C., Torrisi, A., Pantelidou, M., Santama, N., & Cavallaro, S. (2007). Pathways and genes differentially expressed in the motor cortex of patients with sporadic amyotrophic lateral sclerosis. *BMC Genomics*, 8: 26.

Lee, H., Blasco, M., Gottlieb, G., Horner, J. I., Greider, C., & DePinho, R. (1998). Essential role of mouse telomerase in highly proliferative organs. *Nature*, 392, 569–574.

Lee, K., Dietrich, P., & Jessell, T. (2000). Genetic ablation reveals that the roof plate is essential for dorsal interneuron specification. *Nature*, 403(6771):734-40.

Lee, S., Simons, S., Heldt, S., Zhao, M., Schroeder, J., & Vellano, C. (2010). RGS14 is a natural suppressor of both synaptic plasticity in CA2 neurons and hippocampal-based learning and memory. *Proc. Natl. Acad. Sci. U.S.A*, 107, 16994–16998.

Lee, S., Tole, S., Grove, E., & McMahon, A. (2000). A local Wnt-3a signal is required for development of the mammalian hippocampus. *Development*, 127:457–467.

Lehtinen, M., Zappaterra, M., Chen, X., Yang, Y., Hill, A., Lun, M., . . . Walsh, C. (2011). The cerebrospinal fluid provides a proliferative niche for neural progenitor cells. *Neuron*, 69, 893–905.

Li, J., Xie, X., Yu, J., Sun, Y., Liao, X., Wang, X., . . . Si, T. (2017). Suppressed Calbindin Levels in Hippocampal Excitatory Neurons Mediate Stress-Induced Memory Loss. *Cell Rep*, 21(4):891-900.

Liddelow, S. (2015). Development of the choroid plexus and blood-CSF barrier. *Front. Neurosci*, 9:32.

Liddelow, S., Dziegielewska, K., Vandeberg, J., & Saunders, N. (2010). Development of the lateral ventricular choroid plexus in a marsupial, Monodelphis domestica. *Cerebrospinal Fluid Res*, 7:16.

Lie, D., Colamarino, S., Song, H., Désiré, L., Mira, H., Consiglio, A., . . . Gage, F. (2005). Wnt signalling regulates adult hippocampal neurogenesis. *Nature*, 437(7063).

Lin, H., Shaffer, K., Sun, Z., Jay, G., He, W., & Ma, W. (2004). AF1q, a differentially expressed gene during neuronal differentiation, transforms HEK cells into neuron-like cells. *Brain Res. Mol. Brain Res*, 131:126-130.

Lin, Y., Wang, H., Huang, D., Hsieh, P., Lin, M., Chou, C., . . . Huang, H. (2016). Neuronal Splicing Regulator RBFOX3 (NeuN) Regulates Adult Hippocampal Neurogenesis and Synaptogenesis. *PLoS One*, 11(10):e0164164.

Lledo, P., Alonso, M., & Grubb, M. (2006). Adult neurogenesis and functional plasticity in neuronal circuits. *Nat Rev Neurosci*, 7(3):179-93.

Llorens-Martín, M., Rábano, A., & Ávila, J. (2016). The Ever-Changing Morphology of Hippocampal Granule Neurons in Physiology and Pathology. *Front Neurosci*, 9: 526.

Lou, S., Liu, J., Chang, H., & Chen, P. (2008). Hippocampal neurogenesis and gene expression depend on exercise intensity in juvenile rats. *Brain Res*, 1210:48-55.

Lu, T., Aron, L., Zullo, J., Pan, Y., Kim, H., Chen, Y., . . . Yankner, B. (2014). REST and stress resistance in ageing and Alzheimer's disease. *Nature*, 507(7493):448-54.

Lun, M., Monuki, E., & Lehtinen, M. (2015). Development and functions of the choroid plexus–cerebrospinal fluid system. *Nat Rev Neurosci*, 16, 445–457.

Machon, O., Backman, M., Machonova, O., Kozmik, Z., Vacik, T., Andersen, L., & Krauss, S. (2007). A dynamic gradient of Wnt signaling controls initiation of neurogenesis in the mammalian cortex and cellular specification in the hippocampus. *Dev Biol*, 311, 223-237.

Madisen, L., Zwingman, T., Sunkin, S., Oh, S., Zariwala, H., Gu, H., . . . Zeng, H. (2010). A robust and high-throughput Cre reporting and characterization system for the whole mouse brain. *Nat Neurosci*, 13(1):133-40.

Maekawa, M., Takashima, N., Arai, Y., Nomura, T., Inokuchi, K., Yuasa, S., & Osumi, N. (2005). Pax6 is required for production and maintenance of progenitor cells in postnatal hippocampal neurogenesis. *Genes Cells*, 10(10):1001-14.

Mandel, G., Fiondella, C., Covey, M., Lu, D., LoTurco, J., & Ballas, N. (2011). Repressor element 1 silencing transcription factor (REST) controls radial migration and temporal neuronal specification during neocortical development. *Proc Natl Acad Sci U S A*, 108(40): 16789–16794.

Mangale, V., Hirokawa, K., Satyaki, P., Gokulchandran, N., Chikbire, S., Subramanian, L., . . . Mai, M. (2008). Lhx2 selector activity specifies cortical identity and suppresses hippocampal organizer fate. *Science*, 319, 304-309.

Marín, O., Valiente, M., Ge, X., & Tsai, L. (2010). Guiding Neuronal Cell Migrations. *Cold Spring Harb Perspect Biol*, 2(2): a001834.

Marxreiter, F., Regensburger, M., & Winkler, J. (2013). Adult neurogenesis in Parkinson's disease. *Cell Mol Life Sci*, 70(3):459-73.

Mathews, E., Morgenstern, N., Piatti, V., Zhao, C., Jessberger, S., Schinder, A., & Gage, F. (2010). A distinctive layering pattern of mouse dentate granule cells is generated by developmental and adult neurogenesis. *J Comp Neurol*, 518(22):4479-90.

McNeil, E., Capaldo, C., & Macara, I. (2006). Zonula occludens-1 function in the assembly of tight junctions in Madin-Darby canine kidney epithelial cells. *Mol Biol Cell*, 17(4):1922-32.

Meier, S., Alfonsi, F., Kurniawan, N., Milne, M., Kasherman, M., Delogu, A., . . . Coulson, E. (2019). The p75 neurotrophin receptor is required for the survival of neuronal progenitors and normal formation of the basal forebrain, striatum, thalamus and neocortex. *Development*, 146(18).

Meyer, G. (2010). Building a human cortex: the evolutionary differentiation of Cajal–Retzius cells and the cortical hem. *J. Anat*, 217, 334–343.

Meyer, G., Perez-Garcia, C., Abraham, H., & Caput, D. (2002). Expression of p73 and Reelin in the Developing Human Cortex. *Journal of Neuroscience*, 22(12):4973-4986.

Ming, G., & Song, H. (2011). Adult Neurogenesis in the Mammalian Brain: Significant Answers and Significant Questions. *Neuron*, 70(4): 687–702.

Mirzadeh, Z., Merkle, F., Soriano-Navarro, M., Garcia-Verdugo, J., & Alvarez-Buylla, A. (2008). Neural Stem Cells Confer Unique Pinwheel Architecture to the Ventricular Surface in Neurogenic Regions of the Adult Brain. *Cell Stem Cell*, 3,285-278.

Mizuseki, K., Diba, K., Pastalkova, E., & Buzsaki, G. (2011). Hippocampal CA1 pyramidal cells form functionally distinct sublayers. *Nat Neurosci*, 14: 1174–1181.

Monuki, E., Porter, F., & Walsh, C. (2001). Patterning of the Dorsal Telencephalon and Cerebral Cortex by a Roof Plate-Lhx2 Pathway. *Neuron*, 32(4):591-604.

Moss, J., Gebara, E., Bushong, E., Sánchez-Pascual, I., O'Laoi, R., El M'Ghari, I., . . . Toni, N. (2016). Fine processes of Nestin-GFP–positive radial glia-like stem cells in the adult dentate gyrus ensheathe local synapses and vasculature. *Proc Natl Acad Sci U S A*, 113(18):E2536-45.

Mouton, P. (2002). *Principles and practices of unbiased stereology: an introduction for bioscientists.* Baltimore: Johns Hopkins University Press.

Mozzi, A., Guerini, F., Forni, D., Costa, A., Nemni, R., Baglio, F., . . . Cagliani, R. (2017). REST, a master regulator of neurogenesis, evolved under strong positive selection in humans and in non human primates. *Scientific Reports*, 7, 9530.

Murray, E., Wise, S., & Graham, K. (2018). Representational specializations of the hippocampus in phylogenetic perspective. *Neuroscience Letters*, 680,4-12.

Nicola, Z., Fabel, K., & Kempermann, G. (2015). Development of the adult neurogenic niche in the hippocampus of mice. *Front Neuroanat*, 9:53.

Nottebohm, F. (2002). Why are some neurons replaced in adult brain? *J Neurosci*, 22(3), 624-8.

Okamoto, M., Inoue, K., Iwamura, H., Terashima, K., Soya, H., Asashima, M., & Kuwabara, T. (2011). Reduction in paracrine Wnt3 factors during aging causes impaired adult neurogenesis. *FASEB J*, 25(10):3570-82.

O'Mara, S. (2005). The subiculum: what it does, what it might do, and what neuroanatomy has yet to tell us. *J Anat*, 207(3): 271–282.

Pappas, G., Kriho, V., & Pesold, C. (2002). Reelin in the extracellular matrix and dendritic spines of the cortex and hippocampus: a comparison between wild type and heterozygous reeler mice by immunoelectron microscopy. *J Neurocytol*, 30, 413–425.

Park, J., Schlederer, M., Schreiber, M., Ice, R., Merkel, O., Bilban, M., . . . Tse, W. (2015). AF1q is a novel TCF7 co-factor which activates CD44 and promotes breast cancer metastasis. *Oncotarget*, 6(24):20697-710.

Patel, S., Clayton, N., & Krebs, J. (1997). Spatial learning induces neurogenesis in the avian brain. *Behavioural Brain Research*, 89(1-2), 115-128.

Paton, J., & Nottebohm, F. (1984). Neurons generated in the adult brain are recruited into functional circuits. *Science*, 225(4666):1046-8.

Phillips, W., Morton, A., & Barker, R. (2005). Abnormalities of neurogenesis in the R6/2 mouse model of Huntington's disease are attributable to the in vivo microenvironment. *J Neurosci*, 25(50):11564-76.

Pleasure, S., Collins, A., & LoInstein, D. (2000). Unique expression patterns of cell fate molecules delineate sequential stages of dentate gyrus development. *J Neurosci*, 20: 6095–6105.

Prajerova, I., Honsa, P., Chvatal, A., & Anderova, M. (2010). Distinct effects of sonic hedgehog and Wnt-7a on differentiation of neonatal neural stem/progenitor cells in vitro. *Neuroscience*, 171(3):693-711.

Qu, Q., Sun, G., Murai, K., Ye, P., Li, W., Asuelime, G., . . . Shi, Y. (2013). Wnt7a regulates multiple steps of neurogenesis. *Mol Cell Biol*, 33(13):2551-9.

Quattrocolo, G., & Maccaferri, G. (2014). Optogenetic activation of cajal-retzius cells reveals their glutamatergic output and a novel feedforward circuit in the developing mouse hippocampus. *J Neurosci*, 34, 13018–13032.

Rallu, M., Machold, R., Gaiano, N., Corbin, J., McMahon, A., & Fishell, G. (2002). Dorsoventral patterning is established in the telencephalon of mutants lacking both Gli3 and Hedgehog signaling. *Development*, 129(21):4963-74.

Ramon y Cajal, S. (1899). Estudios sobre la corteza cerebral humana I: corteza visual. *Rev. Trim. Micrográf. Madrid*, 4, 117–200.

Remedios, R., Huilgol, D., Saha, B., Hari, P., Bhatnagar, L., Kowalczyk, T., . . . Tole, S. (2007). A stream of cells migrating from the caudal telencephalon reveals a link between the amygdala and neocortex. *Nat Neurosci*, 10(9):1141-50.

Retzius, G. (1893). Die Cajal'schen Zellen der Grosshirnrinde beim Menschen und bei Säiugerthieren. *Biologisches Untersuchungen*, 5:1.

Reynolds, B., & Iiss, S. (1992). Generation of neurons and astrocytes from isolated cells of the adult mammalian central nervous system. *Science*, 255(5052):1707-10.

Richards, L., Kilpatrick, T., & Bartlett, P. (1992). De novo generation of neuronal cells from the adult mouse brain. *Proc Natl Acad Sci*, 89(18):8591-5.

Rockland, K., & DeFelipe, J. (2018). Editorial: Why Have Cortical Layers? What Is the Function of Layering? Do Neurons in Cortex Integrate Information Across Different Layers? *Front Neuroanat*, 12:78.

Roy, A., Gonzalez-Gomez, M., Pierani, A., Meyer, G., & Tole, S. (2014). Lhx2 Regulates the Development of the Forebrain Hem System. *Cerebral Cortex*, 24(5): 1361–1372.

Roybon, L., Hjalt, T., Stott, S., Guillemot, F., Li, J., & Brundin, P. (2009). Neurogenin2 directs granule neuroblast production and amplification while NeuroD1 specifies neuronal fate during hippocampal neurogenesis. *PLoS One*, 4(3):e4779.

Sawamoto, K., Wichterle, H., Gonzalez-Perez, O., Cholfin, J., Yamada, M., Spassky, N., . . . Alvarez-Buylla, A. (2006). New neurons follow the flow of cerebrospinal fluid in the adult brain. *Science*, 311(5761):629-32.

Scharfman, H. (2007). The CA3 "Backprojection" to the Dentate Gyrus. *Prog Brain Res*, 163: 627–637.

Schindelin, J., Arganda-Carreras, I., Frise, E., Kaynig, V., Longair, M., Pietzsch, T., . . . Cardona, A. (2012). Fiji: an open-source platform for biological-image analysis. *Nature Methods*, 9, 676–682.

Seri, B., García-Verdugo, J., Collado-Morente, L., MceIn, B., & Alvarez-Buylla, A. (2004). Cell types, lineage and architecture of the germinal zone in the adult dentate gyrus. *J. Comp. Neurol*, 478, 359–378.

Seri, B., García-Verdugo, J., McEIn, B., & Alvarez-Buylla, A. (2001). Astrocytes give rise to new neurons in the adult mammalian hippocampus. *J Neurosci*, 21(18):7153-60.

Silva-Vargas, V., Crouch, E., & Doetsch, F. (2013). Adult neural stem cells and their niche: a dynamic duo during homeostasis, regeneration, and aging. *Curr. Opin. Neurobiol*, 23, 935–942.

Silverberg, G., Heit, G., Huhn, S., Jaffe, R., Chang, S., Bronte-Stewart, H., . . . Saul, T. (2001). The cerebrospinal fluid production rate is reduced in dementia of the Alzheimer's type. *Neurology*, 57(10):1763-6.

Spuch, C., & Carro, E. (2011). The p75 neurotrophin receptor localization in blood-CSF barrier: expression in choroid plexus epithelium. *BMC Neurosci*, 12:39.

Subramanian, L., & Tole, S. (2009). Mechanisms Underlying the Specification, Positional Regulation, and Function of the Cortical Hem. *Cerebral Cortex*, 19, 90-5.

Subramanian, L., Remedios, R., Shetty, A., & Tole, S. (2009). Signals from the edges: The cortical hem and antihem in telencephalic development. *Semin Cell Dev Biol*, 20(6-10): 712–718.

Sugiyama, T., Osumi, N., & Katsuyama, Y. (2013). The germinal matrices in the developing dentate gyrus are composed of neuronal progenitors at distinct differentiation stages. *Dev. Dyn*, 242, 1442–1453.

Supèr, H., Del Río, J., Martínez, A., Pérez-Sust, P., & Soriano, E. (2000). Disruption of Neuronal Migration and Radial Glia in the Developing Cerebral Cortex Following Ablation of Cajal–Retzius Cells. *Cerebral Cortex*, 10(6):602–613.

Takada, S., Stark, K., Shea, M., Vassileva, G., McMahon, J., & McMahon, A. (1994). Wnt-3a regulates somite and tailbud formation in the mouse embryo. *Genes Dev*, 8(2):174-89.

Talos, F., Abraham, A., Vaseva, A., Holembowski, L., Tsirka, S., Scheel, A., . . . Moll, U. (2010). p73 is an essential regulator of neural stem cell maintenance in embryonal and adult CNS neurogenesis. *Cell Death Differ*, 17, 1816–1829.

Taupin, P. (2007). BrdU immunohistochemistry for studying adult neurogenesis: paradigms, pitfalls, limitations, and validation. *Brain Res Rev*, 53(1):198-214.

Tietz, S., & Engelhardt, B. (2015). Brain barriers: Crosstalk between complex tight junctions and adherens junctions. *J Cell Biol*, 209(4):493-506.

Tole, S., Goudreau, G., Assimacopoulos, S., & Grove, E. (2000). Emx2 is required for growth of the hippocampus but not for hippocampal field specification. *J Neurosci*, 20:2618-2625.

Tse, W., Zhu, W., Chen, H., & Cohen, A. (1995). A novel gene, AF1q, fused to MLL in t(1;11) (q21;q23), is specifically expressed in leukemic and immature hematopoietic cells. *Blood*, 85(3):650-6.

Urbán, N., & Guillemot, F. (2014). Neurogenesis in the embryonic and adult brain: same regulators, different roles. *Front Cell Neurosci*, 8: 396.

van den Berge, S., van Strien, M., Korecka, J., Dijkstra, A., Sluijs, J., Kooijman, L., . . . Hol, E. (2011). The proliferative capacity of the subventricular zone is maintained in the parkinsonian brain. *Brain*, 134(11):3249-63.

Van Praag, H., Schinder, A., Christle, B., Toni, N., Palmer, T., & Gage, F. (2002). Functional neurogenesis in the adult hippocampus. *Nature*, 415(6875):1030-1034.

van Strien, N., Cappaert, N., & Witter, M. (2009). The anatomy of memory: an interactive overview of the parahippocampal–hippocampal network. *Nat Rev Neurosci*, 10, 272–282.

von Bohlen Und Halbach, O. (2007). Immunohistological markers for staging neurogenesis in adult hippocampus. *Cell Tissue Res*, 329(3):409-20.

Vorhees, C., & Williams, M. (2006). Morris water maze: procedures for assessing spatial and related forms of learning and memory. *Nat Protoc*, 1(2):848-58.

Walf, A., & Frye, C. (2007). The use of the elevated plus maze as an assay of anxiety-related behavior in rodents. *Nat Protoc*, 2(2):322-8.

Wang, B., Fallon, J., & Beachy, P. (2000). Hedgehog-regulated processing of Gli3 produces an anterior/posterior repressor gradient in the developing vertebrate limb. *Cell*, 100(4):423-34.

Wang, H., Hsieh, P., Huang, D., Chin, P., Chou, C., Tung, C., . . . Huang, H. (2015). RBFOX3/NeuN is Required for Hippocampal Circuit Balance and Function. *Sci Rep*, 5:17383.

Watanabe, Y., Müller, M., von Engelhardt, J., Sprengel, R., Seeburg, P., & Monyer, H. (2016). Age-Dependent Degeneration of Mature Dentate Gyrus Granule Cells Following NMDA Receptor Ablation. *Front Mol Neurosci*, 8: 87.

Willert, J., Epping, M., Pollack, J., Brown, P., & Nusse, R. (2002). A transcriptional response to Wnt protein in human embryonic carcinoma cells. *BMC Developmental Biology*, 2, 8.

Wilson, S., & Houart, C. (2004). Early steps in the development of the forebrain. *Dev Cell*, 6(2):167-81.

Wilson, S., & Rubenstein, J. (2000). Induction and dorsoventral patterning of the telencephalon. *Neuron*, 28(3):641-51.

Wittmann, W., Iulianella, A., & Gunhaga, L. (2014). Cux2 acts as a critical regulator for neurogenesis in the olfactory epithelium of vertebrates. *Dev Biol*, 388(1):35-47.

Yamada, M., Clark, J., & Iulianella, A. (2014). MLLT11/AF1q is differentially expressed in maturing neurons during development. *Gene Expression Patterns* , 15(2).

Yamada, M., Clark, J., McClelland, C., Capaldo, E., Ray, A., & Iulianella, A. (2015). Cux2 activity defines a subpopulation of perinatal neurogenic progenitors in the hippocampus. *Hippocampus*, 25(2):253-67.

Yang, A., Walker, N., Bronson, R., Kaghad, M., OosterIgel, M., Bonnin, J., . . . Caput, D. (2000). p73-deficient mice have neurological, pheromonal and inflammatory defects but lack spontaneous tumours. *Nature*, 404(6773):99-103.

Yasuda, M., Johnson-Venkatesh, E., Zhang, H., Parent, J., Sutton, M., & Umemori, H. (2011). Multiple Forms of Activity-Dependent Competition Refine Hippocampal Circuits In Vivo. *Neuron*, 70(6):1128-42.

Yoshida, M., Assimacopoulos, S., Jones, K., & Grove, E. (2006). Massive loss of Cajal-Retzius cells does not disrupt neocortical layer order. *Development*, 133, 537-545.

Yu, J., Kim, J., Song, G., & Jung, J. (2006). Increase in proliferation and differentiation of neural progenitor cells isolated from postnatal and adult mice brain by Wnt-3a and Wnt-5a. *Mol Cell Biochem*, 288(1-2):17-28.

Zechner, D., Fujita, Y., Hülsken, J., Müller, T., Walther, I., Taketo, M., . . . Birchmeier, C. (2003). beta-Catenin signals regulate cell growth and the balance between progenitor cell expansion and differentiation in the nervous system. *Dev Biol*, 258(2):406-18.

Zhang, H., Ren, R., Du, J., Sun, T., Wang, P., & Kang, P. (2017). AF1q Contributes to Adriamycin-Induced Podocyte Injury by Activating Wnt/β-Catenin Signaling. *Kidney Blood Press Res*, 42(5):794-803.

Zhao, C., Teng, E., Summers, R., Ming, C., & Gage, F. (2006). Distinct morphological stages of dentate granule neuron maturation in the adult mouse hippocampus. *J Neurosci*, 26: 3–11.

Zhao, T., Kraemer, N., Oldekamp, J., Çankaya, M., Szabó, N., Conrad, S., . . . Alvarez-Bolado, G. (2006). Emx2 in the developing hippocampal fissure region. *European Journal of Neuroscience*, 23(11):2895-2907.

Zimmer, C., Tiveron, M., Bodmer, R., & Cremer, H. (2004). Dynamics of Cux2 expression suggests that an early pool of SVZ precursors is fated to become upper cortical layer neurons. *Cereb Cortex*, 14(12):1408-20.